Politecnico di Torino

Politecnico di Torino

Master's Degree in Aerospace Engineering

Academic year 2023/2024

Constellation optimization

Supervisors:

Prof. Casalino Lorenzo
Dr. Fasano Giorgio
Eng. Berga Marco

Candidate:

Marzullo Anna

April 2024

Summary

1 Introduction 7

2 Satellite navigation 10

2.1 Earth constellations 10

2.2 Dilution of precision 14

3 Problem statement 19

3.1 Physical models 21

3.1.1 Two-body approximation 21

3.1.2 N-body dynamics 23

3.2 Geometric dilution of precision 24

3.3 Optimization mathematical models 25

4 Support mathematical concepts 29

4.1 General optimization methods 29

4.1.1 Black-box approach 30

4.1.2 Sequential quadratic programming 31

4.1.3 Genetic algorithms 31

4.2 Clustering 32

4.3 Path-relinking technique 33

4.4 Multi-objective optimization 34

5 Experimental analysis 36

5.1 Basic assumptions 36

5.2 Global approach from scratch 39

5.3 Local approach from guess solutions 57

5.4 Orbit number reduction 65

5.5 Path-relinking solutions 77

5.6 Global approach from guess solutions 82

5.7 Solution analysis 85

5.8 Analysis summary 87

6 Extensions and future improvements 90

7 Conclusions 94

8 Bibliography 95

9 Acknowledgements 96

List of figures

Figure 1.1: Moonlight initiative representation 7
Figure 1.2: LCNS schematic representation 8
Figure 1.3: lunar terrain representation 9
Figure 2.1: Earth constellations representation 10
Figure 2.2: representation of different orbits 12
Figure 2.3: GPS trilateration 14
Figure 2.4: one satellite signal representation 15
Figure 2.5: two satellite signal representation 15
Figure 2.6: three satellite signal representation 15
Figure 2.7: satellite geometry influence on DOP factors 17
Figure 3.1: J2000 reference frame centered on Earth 19
Figure 3.2: J2000 reference frame centered in the Moon 20
Figure 3.3: Keplerian orbital parameters representation 22
Figure 3.4: three-body geometry in a general inertial reference system 23
Figure 4.1: Black-box schematic representation 31
Figure 4.2: genetic algorithm flow chart 32
Figure 4.3: clustering example representation 33
Figure 4.4: path-relinking approach 34
Figure 4.5: Pareto-front representation 34
Figure 5.1: target area representation (STK) 36
Figure 5.2: case G1 optimal solution 40
Figure 5.3: case G2 optimal solution 41
Figure 5.4: case G3 optimal solution 43
Figure 5.5: case G4 optimal solution 44
Figure 5.6: case G5 optimal solution 46
Figure 5.7: case G6 optimal solution 47
Figure 5.8: case G7 optimal solution 48
Figure 5.9: case G8 optimal solution 50
Figure 5.10: case G9 optimal solution 51
Figure 5.11: case G10 optimal solution 52
Figure 5.12: case G11 optimal solution 53
Figure 5.13: case G12 optimal solution 54
Figure 5.14: case G13 optimal solution 56
Figure 5.15: case S1 guess solution 58
Figure 5.16: case S1 optimal solution 58
Figure 5.17: case S2 guess solution 59
Figure 5.18: case S2 optimal solution 59
Figure 5.19: case S3 guess solution 61
Figure 5.20: case S3 optimal solution 61
Figure 5.21: case S4 guess solution 62
Figure 5.22: case S4 optimal solution 62
Figure 5.23: case S5 optimal solution 64
Figure 5.24: case S5 guess solution 64
Figure 5.25: case AK1 guess solution 66
Figure 5.26: case AK1 clustering solution 66
Figure 5.27: case BK1 guess solution 67
Figure 5.28: case BK1 optimal solution 67

Figure 5.29: case AK2 guess solution 68
Figure 5.30: case AK2 clustering solution 68
Figure 5.31: case BK2 guess solution 70
Figure 5.32: case BK2 optimal solution 70
Figure 5.33: case AK3 clustering solution 71
Figure 5.34: case AK3 guess solution 71
Figure 5.35: case BK3 optimal solution 73
Figure 5.36: case BK3 guess solution 73
Figure 5.37: case AK4 clustering solution 74
Figure 5.38: case AK4 guess solution 74
Figure 5.39: case BK4 optimal solution 76
Figure 5.40: case BK4 optimal solution 76
Figure 5.41: case G1 genetic algorithm 77
Figure 5.42: case G2 genetic algorithm 77
Figure 5.43: case P1 optimal solution 79
Figure 5.44: case P2 optimal solution 80
Figure 5.45: case P3 optimal solution 81
Figure 5.46: case G14 optimal solution 83
Figure 5.47: case G15 optimal solution 84
Figure 5.48: apogee radius variation (%) 85
Figure 5.49: perigee radius variation (%) 85
Figure 5.50: perigee argument variation (%) 86
Figure 5.51: inclination variation (%) 86
Figure 5.52: RAAN variation (%) 86
Figure 5.53: non-dominated solution selection for eight satellite scenarios 88
Figure 5.54: non-dominated solution selection for seven satellite scenarios 89
Figure 6.1: representation of the equatorial target area (STK) 90
Figure 6.2: equatorial optimal solution 92
Figure 6.3: stable and unstable orbits comparison 92
Figure 6.4: GDOP trend over time 93
Figure 6.5: satellite inter-link communication 93

List of tables

Table 2.1: summary of navigation constellations 13
Table 5.1: target area coordinates 36
Table 5.2: variable upper and lower bounds 37
Table 5.3: GDOP values indicators 38
Table 5.4: case G1 orbital parameters 39
Table 5.5: case G1 GDOP values 39
Table 5.6: case G2 optimization variables 40
Table 5.7: case G2 orbital parameters 41
Table 5.8: case G2 GDOP values 41
Table 5.9: case G3 optimization variables 42
Table 5.10: case G3 orbital parameters 42
Table 5.11: case G3 orbital parameters 42
Table 5.12: case G4 optimization variables 43
Table 5.13: case G4 orbital parameters 44
Table 5.14: case G4 GDOP values 44
Table 5.15: case G5 orbital parameters 45
Table 5.16: case G5 GDOP values 45
Table 5.17: case G6 optimization variables 46
Table 5.18: case G6 orbital parameters 47
Table 5.19: case G6 GDOP values 47
Table 5.20: case G7 optimization variables 48
Table 5.21: case G7 orbital parameters 48
Table 5.22: case G7 GDOP values 48
Table 5.23: case G8 optimization variables 49
Table 5.24: case G8 orbital parameters 49
Table 5.25: case G8 GDOP values 49
Table 5.26: case G9 orbital parameters 50
Table 5.27: case G9 GDOP values 51
Table 5.28: case G10 optimization variables 51
Table 5.29: case G10 orbital parameters 52
Table 5.30: case G10 GDOP values 52
Table 5.31: case G11 optimization variables 53
Table 5.32: case G11 orbital parameters 53
Table 5.33: case G11 GDOP values 53
Table 5.34: case G12 orbital parameters 54
Table 5.35: case G12 GDOP values 54
Table 5.36: case G13 optimization variables 55
Table 5.37: case G13 orbital parameters 55
Table 5.38: case G13 GDOP values 55
Table 5.39: global approach optimal solutions: 56
Table 5.40: case S1 orbital parameters 57
Table 5.41: case S1 GDOP values 57
Table 5.42: case S2 optimization variables 58
Table 5.43: case S2 orbital parameters 58
Table 5.44: case S2 GDOP values 59
Table 5.45: case S3 optimization variables 60
Table 5.46: case S3 orbital parameters 60

Table 5.47: case S3 GDOP values 60
Table 5.48: case S4 optimization variables 61
Table 5.49: case S4 orbital parameters 62
Table 5.50: case S4 GDOP values 62
Table 5.51: case S5 optimization variables 63
Table 5.52: case S5 orbital parameters 63
Table 5.53: case S5 GDOP values 63
Table 5.54: local approach optimal solutions 64
Table 5.55: case AK1 orbital parameters 65
Table 5.56: case AK1 GDOP values 65
Table 5.57: case BK1 optimization variables 66
Table 5.58: case BK1 orbital parameters 67
Table 5.59: case BK1 GDOP values 67
Table 5.60: case AK2 orbital parameters 68
Table 5.61: case AK2 GDOP values 68
Table 5.62: case BK2 optimization variables 69
Table 5.63: case BK2 orbital parameters 69
Table 5.64: case BK2 GDOP values 70
Table 5.65: case AK3 orbital parameters 70
Table 5.66: case AK3 GDOP values 71
Table 5.67: case BK3 optimization variables 72
Table 5.68: case BK3 orbital parameters 72
Table 5.69: case BK3 GDOP values 72
Table 5.70: case AK4 orbital parameters 73
Table 5.71: case AK4 GDOP values 74
Table 5.72: case BK4 optimization variables 75
Table 5.73: case BK4 orbital parameters 75
Table 5.74: case BK4 GDOP values 75
Table 5.75: orbital parameters subdivision 77
Table 5.76: upper and lower bounds 77
Table 5.77: case P1 orbital parameters 78
Table 5.78: case P1 GDOP values 78
Table 5.79: case P2 orbital parameters 79
Table 5.80: case P2 GDOP values 79
Table 5.81: case P3 orbital parameters 80
Table 5.82: case P3 GDOP values 81
Table 5.83: case G14 orbital parameters 82
Table 5.84: case G14 GDOP values 82
Table 5.85: case G15 orbital parameters 83
Table 5.86: case G15 GDOP values 84
Table 5.87: summary of the optimal solutions obtained 87
Table 6.1: equatorial target area coordinates 90
Table 6.2: variable upper and lower bounds 90
Table 6.3: equatorial area orbital parameters 91
Table 6.4: equatorial area GDOP values 91

1 Introduction

The exploration of the Moon is becoming a primary focus in global space initiatives, with both government and commercial entities gearing up for ambitious missions over the next decades. The importance of moon exploration for the future cannot be ignored, in fact, the Moon serves as a testing ground for new technologies and innovative experiments, improving essential skills and knowledge vital for broader space endeavors. Apart from its technical value, the Moon has invaluable resources like water ice, which could sustain future lunar settlements and serve as a launchpad for deeper space exploration. Moreover, a sustained presence on the lunar surface can facilitate groundbreaking scientific research. The return to the Moon signifies not just human curiosity but also lays the foundation for a new chapter in human space exploration.

The challenges posed by lunar exploration, such as enduring long-duration missions and extreme temperatures, provide invaluable opportunities to develop and refine capabilities essential for more ambitious ventures, such as crewed missions to Mars. Crucial resources like water ice are vital for life support and potentially enabling sustainable lunar colonies, thereby making prolonged human presence in space more viable. Additionally, water can be utilized as rocket fuel, manufactured in situ on the Moon, significantly mitigating the costs and complexities associated with space travel.

Moreover, the Moon holds immense scientific importance, revealing insights into its geology, composition, and preserving vital information about the early history of our solar system. Finally, the Moon serves as a stepping stone for further solar system exploration and beyond. Establishing a lasting human presence on the Moon can serve as a launchpad for ambitious deep space missions, extending the frontiers of space exploration. The confluence of technological advancement, resource utilization, scientific discovery, and strategic positioning makes the Moon an irresistible destination for exploration in the forthcoming decades.

Figure 1.1: Moonlight initiative representation

The ESA Moonlight Initiative, as represented in Figure 1.1, encompasses a comprehensive array of missions, projects, and initiatives designed to explore every facet of the lunar landscape (see e.g., ESA 2024b). From robotic rovers exploring the lunar surface for signs of water ice to orbiting satellites mapping the Moon's topography in detail, ESA is deploying a wide range of cutting-edge technologies and scientific instruments to allow each type of experimental research. These missions not only provide valuable insights into the

Moon's geology, composition, and history but also lay the groundwork for future human exploration and settlement.

In this context, space communications and navigation are crucial elements, representing crucial components in space exploration, enabling various data transmission and positional accuracy in a mission scenario. Satellite networks in lunar orbit play a pivotal role in communication. These satellites facilitate data transfer between the Moon and Earth. They act as data-relays for signals between lunar bases, rovers, and spacecraft, enabling seamless communication despite the vast distances. The communication between Earth and the Moon involves complex systems, including powerful transmitters and receivers. Signals travel vast distances, facing challenges like signal degradation and latency. Advanced modulation techniques and error-correction mechanisms are employed to ensure reliable data transmission.

In addition to satellite communication, accurate navigation on the lunar surface is essential for missions and exploration. Navigation systems on lunar rovers and spacecraft utilize a combination of sensors, including gyroscopes, accelerometers, and celestial navigation tools, to determine position and orientation relative to the Moon's surface. Precision in navigation relies on synchronization with Earth-based systems. The integration of data from Earth's positional information, combined with lunar-specific mapping and positioning algorithms, ensures accurate navigation and alignment of spacecraft and assets on the lunar surface. Lunar communications and navigation services (LCNS) faces all these problems, as represented in Figure 1.2.

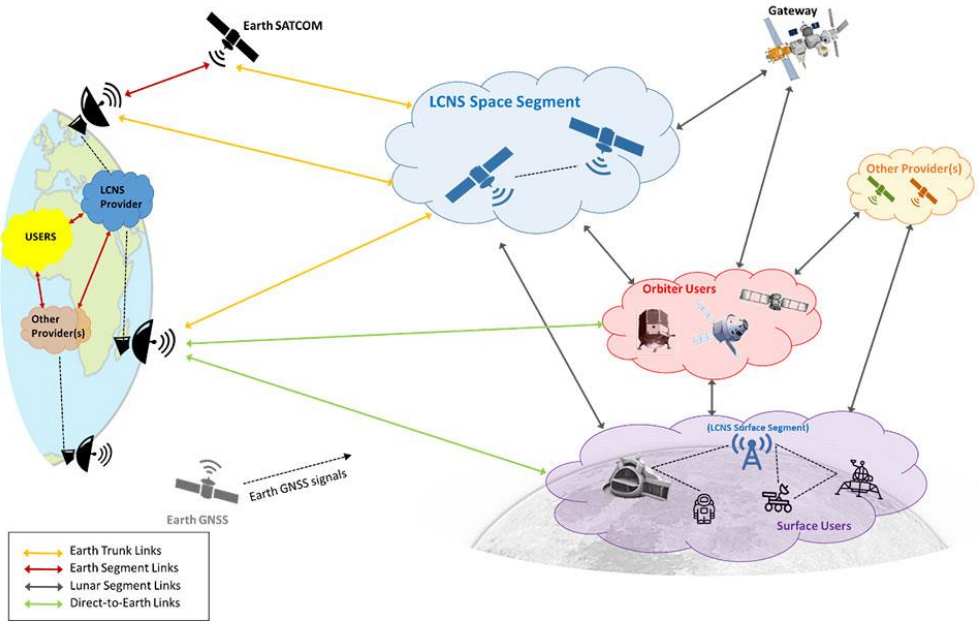

Figure 1.2: LCNS schematic representation

The unique lunar terrain, with its craters and mountains, poses challenges for communication and navigation. Overcoming these obstacles requires adaptive systems, guided navigation, and real-time data analysis to ensure safe communication and data transmission. The Moon's harsh environment, including extreme temperatures and cosmic radiation, demands robust and resilient communication and navigation systems. Advances in materials science and system design are essential for withstanding these conditions.

Lunar communications and navigation systems continue to evolve as space agencies and private companies plans for extensive lunar missions, including long-term lunar bases and scientific exploration. Innovations in quantum communication, autonomous navigation, and sustainable power sources are anticipated to revolutionize lunar communication and navigation in the coming decades.

The captivating interplay between moonlight and the advancements in lunar communication and navigation systems not only fuels our curiosity but also serves as a cornerstone in humanity's quest to explore and inhabit the scenarios beyond Earth.

Figure 1.3: lunar terrain representation

2 Satellite navigation

The following chapter deals with an introduction about the modern satellite navigation systems and the principles that drive such designs. A summary of the existing earth architectures for these kinds of applications are showed. Finally, the parameters of the dilution of precision are explained.

2.1 Earth constellations

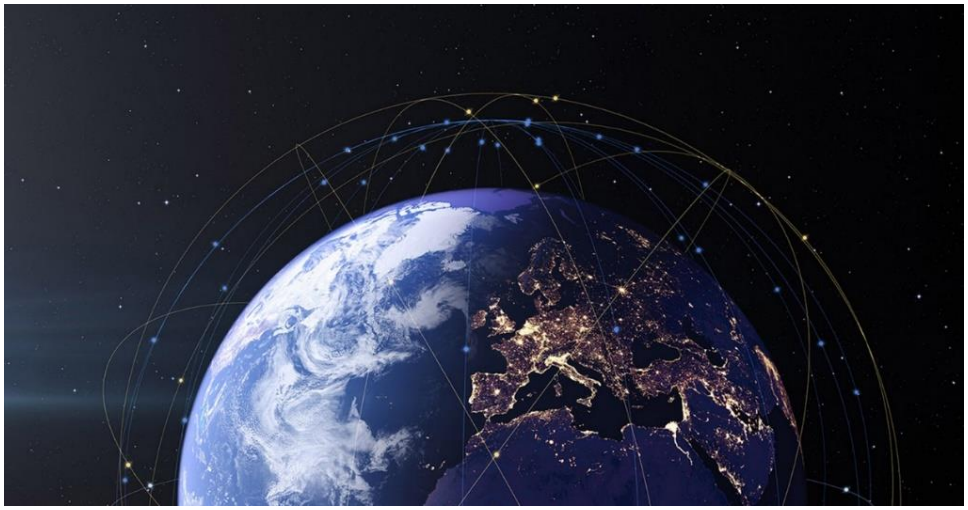

Figure 2.1: Earth constellations representation

Satellite constellations are groups of satellites strategically positioned in orbit around the Earth to achieve specific objectives, such as communication, Earth observation, navigation, or scientific research. Figure 2.1 gives a representation of these systems. The constellations are composed by multiple satellites working together to provide coverage, redundancy, and enhanced capabilities.

In general, constellations can be categorized based on various aspects such as operational function, the methodology used in designing the constellation, and the characteristics of the satellite orbits. Among these, the ability to provide global or local coverage is relevant.

Satellite orbits can be classified based on several factors (see e.g., ESA 2020). In the following section the main subdivision is reported:

- Low Earth Orbit (LEO) are orbit with an altitude from 160 km above Earth to less than 1000 km. It is the orbit most frequently used for satellite imaging, as being near the surface allows it to take images of higher resolution. Although individual LEO satellites are less useful for tasks such as telecommunications, because they require a lot of effort to track from ground stations, they often work as part of a large constellation to provide constant coverage of large areas simultaneously, by working together. These orbits provide the best ground resolution and the lowest orbital insertion cost. They also provide broadband signal transmission with reduced latency. Because of these characteristics, they are used for Earth observation missions (environmental remote sensing), while they are rarely used for navigation systems.

- Medium Earth Orbit (MEO) are orbits with altitude between LEO and geostationary earth orbit (GEO) orbit, from 2000 km and 35,786 km. Due to significant limitations caused by the presence of the Van Allen radiation belts within this altitude range, the use of these orbits is limited to altitudes above 19,000 km, where the effects of the belts are less influent. MEO orbits are frequently used in navigation and terrestrial geodesy missions, particularly for altitudes between 19,000 km and 25,000 km.

- High Earth Orbit (HEO) are orbits with an altitude greater than 35,768 km. A geosynchronous orbit (GSO) is an Earth-centered orbit with an orbital period equivalent to the Earth's rotation on its axis. A satellite in a geosynchronous orbit returns to the same position in the sky after a period of one sidereal day. A circular geosynchronous orbit has a constant altitude of 35,786 km. A relevant case of a geosynchronous orbit is termed Geostationary Earth Orbit (GEO), which is a circular and equatorial orbit (i = 0°, e = 0). The satellite describes a fixed and repeated ground track (on the Equator) on Earth surface, allowing the satellite to continuously observe the same region with identical geometric characteristics. Due to these properties, GEO orbits are crucial for applications requiring continuous coverage on a specific region such as telecommunications, meteorology, and navigation. However, GEO orbits do not provide global coverage.

Satellite constellations can be composed by different types of orbits. Generally, architectures structured with similar satellite orbits ensures that external dynamic perturbations affect each satellite in a comparable way. By maintaining this uniformity, the geometric configuration can be preserved with minimal station-keeping maneuvers, leading to reduced fuel consumption and longer satellite lifetime. Additionally, careful consideration is given to the phasing of satellites within orbital planes to maintain adequate separation, mitigating the risk of collisions or interference at orbit plane intersections. Circular orbits are often preferred due to the consistent altitude they provide, necessitating a steady signal strength for communication.
One popular class of circular orbit geometries is the Walker constellation (see e.g., Walker 1984). This configuration is described using the following short notation:

$$i: N_s/N_p/f$$

where:

- i is the orbit inclination;
- N_s is the total number of satellites;
- N_p is the number of equally spaced orbital planes;
- f is the phasing between satellites in adjacent planes, specified as a scalar integer greater than or equal to 0.

One popular Walker constellation is the Iridium constellation. The active satellites in the full Iridium constellation form a Walker Star with $i = 86.4°$, $N_s = 66$, $N_p = 6$ and $f = 2$ ($86.4°: 66/6/2$), i.e., the satellite return to the same true anomaly value after two planes. These sets of circular orbits at constant altitude are sometimes referred to orbital shells.

A summary of satellite constellations along with some technical information are reported:

- communication satellite constellations: they consist of interconnected satellites orbiting the Earth in coordinated patterns, like Starlink or Iridium constellations. These constellations are designed to facilitate global communication, by ensuring continuous coverage across different regions. They are typically positioned in Low Earth Orbit (LEO) to reduce latency and improve coverage, using phased array antennas, inter-satellite links, and advanced signal processing to facilitate seamless communication coverage across the globe. The strategic placement and synchronization of satellites within the constellation ensure efficient and robust communication services for various applications, including telecommunications, internet connectivity, and remote sensing.

- Earth observation satellite constellations: they allow comprehensive monitoring of the Earth's surface, atmosphere, and oceans, enabling a wide range of applications such as environmental monitoring, disaster management, urban planning, and agricultural assessment. With multiple satellites working together, typically in LEO orbit or sun-synchronous orbit (SSO), these constellations offer frequent revisit times and global coverage, allowing for real-time or near-real-time data acquisition. Advanced sensors onboard these satellites capture high-resolution imagery,

multispectral data, and other geospatial information, which are then processed and analyzed to derive valuable information into Earth's dynamic processes and changes over time.

- Navigation satellite constellations: they provide precise positioning, navigation, and timing services globally. Satellites are typically deployed in medium Earth orbit (MEO) to ensure global coverage and accuracy. These constellations rely on signals transmitted by the satellites to determine the exact location of users' devices on or near the Earth's surface. Each satellite continuously broadcasts its precise time and position information, allowing receivers to triangulate their positions by calculating the time it takes for signals to travel from multiple satellites to the receiver. Navigation satellite constellations support a wide range of applications, including aviation, maritime navigation, land surveying, transportation, and personal navigation devices, contributing to increased safety, efficiency, and precision in various fields.

- Space science satellite constellations: they are specifically dedicated to scientific exploration and observation beyond Earth's atmosphere. These constellations play a pivotal role in advancing the understanding of the cosmos, studying phenomena such as celestial bodies, cosmic rays, and high-energy particles. Equipped with specialized instruments and sensors, these satellites capture data across various wavelengths, enabling scientists to conduct detailed analyses of astronomical events and cosmic structures. Satellites may have various orbits depending on the specific scientific objectives, including polar orbits or highly elliptical orbits. By deploying multiple satellites, these constellations offer broader coverage, increased observational frequency, and the ability to conduct coordinated observations, ultimately contributing to the advancement of space science.

These satellite constellations represent a diverse range of applications and technical implementations, each contributing to scientific research, technological advancements, and practical applications in various fields.

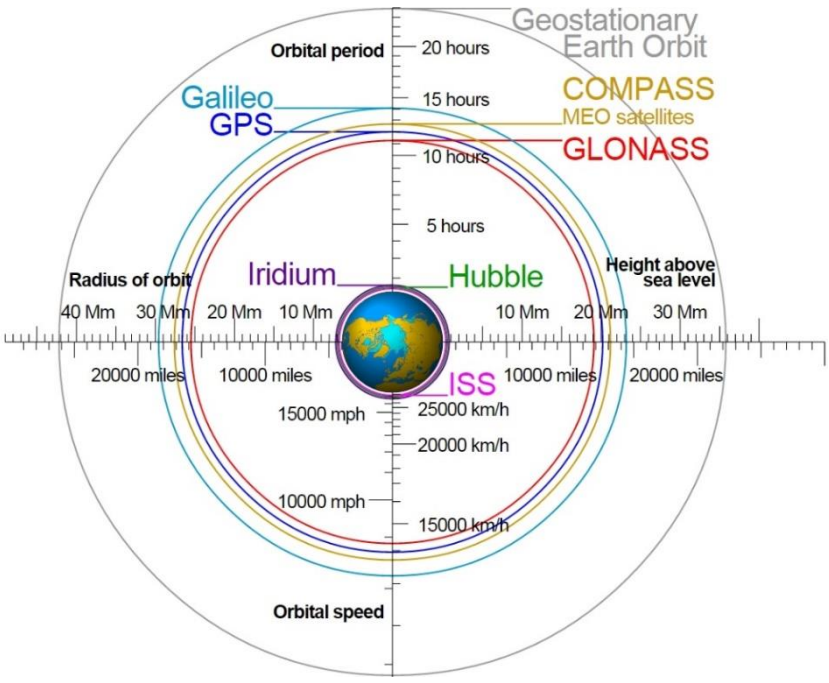

Figure 2.2: representation of different orbits

In the context of navigation satellites (see ESA 2024a), here are some of the most prominent constellations able to ensure continuous and accurate positioning, navigation, and timing (PNT) services:

- Global Positioning System (GPS): developed and operated by the United States Department of Defence, the GPS constellation is the most widely used navigation satellite system globally. It consists of a constellation of around 30 satellites orbiting the Earth at approximately 20,000 km above the surface. These satellites continuously transmit signals that can be received and used by GPS receivers to determine precise positioning, velocity, and timing information.
- GLONASS (Global Navigation Satellite System): GLONASS is the Russia counterpart to the GPS system. It consists of a constellation of around 24 operational satellites orbiting the Earth. GLONASS provides global coverage and is interoperable with GPS, allowing users to receive signals from both systems simultaneously to improve positioning accuracy and reliability.
- Galileo: developed by the European Union and the European Space Agency (ESA), Galileo is Europe's independent global navigation satellite system. It consists of a constellation of around 30 satellites in orbit, providing highly accurate positioning, navigation, and timing services to users worldwide. Galileo aims to offer greater coverage and reliability than existing systems and is designed to be interoperable with GPS and GLONASS.
- BeiDou Navigation Satellite System (BDS): BeiDou is China's navigation satellite system, providing positioning, navigation, and timing services to users in China and the Asia-Pacific region. It initially started as a regional system but has since expanded to global coverage with a constellation of over 30 satellites. BeiDou is designed to provide enhanced positioning accuracy and availability, particularly in challenging urban environments and for mobile applications.
- Quasi-Zenith Satellite System (QZSS): developed by Japan, QZSS is a regional satellite navigation system designed to complement existing global navigation satellite systems like GPS. It consists of a constellation of multiple satellites, including one or more satellites in quasi-zenith orbits (QZO) to provide enhanced coverage over Japan and the surrounding region. QZSS aims to improve positioning accuracy, particularly in urban environments with obstructed views of the sky.

GNSS	Galileo	GLONASS	GPS	BDS		
Orbit type	MEO	MEO	MEO	GEO	IGSO	MEO
Satellite Number	24	24	30	3	3	24
Altitude	20180 km	19100 km	23220 km	35786 km	35786 km	21528
Inclination	56°	64.8°	56°	0°	55°	55°
Constellation	6 planes	Walker (24/3/1)	Walker (24/3/1) + 6 backups	Located at 80°E, 110.5°E, and 140°E	RAAN of 118°E	Walker (24/3/1)
Total number	24	24	30	30		

Table 2.1: summary of navigation constellations

These navigation satellite constellations work together to provide global coverage and ensure redundancy, resilience, and reliability in positioning and timing services for various applications, including aviation, maritime navigation, surveying, agriculture, transportation, and personal navigation.

2.2 Dilution of precision

In the vast space environment, where distances span millions of kilometers and the smallest error can have significant consequences, satellite navigation systems represent a testament to human ingenuity. Operating through a network of orbiting satellites, these systems give us the remarkable ability to define our location with high accuracy (see e.g., GISgeography 2024). Satellite navigation has revolutionized the way we navigate and explore the world around us, becoming indispensable tools in countless applications. As technology continues to evolve, the possibilities for improving navigation accuracy are increasing. paving the way for a future where we can navigate with unprecedented accuracy and confidence.

At the heart of satellite navigation lies a constellation of satellites orbiting the central planet. These satellites continuously broadcast signals that are acquired by receivers on the ground or in other vehicles. The receiver can calculate its own position using a process known as trilateration. The principle is represented in Figure 2.3.

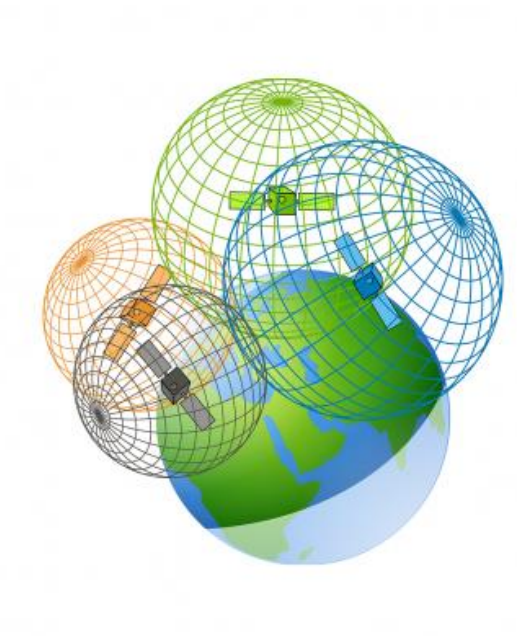

Figure 2.3: GPS trilateration

The trilateration is often confused with the concept of triangulation, in fact trilateration involves measuring distances while, on the other hand, triangulation measures angles. The following two-dimensional example explains the process, involving three satellites, as represented in figure 2.4, 2.5, and 2.6.

Figure 2.4: one satellite signal representation

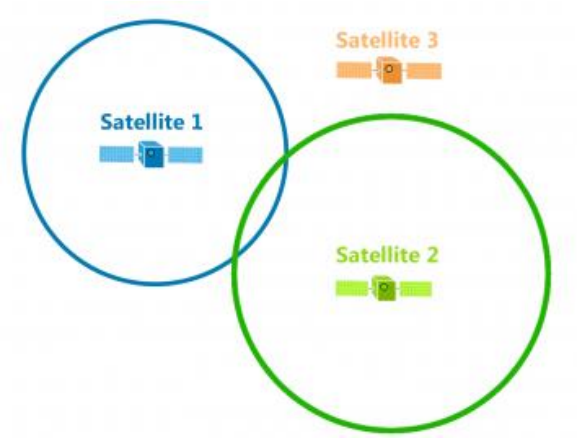

Figure 2.5: two satellite signal representation

Figure 2.6: three satellite signal representation

Satellites broadcast signals for the GPS receiver to define its position, with both time and distance information. When the satellite one transmits a signal and it reaches the receiver, the distance between them is calculated, forming a circle of possible positions around the receiver. Consequently, the GPS position could lie anywhere on this circular path at the specified radius (see Fig. 2.4). The same thing occurs with the signal from a satellite two. The distance is uniformly broadcast until it reaches the receiver, potentially placing the receiver anywhere along the circle (see Fig. 2.5). However, with two known distances from two satellites, the precise position could be on the two intersection points where the circles meet. The involvement of a third satellite defines the accurate location at the intersection of all three circles. Trilateration utilizes these three distances to calculate the exact position (see Fig. 2.6). As the GPS receiver moves, the radius of each circle (distance) change consequently. In three-dimensional reality, GPS satellites broadcast signals in a spherical pattern, measuring distances to calculate the precise location. Yet several factors such as the atmosphere can affect the GPS precision and errors.

The Global Navigation Satellite System (GNSS) typically requires signals from at least four visible satellites, to work effectively. This requirement comes from the basic principle of how the positioning systems work. Thanks to the trilateration principle, it is possible to determine a receiver position by calculating its distance from at least three visible satellites. With signals from three satellites, the receiver can determine

approximately its position but the clock of the receiver is not synchronized with the atomic clocks on the satellites. The addition of a fourth satellite is essential for precise 3D positioning and time synchronization. This is because the receiver also needs to account for its own internal clock inaccuracies. By receiving signals from a fourth satellite, the receiver can correct any clock discrepancies and accurately calculate its position in three dimensions. In reality, more satellites provide better precision and redundancy. While four satellites are the minimum required for basic positioning, additional visible satellites further improve precision and reliability. By receiving signals from more satellites, the receiver can better mitigate errors caused by factors like atmospheric interference or satellite clock inaccuracies.

In the context of satellite navigation and positioning systems, the accuracy and reliability of positioning are paramount. The phenomenon termed dilution of precision (DOP) represents and profoundly shapes the reliability of location-based measurements, and among its manifestations, the geometric dilution of precision (GDOP) emerges as a pivotal factor (see e.g., Tsui 2000). The DOP is a parameter to specify the error propagation as a mathematical effect of navigation satellite geometry on positional measurement precision, in particular it quantifies the effect of satellite geometry on positioning precision. The DOP defines how errors in the measurement as geometric perturbations, will affect the final state estimation, leading to changes in the measured data. Ideally, minor variations in the measured data should not yield significant variations in the final data. Conversely, sensitivity to measurement errors indicates a less desirable scenario where small variations in input lead to considerable changes in output. Not considering ionospheric and tropospheric effects, the signals from navigation satellites are defined. In particular, the relative satellite-receiver geometry plays the major role in determining the precision of estimated positions and times. Generally, a low DOP value represents a better positional precision. The DOP include the Geometric Dilution of Precision (GDOP), the Position Dilution of Precision (PDOP), the Time Dilution of Precision (TDOP) and the Vertical Dilution of Precision (VDOP):

- Horizontal Dilution of Precision (HDOP): HDOP is a measure of the effect of satellite geometry on the accuracy of horizontal positioning. It quantifies how well the satellites are spread out across the sky in relation to the user's position. A lower HDOP value indicates better satellite geometry and therefore better horizontal positioning accuracy. HDOP values typically range from one to infinity, with values closer to one indicating better accuracy.

- Vertical Dilution of Precision (VDOP): VDOP measures the effect of satellite geometry on the accuracy of vertical positioning. It assesses how well the satellites are distributed in relation to the user's altitude. Similar to HDOP, a lower VDOP value indicates better satellite geometry and therefore better vertical positioning accuracy. VDOP values also typically range from one to infinity.

- Geometric Dilution of Precision (GDOP): GDOP is a combined measure of the effect of satellite geometry on both horizontal and vertical positioning accuracy. It considers both HDOP and VDOP to provide an overall assessment of positioning accuracy. A lower GDOP value indicates better overall satellite geometry and therefore better overall positioning accuracy.

- Time Dilution of Precision (TDOP): TDOP measures the effect of satellite geometry on the accuracy of time measurements in satellite navigation systems. It quantifies how well the satellites are distributed in relation to the user's location in time. Similar to HDOP and VDOP, a lower TDOP value indicates better satellite geometry and therefore better time measurement accuracy.

The DOP factors are influenced by various factors:

- Satellite constellation geometry: the satellites position in the sky plays a crucial role in determining the accuracy of the receiver position. When satellites are closely grouped together, the DOP is low, resulting in higher accuracy. Conversely, when satellites are spread out or clustered in specific regions of the sky, the DOP is high, leading to lower accuracy. The concept is represented in Figure

2.7. Higer satellite elevation angles result in lower DOP, improving sensitivity to atmospheric disturbances. This is because, depending on the relative geometry between a satellite and a receiver, the precision of the satellite pseudo-range directly influences each dimension of the receiver's position measurement. The collective precision of multiple satellites in view of a receiver is determined by their relative positions, thus impacting the accuracy across each dimension of the receiver's measurement.

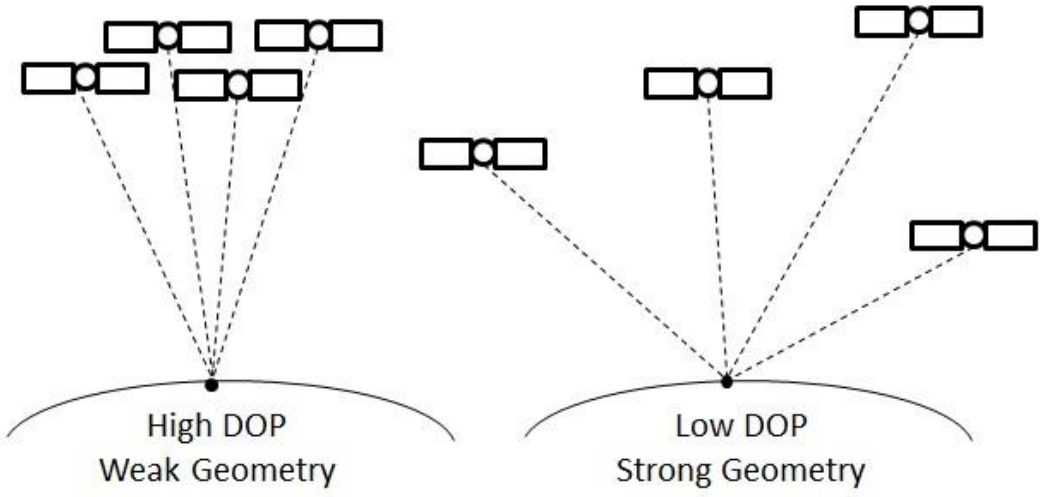

Figure 2.7: satellite geometry influence on DOP factors

- Receiver position: the receiver location on the surface affects the visible satellites and their angles, thereby it influences the GDOP.
- Atmospheric conditions: the atmosphere can introduce errors in satellite signals due to factors such as, for example in the Earth case, ionospheric and tropospheric delays. These delays can vary based on factors like weather conditions, time of day, and geographic location, thereby affecting the accuracy of position measurements.
- Satellite signal quality: the strength and integrity of satellite signals received by the receiver device also impact the DOP. Interference from nearby structures, terrain, or electronic devices can degrade the quality of signals, leading to increased uncertainty in position calculation.
- Receiver sensitivity and multipath effects: The sensitivity of the receiver device to satellite signals, as well as multipath effects caused by signal reflections off nearby surfaces, can introduce errors in position calculations. Receiver design, antenna placement, and signal processing techniques play crucial roles in mitigating these effects.

While DOP presents challenges to achieving accurate position fixes, there are several strategies to mitigate its effects. Effective satellite selection, strategic antenna placement, optimized receiver design, and real-time monitoring with corrections are crucial elements for enhancing the accuracy of position measurements in advanced positioning systems. By prioritizing satellites with favorable geometries and visibility, users can minimize dilution of precision (DOP) and elevate measurement accuracy, often facilitated by algorithms that dynamically optimize satellite selection based on prevailing conditions. Additionally, strategic antenna placement enhances satellite visibility and geometric conditions, further reducing DOP. Receiver design and calibration play a pivotal role in mitigating the impact of receiver sensitivity and multipath effects on accuracy

through optimization of design, placement, and signal processing algorithms. Moreover, continuous real-time monitoring of satellite positions coupled with correction algorithms recalibrates positioning calculations on-the-fly, effectively mitigating DOP effects and ensuring consistent accuracy in position measurements.

3 Problem statement

The following chapter deals with the description of the mathematical model and assumptions defined to describe the problem. The optimization algorithms are applied on the model formulated. The dynamic models, control variables and constraints are showed in detail.

The problem consists in analyzing the motion of a group of satellites around a central body, in our case the Moon, to calculate the time intervals of visibility of every satellite with respect to the target points on the body surface, and the time intervals of visibility of every satellite with respect to the Earth. The following scenario is considered:

- a set of satellites S_α with $\alpha = 1, \dots, N_S$ is considered.
- the time period considered is $[0, T]$;
- a grid of target points $P_i = (\lambda_i, \varphi_i)$ (λ_i latitude and φ_i longitude), with $\lambda_i = [0, \pm\frac{\pi}{2}]$, $\varphi_i = [0, 2\pi]$ and $i = 1, \dots, N_P$, on the Moon surface is given;

The model is aimed at minimizing the geometric dilution of precision GDOP, as defined in Section 3.3 (GDOP, Langley 1999a, 1999b). The visibility of at least four satellites from each single point (on the lunar surface) must be permanently guaranteed. Analogously, the visibility of at least one satellite from Earth must be permanently guaranteed. In the present work is understood that the mutual communication between all the satellites is always possible (this guarantees that the visibility of a single satellite from Earth is sufficient for the scope). The following reference frames are introduced:

- Earth centered inertial (ECI) reference frame. The fundamental $x_E y_E$ plane is the Earth equatorial plane, the x_E axis is permanently fixed in the direction of the vernal equinox while the z_E axis is permanently oriented to the north pole. The origin O_E is fixed in the center of the Earth. One commonly used ECI frame is defined with the Earth's Mean Equator and Mean Equinox (MEME) at 12:00 Terrestrial Time on 1 January 2000 (represented in Fig. 3.1). The z_E axis is aligned with the Earth's rotation axis (or equivalently, the celestial North Pole) as it was at that time. The x_E and y_E axes are defined as previously. The ECI reference system will be indicated herein by (O_E,x_E,y_E, z_E).

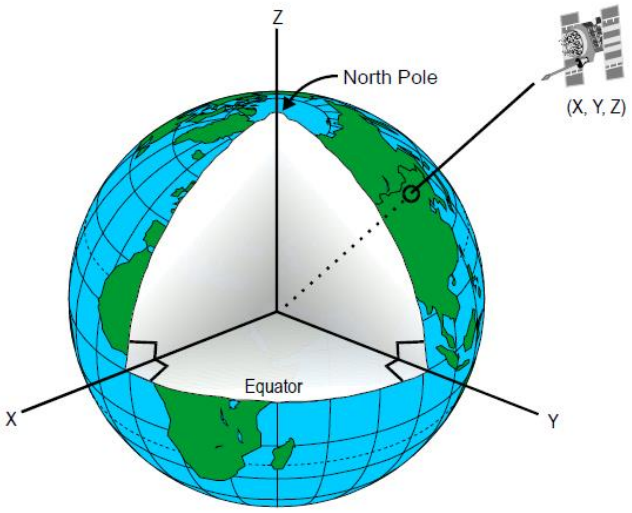

Figure 3.1: J2000 reference frame centered on Earth

- Moon centered (MC) reference frame with axes always parallel to the corresponding axes of the J2000 reference frame ($x_E//x_M$, $y_E//y_M$, $z_E//z_M$) as represented in Figure 3.2. The origin of O_M is fixed in the center of the Moon; the MC reference system will be indicated herein by (O_M,x_M,y_M, z_M). In the following, if not differently specified, the Cartesian coordinates are adopted for both reference frames.

For the specific case it will be considered the Moon centered reference frame to propagate satellite orbit for all the dynamical models implemented. In Figure 3.2 the red line represents the Moon equator.

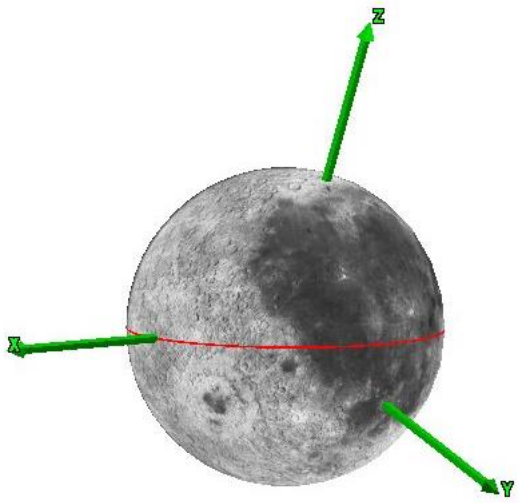

Figure 3.2: J2000 reference frame centered in the Moon

The conversion of a state vector from one inertial reference system to a second inertially one, can be obtained with the definition of the matrix rotation, starting from the Euler angles defined between the two inertial reference systems. The three Euler angles usually represent rotations about the axes of a fixed coordinate system. The sequence of rotations and the order of the axes determine the final orientation. A common rotation applied is the Tait-Bryan 321 rotation where 3 indicates that the first rotation is about the third axis (z axis), 2 indicates that the second rotation is about the second axis (y axis) and 1 indicates that the third rotation is about the first axis (x axis). For each elemental rotation, a 3x3 rotation matrix representing the rotation about a specific axis is expressed. The rotation matrices for the elemental rotations can be derived based on trigonometric functions (such as sine and cosine) of the corresponding Euler angles. The following expressions represent the main rotation matrices, for an angle rotation α about the x axis, an angle rotation β about the y axis and an angle rotation γ about the z axis to obtain:

$$R_x(\alpha) = \begin{bmatrix} 1 & 0 & 0 \\ 0 & \cos(\alpha) & -\sin(\alpha) \\ 0 & \sin(\alpha) & \cos(\alpha) \end{bmatrix}, \tag{3.1}$$

$$R_y(\beta) = \begin{bmatrix} \cos(\beta) & 0 & \sin(\beta) \\ 0 & 1 & 0 \\ -\sin(\beta) & 0 & \cos(\beta) \end{bmatrix}, \tag{3.2}$$

$$R_z(\gamma) = \begin{bmatrix} \cos(\gamma) & -\sin(\gamma) & 0 \\ \sin(\gamma) & \cos(\gamma) & 0 \\ 0 & 0 & 1 \end{bmatrix}. \tag{3.3}$$

Following the 321 rotation sequence, the state vector in the new reference system F_2 ($\boldsymbol{X}_{F_2}$) can be obtained starting from the vector in the first reference system ($\boldsymbol{X}_{F_1}$) as follow:

$$\boldsymbol{X}_{F_2} = R_z(\gamma) * R_y(\beta) * R_x(\alpha) * \boldsymbol{X}_{F_1} . \quad (3.4)$$

3.1 Physical models

The following chapter is based on the celestial mechanical theory as discussed in Fundamentals of Astrodynamics and applications (Vallado, 2013).

3.1.1 Two-body approximation

There are various equivalent forms to define the state of a satellite in space at a specific time. A widely used form, is the state vector expression $\boldsymbol{X}(t)$, which represents the position $\boldsymbol{r}(t)$ and velocity $\dot{\boldsymbol{r}}(t)$ vectors of the satellite, as reported in 3.5:

$$\boldsymbol{X}(t) = [\boldsymbol{r}(t), \dot{\boldsymbol{r}}(t)] = [\boldsymbol{r}_x(t), \boldsymbol{r}_y(t), \boldsymbol{r}_z(t), \dot{\boldsymbol{r}}_x(t), \dot{\boldsymbol{r}}_y(t), \dot{\boldsymbol{r}}_z(t)] . \quad (3.5)$$

The state vector can be also expressed as function of the Keplerian orbital parameters:

$$\boldsymbol{X}(t) = [\boldsymbol{r}(t), \dot{\boldsymbol{r}}(t)] = \boldsymbol{f}(S_a, e, i, \Omega, \omega, \nu_0) . \quad (3.6)$$

Here, the Keplerian orbital elements are utilized, i.e., S_a is the semi-major axis, e the eccentricity, i the inclination, Ω is the right ascension of the ascending node, ω is the argument of periapsis and ν_0 is the true anomaly at $t = 0$. More specifically:

- Semi-major axis (S_a): it represents half the sum of perigee r_p and apogee r_a radius of the orbit. The apogee is denoted as the farthest point in the orbit from the secondary body about the primary one, while the perigee as the nearest point.
- Eccentricity (e): it describes the elongation of the ellipse in relation to a circle.
- Inclination (i): it represents the orientation of the ellipse with respect to the reference plane, measured at the ascending node.
- Right ascension of the ascending node (Ω): it represents the angle orientation of the ascending node line of the orbit, with respect to the reference frame vernal point.
- Argument of periapsis (ω): it indicates the orientation of the ellipse within the orbital plane, measuring the angle from the ascending node to the periapsis.
- True anomaly at epoch $t = 0$ (ν_0): it describes the orbiting body position along the ellipse at a specific time.

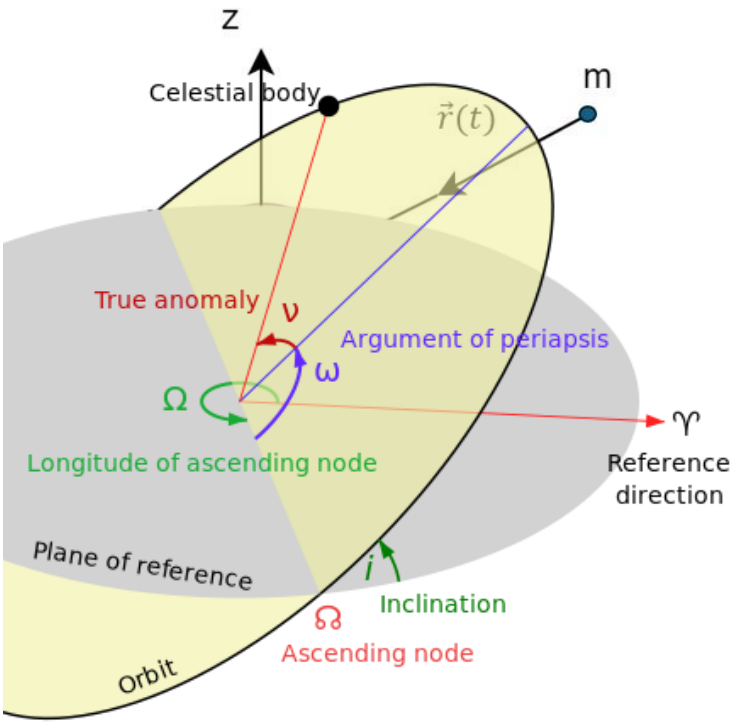

Figure 3.3: Keplerian orbital parameters representation

The inclination, right ascension of the ascending node, and argument of periapsis can also be described as Euler angles, defining the orbit orientation relative to the reference coordinate system. The Keplerian orbital elements (as represented in Fig. 3.3) are the parameters required to uniquely identify a specific orbit. In celestial mechanics these elements are considered in two-body systems using a Kepler orbit. A real orbit elements change over time due to the dynamic perturbations caused by other celestial bodies and the effects of their gravity field. A Kepler orbit is an idealized approximated orbit at a particular time. With reference to a secondary body orbiting around a primary central one with an inertial reference system centered on it, the shape and size of the ellipse orbit are defined.
The two-body equation describe the motion of two points body under the influence of their mutual gravitational attraction, as described by Newtonian mechanics. The equation is obtained from several assumptions.

1. The mass of the satellite is negligible compared to the mass of the attracting body. This is reasonable for the motion of artificial satellites.
2. The coordinate system chosen is inertial. The importance of this assumption becomes apparent in the derivations necessary to obtain the equation.
3. The bodies of the satellite and attracting body are spherically symmetrical, with uniform density. In consequence they can be treated as point masses.
4. On the system is present only the gravitational force, which act along a line joining the centers of the two bodies.

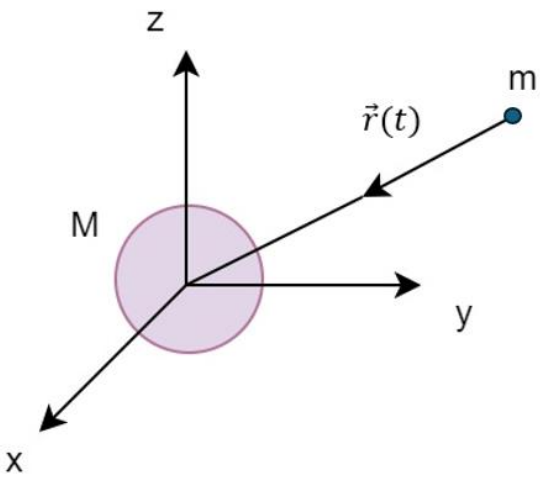

Figure 3.3: Two body problem representation

The two-body equation in an inertial reference frame can be expressed as follows:

$$\ddot{\boldsymbol{r}}(t) = -\frac{\mu}{\|\boldsymbol{r}(t)\|^3}\boldsymbol{r}(t)\,, \tag{3.7}$$

with $\mu = GM$.
Where $\ddot{\boldsymbol{r}}(t)$ is the satellite acceleration vector, μ is the gravitational parameter of the central body, G is the universal constant of gravitation, M is the mass of the central attracting body and $\boldsymbol{r}(t)$ is the position vector of the satellite. For the specific case the Moon is the central body.

3.1.2 N-body dynamics

The perturbed dynamic model describes the motion of the satellite under the influence of the central body gravitational force, and the perturbative gravitational forces derived from the presence of third bodies. Figure 3.3 represents a general inertial reference system with a central body and other secondar bodies, like Moon or Sun, and can helps to understand the position vectors and relative positions, that have to be considered.

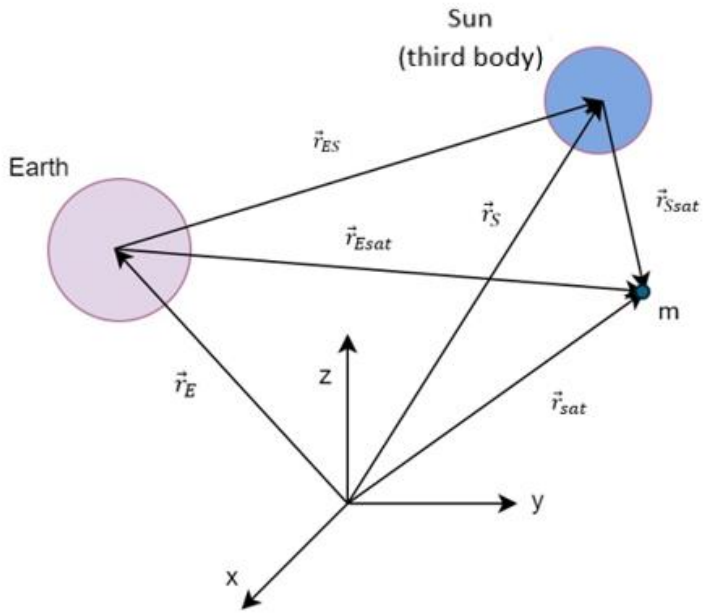

Figure 3.4: three-body geometry in a general inertial reference system

By analytical derivations, it is possible to achieve the N-body expression, relative to an inertial reference system, with the origin in the mass center of the primary central body. The subscript '1' refers to the primary central body, the subscript 'sat' refers to the satellite and 'j' to the third body considered. In particular the (n) perturbative bodies considered for $3 \leq j \leq n$:

$$\ddot{\boldsymbol{r}}_{1sat}(t) = -G\frac{(m_1+m_{sat})}{\|\boldsymbol{r}_{1sat}(t)\|^3}\boldsymbol{r}_{1sat}(t) + G\sum_{j=3}^{n} m_j\left(\frac{\boldsymbol{r}_{satj}(t)}{\|\boldsymbol{r}_{satj}(t)\|^3} - \frac{\boldsymbol{r}_{1j}(t)}{\|\boldsymbol{r}_{1j}(t)\|^3}\right), \tag{3.8}$$

From the equation can be seen the presence of several effects. The first one is the two-body gravity acceleration of the primary central body on the satellite. The second part of the equation has two parts, and it represents the gravity perturbation derived from the third bodies. A direct effect is caused from the third bodies directly on the satellite, derived from the state vector $\boldsymbol{r}_{satj}(t)$. The last term represents the indirect effect, caused by the acceleration of the third bodies on the central one (derived from the state vector $\boldsymbol{r}_{1j}(t)$).

3.2 Geometric dilution of precision

The mathematical formulation of the GDOP is here described (with reference to the Moon surface). At a given time, we consider a surface point to be observed contemporarily by at least four satellites. The formulation presented considers the case of four visible satellites but can be generalized in the case the satellites are more than four.

The satellite position vectors are introduced for each satellite respectively: $r_{M1} = [x_{M1}, y_{M1}, z_{M1}]$, $r_{M2} = [x_{M2}, y_{M2}, z_{M2}]$, $r_{M3} = [x_{M3}, y_{M3}, z_{M3}]$, $r_{M4} = [x_{M4}, y_{M4}, z_{M4}]$, and component vectors of the surface point $r_M = [x_M, y_M, z_M]$. The distance between surface point and any of the four satellites is represented by:

$$\delta r_{M\alpha} = \sqrt{(x_{M\alpha} - x_M)^2 + (y_{M\alpha} - y_M)^2 + (z_{M\alpha} - z_M)^2}\,, \tag{3.9}$$

where α is any satellite ($\alpha = 1, \ldots, 4$).

The following matrix A is introduced:

$$A = \begin{bmatrix} \frac{(x_{M1}-x_M)}{\delta r_{M1}} & \frac{(y_{M1}-y_M)}{\delta r_{M1}} & \frac{(z_{M1}-z_M)}{\delta r_{M1}} & 1 \\ \frac{(x_{M2}-x_M)}{\delta r_{M2}} & \frac{(y_{M2}-y_M)}{\delta r_{M2}} & \frac{(z_{M2}-z_M)}{\delta r_{M2}} & 1 \\ \frac{(x_{M3}-x_M)}{\delta r_{M3}} & \frac{(y_{M3}-y_M)}{\delta r_{M3}} & \frac{(z_{M3}-z_M)}{\delta r_{M3}} & 1 \\ \frac{(x_{M4}-x_M)}{\delta r_{M4}} & \frac{(y_{M4}-y_M)}{\delta r_{M4}} & \frac{(z_{M4}-z_M)}{\delta r_{M4}} & 1 \end{bmatrix}. \tag{3.10}$$

The following matrix Q is defined:

$$Q = \begin{bmatrix} \sigma_x^2 & \sigma_{xy}^2 & \sigma_{xz}^2 & \sigma_{x\tau}^2 \\ \sigma_{yx}^2 & \sigma_y^2 & \sigma_{yz}^2 & \sigma_{y\tau}^2 \\ \sigma_{zx}^2 & \sigma_{zy}^2 & \sigma_z^2 & \sigma_{z\tau}^2 \\ \sigma_{\tau x}^2 & \sigma_{\tau y}^2 & \sigma_{\tau z}^2 & \sigma_\tau^2 \end{bmatrix} = (A^T * A)^+ . \tag{3.11}$$

The calculation of the Q matrix involves the implementation of the transpose matrix A^T and the pseudoinverse $(A^T * A)^+$ of the term $(A^T * A)$. The pseudoinverse (see e.g., Israel et al., 2003) is also known as the Moore-Penrose inverse and it represents the generalization of the inverse matrix for non-square or singular matrices. It is defined as follows:

It is used when the matrix does not have an inverse, i.e., when it is not a square matrix or when it is singular (its determinant is zero). The pseudoinverse provides a solution that is as close as possible to a true inverse, allowing to solve systems of linear equations even when the matrix doesn't meet the criteria for a traditional inverse. The main characteristics of the inverse and the pseudoinverse of a matrix are reported below.

- Applicability: the inverse of a matrix exists if and only if the matrix is square and non-singular. In contrast, the pseudoinverse can be calculated for any matrix, regardless of its dimensions or singularity.
- Existence: not all matrices have an inverse, but every matrix has a pseudoinverse.
- Computation: while the inverse of a matrix can be computationally expensive to calculate, especially for large matrices, the pseudoinverse can be efficiently computed even for singular or rectangular matrices using techniques like singular value decomposition (SVD).
- Use cases: the inverse of a matrix is primarily used to solve systems of linear equations. The pseudoinverse, on the other hand, is often used in applications like least squares regression, optimization, and solving overdetermined systems of linear equations.

If A is a square non-singular matrix, its inverse A^{-1} satisfies the equation $A * A^{-1} = A^{-1} * A = I$, where I is the identity matrix. However, for non-square or singular matrices, no such inverse exists. Instead, the pseudoinverse denoted as A^{+} can be computed, which satisfies certain properties such as $A * A^{-1} = A * A^{+} * A = A$ and $A^{+} * A * A^{+} = A^{+}$. In conclusion, the pseudoinverse is a generalization of the inverse of a matrix, allowing to find approximate solutions to systems of linear equations and perform calculations on matrices that do not meet the criteria for having a true inverse.

The GDOP d is given by:

$$d = \sqrt{\sigma_x^2 + \sigma_y^2 + \sigma_z^2 + \sigma_\tau^2}\ . \tag{3.12}$$

Where $\sigma_x, \sigma_y, \sigma_z$ and σ_τ are the diagonal elements of Q as defined in (3.11). The GDOP d is adimensional.

3.3 Optimization mathematical models

Basic assumptions

In this section we formulate the simplified mathematical models relevant to the constellation optimization problem, assuming the following:

- the satellite dynamics is described with different model: the two body problem (with the Moon as central body) and the perturbed with the Moon as the central body and the Earth and the Sun as the second central bodies;
- the Earth and Sun are described as single points;
- the Moon body is assumed as a perfect sphere;
- the Earth ephemerides are considered to obtain position, velocity and acceleration during the orbital motion with respect to the Moon;
- the Sun ephemerides are considered to obtain position, velocity and acceleration during the orbital motion with respect to the Moon;

GDOP time-function definition

To generalize for any time t and for any point P_i the satellite visibility from the target points the Boolean functions $\delta_{\alpha i}(t)$ are introduced, with the following meaning:

$$\forall t \in [0,T] \qquad \delta_{\alpha i}(t) = \begin{cases} 1 & \gamma_{\alpha i}(t) \geq \underline{\gamma_\alpha} \\ 0 & otherwise \end{cases} . \tag{3.13}$$

As is gartered, the visibility condition for any satellite with respect to the point is satisfied if there is a minimum elevation angle $\underline{\gamma}$ between the satellite and the local horizon of the point at any time t.
In particular $\underline{\gamma_\alpha}$ is the elevation angle lower bound and $\gamma_{\alpha i}$ is the elevation angle of the satellite with respect to the point surface P_i, at a specific time t.
The following time function is introduced for the selection of all visible satellite α.

$\forall t \in [0,T]$,

$\forall i \in [1,N_P]$

$$\hat{d}_{i\alpha}(t) = \begin{cases} \sqrt{\sigma_{xi}^2(t) + \sigma_{yi}^2(t) + \sigma_{zi}^2(t) + \sigma_{\tau i}^2(t)} & if \quad \sum_{\alpha=1}^{N_s} \delta_{\alpha i}(t) \geq 4 \\ +\infty & otherwise \end{cases} , \tag{3.14}$$

where the term $\sqrt{\sigma_{xi}^2(t) + \sigma_{yi}^2(t) + \sigma_{zi}^2(t) + \sigma_{\tau i}^2(t)}$ is obtained from (3.9), (3.10) and (3.11), for all the visible satellite α.

The following function (3.15) represents the GDOP for any point i at a general time t :

$$d_i(t) = \hat{d}_{i\alpha}(t) . \tag{3.15}$$

Satellite Earth visibility

In order to deal with the request of visibility of at least one satellite from Earth, the following Boolean function is defined:

$$\forall t \in [0,T] \qquad \eta_\alpha(t) = \begin{cases} 1 & \alpha \; is \; visible \; from \; the \; Earth \\ 0 & otherwise \end{cases} . \tag{3.16}$$

The above visibility condition can be expressed in the following way.
At a given time t we consider the segment joining the Earth center O_E with the point corresponding to the position of the satellite $P_\alpha(t)$. To reach the visibility of the satellite α from Earth, the segment previously introduced must not intersect the Moon surface.

$$\forall t \in [0,T], \qquad \overline{O_E P_\alpha(t)} \cap S_M = \emptyset , \tag{3.17}$$

Where S_M is the Moon surface.

Objective function

The following optimization criterion is considered, to represent the minimization of the GDOP:

- $min \sum_i^{N_P} \int_0^T d_i(t) dt$ (3.18)

This corresponds to minimizing the GDOP average over all the grid points in the whole time interval $[0,T]$.

Constraints

- Dynamic system constraints

The reference frame considered is the MC frame as defined in Section 3.1.
With reference to the two-body dynamic model implemented, the equation 3.1 can be expressed as follow:

$$\ddot{\boldsymbol{r}}_{M\alpha}(t) = -\frac{\mu_M}{\|\boldsymbol{r}_{M\alpha}(t)\|^3}\boldsymbol{r}_{M\alpha}(t)\,. \tag{3.19}$$

For the perturbed dynamic model, the equation 3.2 is expressed as follow.
To derive the dynamics equations with respect to the MC reference frame, we have to consider the resulting force vector $\boldsymbol{F}_{M\alpha}(t)$ acting on the satellite α at any time t in the MC reference frame. The primary central body is represented by the Moon while the third bodies are the Earth and the Sun.
After analytical passages the following equation is obtained and used to describe the motion:

$$\ddot{\boldsymbol{r}}_{M\alpha}(t) = -\frac{\mu_M}{\|\boldsymbol{r}_{M\alpha}(t)\|^3}\boldsymbol{r}_{M\alpha}(t) + \frac{\mu_E}{\|\boldsymbol{r}_{M\alpha E}(t)\|^3}\boldsymbol{r}_{M\alpha E}(t) + \frac{\mu_S}{\|\boldsymbol{r}_{M\alpha S}(t)\|^3}\boldsymbol{r}_{M\alpha S}(t) - \frac{\mu_E}{\|\boldsymbol{r}_{ME}(t)\|^3}\boldsymbol{r}_{ME}(t) - \frac{\mu_S}{\|\boldsymbol{r}_{MS}(t)\|^3}\boldsymbol{r}_{MS}(t)\,, \tag{3.20}$$

Where:

$\frac{\mu_M}{\|\boldsymbol{r}_{M\alpha}(t)\|^3}\boldsymbol{r}_{M\alpha}(t)$ is the Moon gravitational force acting on the satellite

$\frac{\mu_E}{\|\boldsymbol{r}_{M\alpha E}(t)\|^3}\boldsymbol{r}_{M\alpha E}(t)$ is the Earth gravitational force acting on the satellite.

$\frac{\mu_S}{\|\boldsymbol{r}_{M\alpha S}(t)\|^3}\boldsymbol{r}_{M\alpha S}(t)$ is the Moon gravitational force acting on the satellite

$\frac{\mu_E}{\|\boldsymbol{r}_{ME}(t)\|^3}\boldsymbol{r}_{ME}(t)$ is the Earth gravitational force acting on the Moon

$\frac{\mu_S}{\|\boldsymbol{r}_{MS}(t)\|^3}\boldsymbol{r}_{MS}(t)$ is the Sun gravitational force acting on the Moon

And μ_M is the gravitational parameter of the Moon, μ_E is the gravitational parameter of the Earth and μ_S is the gravitational parameter of the Sun.
In particular the position vectors are expressed as follow:

$\boldsymbol{r}_{M\alpha E}(t) = \boldsymbol{r}_{ME}(t) - \boldsymbol{r}_{M\alpha M}(t)$,

$\boldsymbol{r}_{M\alpha S}(t) = \boldsymbol{r}_{MS}(t) - \boldsymbol{r}_{M\alpha M}(t)$,

Where

$\ddot{\boldsymbol{r}}_{M\alpha}(t) = [\ddot{x}_{M\alpha}(t), \ddot{y}_{M\alpha}(t), \ddot{z}_{M\alpha}(t)]$ acceleration of satellite α at time t w.r.t. MC;

$\boldsymbol{r}_{M\alpha}(t) = [x_{M\alpha}(t), y_{M\alpha}(t), z_{M\alpha}(t)]$ position of satellite α at time t w.r.t. MC;

$\boldsymbol{r}_{M\alpha E}(t) = [x_{M\alpha E}(t), y_{M\alpha E}(t), z_{M\alpha E}(t)]$ position of satellite α with respect to Earth at time t w.r.t. MC;

$\boldsymbol{r}_{M\alpha S}(t) = [x_{M\alpha S}(t), y_{M\alpha S}(t), z_{M\alpha S}(t)]$ position of satellite α with respect to Sun at time t w.r.t. MC;

$\boldsymbol{r}_{ME}(t) = [x_{ME}(t), y_{ME}(t), z_{ME}(t)]$ position of the Earth with respect to the Moon at time t w.r.t. MC;

$\boldsymbol{r}_{MS}(t) = [x_{ME}(t), y_{ME}(t), z_{ME}(t)]$ position of the Sun with respect to the Moon at time t w.r.t. MC;

- Visibility constraints

With reference to equation (3.11), there must be at least four visible satellite at any time t for every point i, i.e.

$$\forall t \in [0,T] \quad \sum_{\alpha=1}^{N_s} \delta_{\alpha i}(t) \geq 4. \tag{3.21}$$

Concerning the visibility of at least one satellite with respect to the Earth at any time t, the following condition is set:

$$\forall t \in [0,T] \quad \sum_{\alpha=1}^{N_s} \eta_{\alpha}(t) \geq 1. \tag{3.22}$$

Regarding the non-intersection conditions (3.22), the following equation is derived:

$$\forall t \in [0,T], \qquad \overline{O_E P_\alpha(t)} \cap S_M = \emptyset \iff \overline{O_E \boldsymbol{r}_{M\alpha}(t)} \cap S_M = \emptyset \tag{3.23}$$

- Visibility constraints

The constraint on the final satellite altitude is reported. It is necessary that each satellite, at the final instant of analysis, report a minimum perigee altitude. The expression 3.24 represent the constraint:

$$\forall \alpha = 1, \dots, N_s \quad r_{p_\alpha}(t = T) - R_{moon} \geq h_{pmin} \tag{3.24}$$

Where N_s is the total number of satellites, R_{moon} is the Moon radius and h_{min} is the minimum perigee altitude required for each satellite in the final instant of time analysis.

Bounds

The bounds for the variables representing the satellite orbit parameters are reported below:

$$\underline{r_{a_\alpha}} \leq r_{a_\alpha} \leq \overline{r_{a_\alpha}}$$
$$\underline{r_{p_\alpha}} \leq r_{p_\alpha} \leq \overline{r_{p_\alpha}}$$
$$\underline{i}_\alpha \leq i_\alpha \leq \overline{i}_\alpha$$
$$\underline{\omega}_\alpha \leq \omega_\alpha \leq \overline{\omega}_\alpha$$
$$\underline{\Omega}_\alpha \leq \Omega_\alpha \leq \overline{\Omega}_\alpha$$
$$\underline{\nu}_{0\alpha} \leq \nu_{0\alpha} \leq \overline{\nu}_{0\alpha}$$

Where for each satellite α:

- r_{a_α} is the apogee radius of the satellite orbit;
- r_{p_α} is the perigee radius of the satellite orbit;
- i_α is the perigee radius of the satellite orbit;
- ω_α is the perigee argument of the satellite orbit;
- Ω_α is the RAAN of the satellite orbit;
- $\nu_{0\alpha}$is the true anomaly at $t = 0$ of the satellite.

4 Support mathematical concepts

In this chapter some basic mathematical concepts are introduced. The principal characteristics and general concepts are briefly explained herein while in the second Section 4.2 the clustering techniques is explained.

4.1 General optimization methods

This chapter deals with an introduction about the most well-known optimization methods and algorithms applied for various type of problems. Optimization problems form a fundamental category in mathematics, encompassing a wide range of applications across various disciplines. At their core, optimization problems involve finding the best solution from a set of feasible options, with the goal of maximizing or minimizing an objective function, while satisfying certain constraints. These problems are applied in real-world scenarios, appearing in fields such as engineering, physics, computer science, economics, and biology. Optimization problems are typically formulated using mathematical expressions. The objective function represents the quantity to be maximized or minimized, while constraints impose limitations on the feasible solutions. Mathematically, an optimization problem can be expressed as (see e.g., Minoux et al. 1986):

$$\begin{cases} \min J(\boldsymbol{x}) \\ \boldsymbol{g}(\boldsymbol{x}) \leq \boldsymbol{0} \\ \boldsymbol{h}(\boldsymbol{x}) = \boldsymbol{0} \\ \underline{\boldsymbol{X}} \leq \boldsymbol{x} \leq \overline{\boldsymbol{X}} \end{cases} \tag{4.1}$$

With

$$\begin{cases} \quad \boldsymbol{x} \in R^n \\ J: \ R^n \to R \\ \boldsymbol{Q}: \ R^n \to R^m \end{cases} \tag{4.2}$$

Here, $\boldsymbol{x}$ represents the vector of decision variables, $\underline{\boldsymbol{X}}$ and $\overline{\boldsymbol{X}}$ are the upper and lower bounds of the decisions variables, $J(\boldsymbol{x})$ is the objective function and $\boldsymbol{g}(\boldsymbol{x})$ and $\boldsymbol{h}(\boldsymbol{x})$ are the inequalities and equalities functions respectively. In the equation 4.1 the expression $\min J(\boldsymbol{x})$ has the same significance of $\max J(\boldsymbol{x})$.

A feasible solution is represented by the set of values taken by the decision variables $\boldsymbol{x}$ which satisfy all the constraints (equalities and inequalities). The set of feasible solutions in the decision variable space identifies the feasibility domain. A solution method can be categorized as either exact, if it precisely identifies and proves the best feasible solution, or heuristic, if it aims to find a satisfactory solution, though not necessarily optimal. Once a mathematical model is formulated, the challenge lies in identifying its solutions. Mathematical programming encompasses both the theoretical aspects and the solution techniques of mathematical programming models. The complexity of these methods strictly depends on the characteristics and properties of the functions f, g and h.

Optimization techniques act as guiding compass through the various possibilities. In the specific framework of optimal control (see e.g., Bryson 1999), there are several methods to face optimization challenges, ranging from classical approaches, such as direct and indirect methods, to evolutionary algorithms.

- Direct methods: they seek the optimal solution by directly examining the objective function and constraints. Among these methods, a famous one is the method of gradient, which involves iterative adjustments to the solution based on the gradient of the objective function, directing towards steepest descent or ascent. Another notable direct method is the Newton-Raphson method, particularly useful at solving nonlinear optimization problems. It refines the solution iteratively by approximating the objective function with a quadratic model and updating the solution using the

Newton direction. Direct methods are valued for their efficacy in uncovering local optima, especially in smooth, convex problems.

- Indirect methods: in contrast, indirect methods approach optimization problems through mathematical formulations or transformations. These methods typically entail converting the optimization problem into a different mathematical form, such as a system of equations or differential equations, which can then be solved using established techniques. An example of an indirect method is the application on Pontrjagin's principle (see e.g., Bryson 1999). While indirect methods may confer advantages in certain scenarios, they can also introduce complexities and computational overhead.
- Evolutionary algorithms: evolutionary algorithms draw inspiration from the principles of natural selection and evolution to address optimization problems. These algorithms maintain a population of candidate solutions, subjecting them to selection, crossover, and mutation operators to iteratively generate new solutions. Across successive generations, the population evolves towards solutions based on their fitness, eventually converging to optimal or near-optimal solutions. Among the most renowned evolutionary algorithms is the genetic algorithm (GA), which mimics natural selection by evolving a population of individuals encoded as chromosomes. Each individual represents a potential solution, and genetic operators like crossover and mutation are applied to produce offspring with potentially traits. GAs are good for complex navigation and prove particularly effective for problems characterized by nonlinearity, discontinuity, or high dimensionality.

Additionally, a diverse array of optimization methods exists, each tailored to address various problem structures, objectives, and constraints. The chosen methods can significantly influence the efficiency and effectiveness of the solution process.

4.1.1 Black-box approach

The back-box approach (see e.g., Alarie 2021) deals with a problem where the analytical expressions of the functions involved is partially or totally not known a priori. The control variables in the black-box approach are the input variables from which the output functions can be calculated.

Formulation of the black box approach: the optimization problem is viewed solely from the standpoint of input and output. The emphasis lies in understanding how inputs (variables, constraints, etc.) correspond to outputs (objective function values, feasible solutions, etc.) without delving into the internal complexities of the problem. The input variables $\boldsymbol{x}$ must be contained within the given upper and lower bounds, as expressed below:

$$\begin{cases} \boldsymbol{y} = f(\boldsymbol{x}) \\ \underline{\boldsymbol{X}} \leq \boldsymbol{x} \leq \overline{\boldsymbol{X}} \end{cases}. \tag{4.4}$$

The cost function and the constraint functions are calculated starting from the output vector and the decisions variables, i.e.,

$$\begin{cases} J(\boldsymbol{x}, \boldsymbol{y}) \\ \boldsymbol{Q}(\boldsymbol{x}, \boldsymbol{y}) \end{cases}. \tag{4.5}$$

The focus lies on efficiently exploring the solution space using optimization techniques like algorithms, heuristics, or machine learning methods. This involves iterative interaction, where initial guesses refine subsequent inputs until satisfactory solutions or convergence criteria are met.

Black-box optimization methods provide a powerful approach to address challenging problems even without a comprehensive knowledge of the system involved. As technology advances, these methods will continue evolving, unlocking new optimization possibilities across various domains.

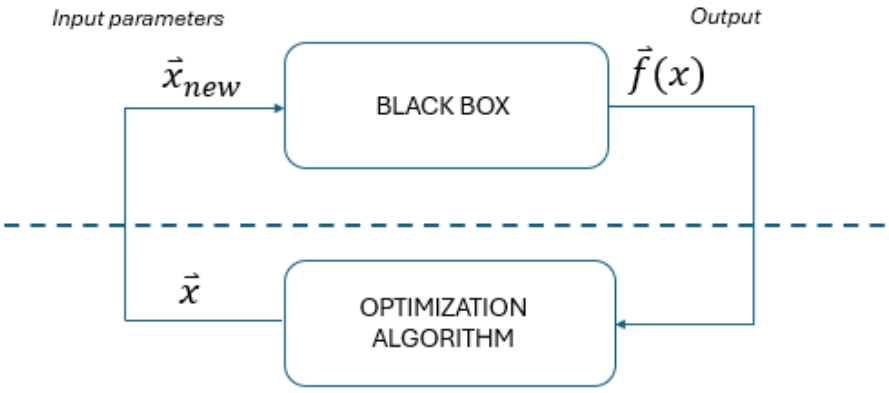

Figure 4.1: Black-box schematic representation

4.1.2 Sequential quadratic programming

Sequential quadratic programming (SQP) is an optimization method widely used for solving nonlinear optimization problems, particularly those with constraints (see e.g., Fletcher 2010). It belongs to the class of iterative algorithms, where at each iteration, it solves a quadratic subproblem approximating the original nonlinear one. SQP iteratively refines the solution by updating the decision variables towards the optimum, subject to constraints, until convergence is achieved. The general steps of the SQP algorithm are as follows:

1. Initialization: choose an initial feasible solution and set iteration counter k = 0.
2. Quadratic programming sub-problem: at iteration k, construct a quadratic approximation of the objective function and constraints around the current point.
3. Solve quadratic sub-problem: solve the quadratic sub-problem to obtain a search direction, typically using methods like interior-point or active-set.
4. Line search: perform a line search to determine the step size along the search direction that minimizes the objective function while satisfying the constraints.
5. Update: update the decision variables using the step size obtained from the line search.
6. Convergence check: check for convergence criteria. If satisfied, stop; otherwise, increment k and go to step 2.

SQP converges to a local minimum when the search direction becomes small enough, or when the change in the objective function and constraints is sufficiently small between iterations. Convergence criteria typically check the optimality conditions, such as the Karush-Kuhn-Tucker (KKT) conditions.

SQP offers efficiency and local convergence for solving a wide number of nonlinear optimization problems with constraints. However, its convergence can be sensitive to the initial guess and computational cost of using derivatives, requiring specific strategies to achieve robust and efficient convergence. Moreover, it may converge to local optima, particularly for ill-conditioned problems or highly nonlinear constraints / objective functions. All in all, despite these limitations, SQP flexibility and derivative-based approach make it a versatile tool.

4.1.3 Genetic algorithms

Genetic Algorithms (GA) are stochastic search algorithms inspired by the principles of natural selection. Their functioning is based on the principles of Darwinian evolution and genetics. Developed by John Holland in the 1970s, genetic algorithms have become a popular method for finding solutions to complex optimization

problems. They are particularly useful for problems with a large search space, non-linearity. By iteratively evolving a population of candidate solutions, genetic algorithms efficiently explore and exploit the search space to find near-optimal solutions.

They maintain a population of individuals, each representing a potential solution to the optimization problem. These individuals are represented as strings of symbols, often referred to as chromosomes or genotypes and the evolution process involves selection, crossover, and mutation, miming the genetic recombination, and mutation processes. The main components of genetic algorithms include:

- Representation: encoding of candidate solutions as chromosomes.
- Initialization: generating an initial population of individuals.
- Selection: choosing individuals from the population for reproduction based on their fitness.
- Crossover: creating new individuals by combining genetic material from selected parents.
- Mutation: introducing random changes to individuals to maintain diversity.
- Fitness evaluation: assessing the quality of individuals based on their performance on the optimization problem.
- Termination criteria: determining when to stop the evolution process, typically based on the number of generations or a given satisfactory criterion.

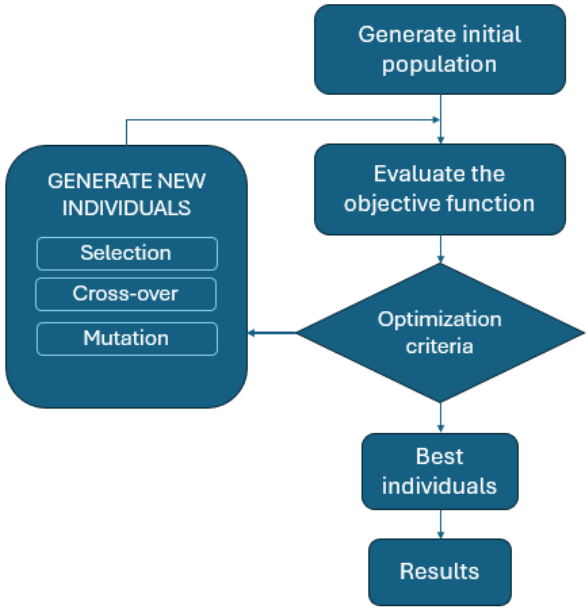

Figure 4.2: genetic algorithm flow chart

The implementation of these components depends on the characteristics of the optimization problem, such as its structure, constraints, and objective(s). Additionally, parameter tuning, and control strategies are crucial for optimizing the performance of genetic algorithms. Genetic algorithms find applications in various fields, including engineering design, scheduling, machine learning, and robotics.

4.2 Clustering

The main goal of clustering is to partition large amount of data into groups, or clusters, where data within the same cluster is more similar than data in other clusters (see Fig 4.3). Clustering is widely used in various fields due to its ability to uncover hidden patterns and structures within data. Various types of clustering algorithms are available. The most popular one is K-means (see e.g., Lloyd 1982), which divides the given

data into K clusters and each element (of the data set) belongs to exactly one cluster. The main steps of K-means are here reported:

- Initialization: the algorithm starts by randomly initializing K cluster centroids. Each centroid represents the “center of mass” of the corresponding cluster.
- Assignment: each element is assigned to the nearest centroid based on some distance metric, typically Euclidean distance.
- Update centroids: after all elements have been assigned to clusters, the centroids are updated by computing the mean of all elements assigned to each cluster.
- Repeat: steps 2 and 3 are repeated iteratively until the centroids no longer change significantly or a specified number of iterations is reached.

The goal of the K-means algorithm is to minimize the within-cluster variance, which is achieved by optimizing the placement of the centroids. Given a set of observations $(x_1, x_2, \dots, x_n)$ where each observation is a d-dimensional real vector, K-means clustering aims to partition the n observations into $\mathrm{k}\ (\leq \mathrm{n})$ sets $\mathrm{S} = \{\mathrm{S}_1, \mathrm{S}_2, \dots, \mathrm{S}_\mathrm{k}\}$ so as to minimize the within-cluster sum of squares (WCSS) (i.e. variance). Formally, the objective is to find:

$$\arg\min_{S} \sum_{i=1}^{k} \sum_{x \in S_i} \|x - \mu_i\|^2,$$

Where μ_i is the mean (also called centroid) of points in S_i, i.e.

$$\mu_i = \frac{1}{|S_i|} \sum_{x \in S_i} x,$$

Where $|S_i|$ is the size of S_i.

Clustering is a versatile and widely used technique with applications across various domains, providing insights into data structures, patterns, and relationships. It finds application a wide variety of scientific and industrial fields.

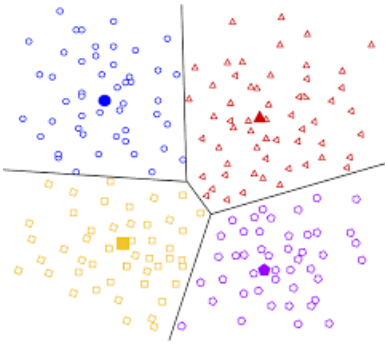

Figure 4.3: clustering example representation

4.3 Path-relinking technique

The path-relinking technique represents a process to generate new sets of reference solutions, creating paths between and beyond known solutions. In fact, a path between solutions in a neighborhood space will generally yield new solutions that share a significant subset of attributes contained in the parent solutions. The generation of such paths in the neighborhood space characteristically "relinks" previous points in ways not achieved in the previous search history, hence giving the approach its name (see Fig 4.4). The creation of paths, joining two selected solutions x' and x" and producing a solution sequence, can first be considered:

$$x' = x(1), x(2), \dots, x(r) = x" \ .$$

To reduce the number of solutions to be considered, the solution $x(i+1)$ may be created from $x(i)$ at each step by choosing the direction that leaves a reduced number of steps remaining to reach x (the "fewest" number of moves). This policy, even if applied without exception, can permit a significant number of alternative choices for generating the next solution at each step. Consequently, additional criteria are relevant to creating the path, as indicated in Figure 4.4 below.

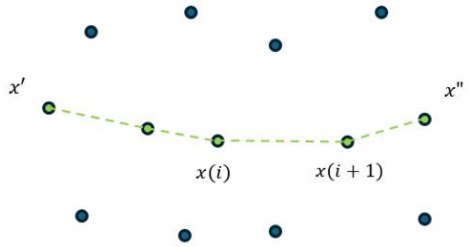

Figure 4.4: path-relinking approach

4.4 Multi-objective optimization

This section deals with the fundamentals of multi-objective optimization (MOO) and its application to optimal control, focusing on the concept of the Pareto front. In the context of optimal control, the problems often present conflicting objectives such as minimizing costs, maximizing performances, and meeting constraints. Unlike a single-objective optimization, where a single optimal solution has to be reached, MOO aims to find a set of solutions, known as the Pareto optimal set. An MOO can be formulated as:

$$min(f_1(x), f_2(x), \dots, f_k(x)) ,$$

where the integer k is the number of objectives to be minimized (or maximized) and the x is the set of decision variables. The decision variables are typically subject to constraint functions. The pareto optimal set consists of solutions where no objective can be improved without worsening at least one other objective. This way, they represent the trade-offs between objectives. A solution is called nondominated, if none of the objective functions can be improved in value without degrading some of the other objective values. In optimal control problems, the Pareto front illustrates the compromise between different control strategies that optimize various objectives simultaneously as represented in Figure 4.5 (MOO minimization problem).

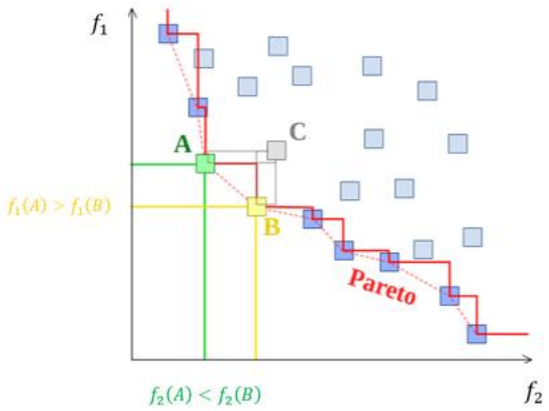

Figure 4.5: Pareto-front representation

Without additional objectives or constraints, there may exist a potentially infinite number of Pareto optimal solutions, all of which are considered equally good. The goal may be to find a representative set of Pareto optimal solutions. Formulating a multi-objective optimal control problem consists in defining the objectives, constraints, and system dynamics explicitly. Various techniques exist for solving MOO problems, ranging from evolutionary algorithms to mathematical programming and direct methods. Evolutionary algorithms like genetic algorithms and particle swarm optimization are well-suited for MOO.

5 Experimental analysis

In the following chapter all the experimental analysis made with the algorithms and methods are reported. The chapter is divided into separate sections to show the results obtained with different dynamic models, total number of satellites and control variables, in addition with different approaches and algorithms to improve the solutions. This chapter discusses solutions that are satisfactory from an engineering perspective. Some solutions may be considered worthwhile in this regard, even if they are not globally optimal. It should be noted that the optimality of the solutions found has not been proven. From a rigorous standpoint, all solutions found should be considered suboptimal. All the optimization analysis are performed in Matlab environment (see e.g., MathWorks 2022), while the results are verified in System Tool-kit (STK) environment (see e.g., STK 2024). The section 5.1 deals with the basic assumptions of the mathematical model used for the optimization, the section 5.2 reports the solution obtained from the genetic algorithm, the section 5.3 represents the solutions obtained through the SQP algorithm and the section 5.4 the improvements made with the clustering methods. The section 5.5 reports the solutions obtained through the Path-linking techniques. Finally, the section 5.6 reports an analysis on some relevant solutions about the influence of the orbital perturbation.

5.1 Basic assumptions

Target area

The mathematical model used in the optimization is defined by constant and defined characteristics that allow the results to be compared at the end of the experimental analysis. The geographical coordinates of the points to be observed on the lunar surface and that define the target reference area are defined and kept constant throughout the analysis.

Minimum latitude	-90°
Maximum latitude	-75°
Minimum longitude	0°
Maximum longitude	360°
Number of points	20

Table 5.1: target area coordinates

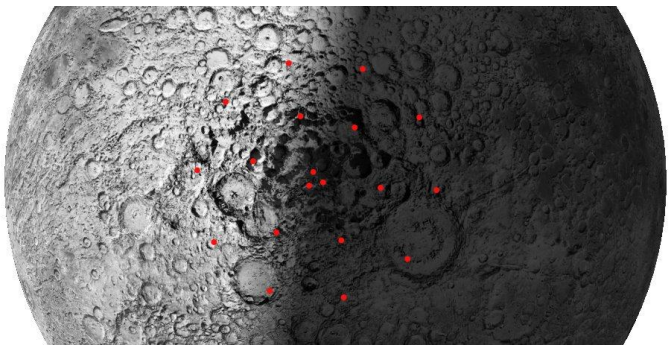

Figure 5.1: target area representation (STK)

Orbit propagation

In the Matlab environment, the orbit propagation and position of target points are calculated for a total time similar to the period of the Moon's revolution around the Earth. The initial time is defined as $t = 0$ while the final time is defined as $t = T$, where $T = 28\ days$. The total time T is divided in subintervals of

10 minutes each, to calculate satellite positions, target point positions and GDOP values. For the results verified in the STK environment, the orbit propagation considers the perturbation effects due to the Earth gravity force and the Sun gravity force, for a total time similar to the period of the Moon's revolution around the Earth. The initial time is defined as $t = 0$ while the final time is defined as $t = T$, where $T = 28\ days$. The total time T is divided in subintervals of 1 minutes each, to calculate satellite positions, target point positions and GDOP values.

Visibility constraint

The visibility constraint is defined with a minimum elevation angle between the surface point and the satellite position (see expression 3.13):

$$\gamma = 5°$$

Variable bounds

The variables bounds are defined as follows:

	[km]	[km]	[deg]	[deg]	[deg]	[deg]
	r_a	r_p	i	Ω	ω	ν
Lower bound	2000	2000	0	0	0	0
Upper bound	15000	15000	180	360	360	360

Table 5.2: variable upper and lower bounds

Where:

- r_a is the orbit apogee radius;
- r_p is the orbit perigee radius;
- i is the orbit inclination;
- Ω is the orbit right ascension of the ascending node;
- ω is the perigee argument;
- ν is the satellite true anomaly at $t = 0$;

GDOP values interpretation

The results obtained report the GDOP values calculated from the satellite and the grid point positions, over the time considered. The Table 5.3 helps us to understand better the GDOP value and its significance:

GDOP value	Rating	Description
<1	Ideal	Highest precision level.
1–2	Excellent	Confidence precision level, positional measurements are considered accurate.
2–5	Good	This level represents the minimum appropriate for accurate measurements.
5–10	Moderate	The quality of positional measurements could be improved.
10–20	Fair	Low confidence level, positional measurement represents an estimate.

>20	Poor	Not sufficient accurate level, measurements should be discarded.

Table 5.3: GDOP values indicators

The results obtained report the following information, e.g. the two objectives to be minimized:

- Mean GDOP: it represents the mean GDOP value over the total time and for each of the 20 target points considered. It is valuated considering all the GDOP values, in particular when the GDOP is greater than 20 is it forcedly set to 20;
- Peak time %: it represents the mean percentage of time for each point with GDOP values greater than 20.

5.2 Global approach from scratch

The following solutions are obtained by the genetic algorithm which is part of the Global Optimization Toolbox of Matlab. In the following cases the initial population is not initialized therefor the algorithm selects by itself the individuals inside the variable bounds, from which starts the process. The implemented mathematical model is defined with the two-body dynamics to calculate the satellite state vector during the orbital motion. The total number of satellites is defined, and, in each case, different variables are selected for the process. In case the results are too different between the Matlab two-body propagation and the STK perturbation analysis, a second optimization process is performed, based on a mathematical model involving the orbital perturbations.

The following case G1, G2, G3, G4 represents a scenario with eight satellites. Each satellite is defined by its six variables (48 total variables): apogee radius r_a, perigee radius r_p, inclination i, right ascension of the ascending node Ω, argument of perigee ω and the true anomaly ν. In each case are reported the variables defined for the optimization process while, if not specified, all the satellite variables are involved. If not specified, the mathematical model used for the optimization is represented by the two-body dynamics.

5.2.1 Case G1

The optimal results of case G1 are reported in Table 5.5, while in Table 5.4 are reported the orbital parameters of each satellite. In Figure 5.2 the optimal solution is represented.

	[km]	[km]	[deg]	[deg]	[deg]	[deg]
	r_a	r_p	i	Ω	ω	ν
S_1	13348.2	2943.2	147.4	246.9	93.2	219.1
S_2	13585.8	2594.0	148.3	247.8	115.7	358.2
S_3	14996.1	2525.6	152.0	126.4	99.9	131.3
S_4	13289.8	5177.1	87.1	267.5	108.8	133.7
S_5	14702.7	2797.5	35.9	171.3	103.9	176.3
S_6	14827.3	2738.6	34.9	221.3	94.5	247.1
S_7	14166.8	2248.9	94.1	219.1	86.5	153.1
S_8	14919.1	3554.9	97.8	149.3	87.8	232.8

Table 5.4: case G1 orbital parameters

	Mean GDOP		Peak time %	
	MATLAB	STK	MATLAB	STK
Optimal solution	2.53	2.65	0.19 %	0.37 %

Table 5.5: case G1 GDOP values

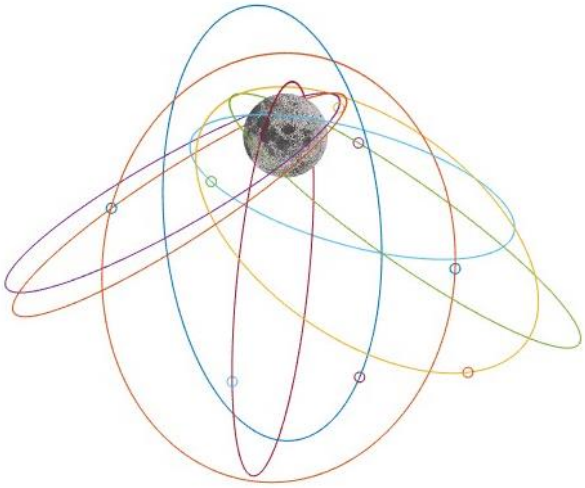

Figure 5.2: case G1 optimal solution

Case G1 represents a scenario with an orbital plane for each satellite involved. Although the architecture is complex, the optimization algorithm has reached a good solution with a low mean GDOP value and mean peak time percentage. Although the solution is not the global optimum (see case G3 and case G14), it is still considered worthwhile thanks to the extensive use of all degrees of freedom.

5.2.2 Case G2

The optimal results of case G2 are reported in Table 5.8, while in Table 5.7 are reported the orbital parameters of each satellite. In Figure 5.3 the optimal solution is represented. The optimization variables selected are reported in Table 5.6: there are eight satellites and two orbital planes. It is reasonable to consider solutions with a reduced number of orbital planes as they are considered more advantageous for reasons of satellite deployment or constellation operability. The satellites S_1, S_2, S_3 and S_4 belong to the first plane so the variables are the plane orbital parameters (apogee radius r_{a1}, the perigee radius r_{p1}, the inclination i_1, the RAAN Ω_1 and the perigee argument ω_1) and the true anomaly of each satellite at $t = 0$. The satellites S_5, S_6, S_7 and S_8 belong to the second plane so the variables are the plane orbital parameters (r_{a2}, r_{p2}, i_2, Ω_2 and ω_2) and the true anomaly of each satellite at $t = 0$.

S_1	S_2	S_3	S_4	S_5	S_6	S_7	S_8
r_{a1}				r_{a2}			
r_{p1}				r_{p2}			
i_1				i_2			
Ω_1				Ω_2			
ω_1				ω_2			
ν_1	ν_2	ν_3	ν_4	ν_5	ν_6	ν_7	ν_8

Table 5.6: case G2 optimization variables

	[km]	[km]	[deg]	[deg]	[deg]	[deg]
	r_a	r_p	i	Ω	ω	ν
S_1	12810.9	2436.8	77.3	259.3	136.9	171.3
S_2	12810.9	2436.8	77.3	259.3	136.9	90.0
S_3	12810.9	2436.8	77.3	259.3	136.9	196.5
S_4	12810.9	2436.8	77.3	259.3	136.9	204.4
S_5	9558.8	2087.3	123.1	340.6	86.8	140.3
S_6	9558.8	2087.3	123.1	340.6	86.8	201.9
S_7	9558.8	2087.3	123.1	340.6	86.8	166.8
S_8	9558.8	2087.3	123.1	340.6	86.8	343.3

Table 5.7: case G2 orbital parameters

	Mean GDOP		Peak time %	
	MATLAB	STK	MATLAB	STK
Optimal solution	3.57	3.66	0.03 %	0.04 %

Table 5.8: case G2 GDOP values

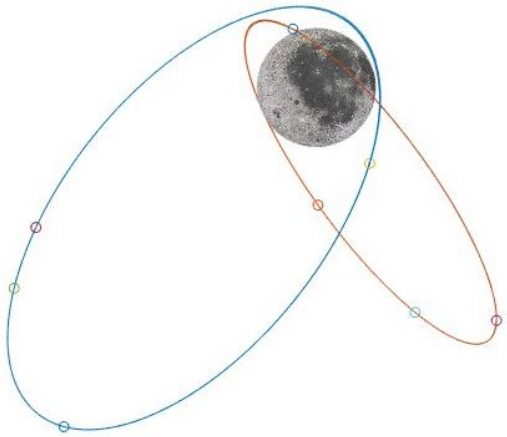

Figure 5.3: case G2 optimal solution

The optimal solution obtained from case G2 represents a scenario with eight satellites and a reduced number of orbital planes. There are fewer variables involved in the optimization process compared to case G1, so the average GDOP value is good, but worse than the results reported in Table 5.5 relative to case G1.

5.2.3 Case G3

The optimal results of case G3 are reported in Table 5.11, while in Table 5.10 are reported the orbital parameters of each satellite. In Figure 5.4 the optimal solution is represented. The optimization variables selected are reported in Table 5.9: there are eight satellites and three orbital planes. The aim is to find a

satellite arrangement with a reduced number of total orbital planes as indicated for case G2. The satellites S_1, S_2, S_3 belong to the first plane so the variables are the plane orbital parameters (apogee radius r_{a1}, the perigee radius r_{p1}, the inclination i_1, the RAAN Ω_1 and the perigee argument ω_1) and the true anomaly of each satellite at $t = 0$. The satellites S_4, S_5 and S_6 belong to the second plane so the variables are the plane orbital parameters (r_{a2}, r_{p2}, i_2, Ω_2 and ω_2) and the true anomaly of each satellite at $t = 0$. The satellites S_7 and S_8 belong to the third plane so the variables are the plane orbital parameters (r_{a3}, r_{p3}, i_3, Ω_3 and ω_3) and the true anomaly of each satellite at $t = 0$.

S_1	S_2	S_3	S_4	S_5	S_6	S_7	S_8
r_{a1}			r_{a2}			r_{a3}	
r_{p1}			r_{p2}			r_{p3}	
i_1			i_2			i_3	
Ω_1			Ω_2			Ω_3	
ω_1			ω_2			ω_3	
ν_1	ν_2	ν_3	ν_4	ν_5	ν_6	ν_7	ν_8

Table 5.9: case G3 optimization variables

	[km]	[km]	[deg]	[deg]	[deg]	[deg]
	r_a	r_p	i	Ω	ω	ν
S_1	14893.8	2634.6	91.1	156.6	93.7	137.3
S_2	14893.8	2634.6	91.1	156.6	93.7	184.6
S_3	14893.8	2634.6	91.1	156.6	93.7	258.9
S_4	13158.5	3798.6	45.6	163.7	99.6	193.6
S_5	13158.5	3798.6	45.6	163.7	99.6	147.7
S_6	13158.5	3798.6	45.6	163.7	99.6	344.6
S_7	14429.7	2548.6	150.1	146.7	70.3	177.2
S_8	14429.7	2548.6	150.1	146.7	70.3	253.2

Table 5.10: case G3 orbital parameters

	Mean GDOP		Peak time %	
	MATLAB	STK	MATLAB	STK
Optimal solution	2.50	2.50	0 %	0 %

Table 5.11: case G3 orbital parameters

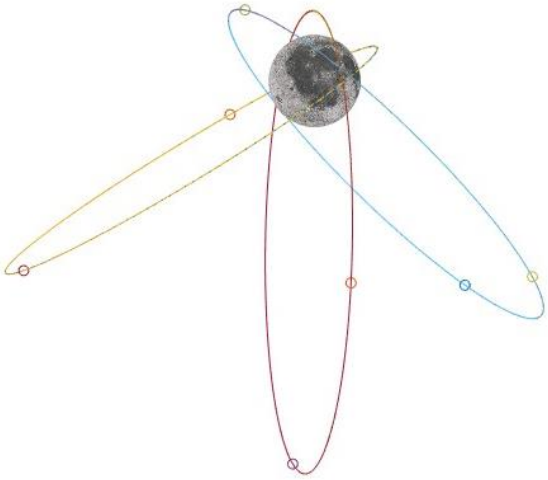

Figure 5.4: case G3 optimal solution

The solution obtained in case G3, as shown in Table 5.11, is a better solution with respect to cases G1 and G2, as can be seen from the mean GDOP and mean peak time percentage values. The architecture involves three orbital planes. Recall that the algorithm adopted, been metaheuristic, cannot prove the optimality of the solution found.

5.2.4 Case G4

The optimal results of case G4 are reported in Table 5.14, while in Table 5.13 are reported the orbital parameters of each satellite. In Figure 5.5 the optimal solution is represented. The optimization variables selected are reported in Table 5.12: there are eight satellites and four orbital planes. As explained for cases G2 and G3 the aim is to find a solution with a limited number of orbital planes. The satellites S_1 and S_2 belong to the first plane so the variables are the plane orbital parameters (apogee radius r_{a1}, the perigee radius r_{p1}, the inclination i_1, the RAAN Ω_1 and the perigee argument ω_1) and the true anomaly of each satellite at $t = 0$. The satellites S_3 and S_4 belong to the second plane so the variables are the plane orbital parameters (r_{a2}, r_{p2}, i_2, Ω_2 and ω_2) and the true anomaly of each satellite at $t = 0$. The satellites S_5 and S_6 belong to the third plane so the variables are the plane orbital parameters (r_{a3}, r_{p3}, i_3, Ω_3 and ω_3) and the true anomaly of each satellite at $t = 0$. The satellites S_7 and S_8 belong to the fourth plane so the variables are the plane orbital parameters (r_{a4}, r_{p4}, i_4, Ω_4 and ω_4) and the true anomaly of each satellite at $t = 0$.

S_1	S_2	S_3	S_4	S_5	S_6	S_7	S_8
r_{a1}		r_{a2}		r_{a3}		r_{a4}	
r_{p1}		r_{p2}		r_{p3}		r_{p4}	
i_1		i_2		i_3		i_4	
Ω_1		Ω_2		Ω_3		Ω_4	
ω_1		ω_2		ω_3		ω_4	
ν_1	ν_2	ν_3	ν_4	ν_5	ν_6	ν_7	ν_8

Table 5.12: case G4 optimization variables

	[km]	[km]	[deg]	[deg]	[deg]	[deg]
	r_a	r_p	i	Ω	ω	ν
S_1	14933.0	2336.6	94.5	137.02	94.4	245.9
S_2	14933.0	2336.6	94.5	137.02	94.4	173.9
S_3	14979.2	2246.2	33.3	278.2	120.9	178.6
S_4	14979.2	2246.2	33.3	278.2	120.9	308.0
S_5	14352.7	13632.2	69.8	303.9	192.5	289.8
S_6	14352.7	13632.2	69.8	303.9	192.5	110.1
S_7	14402.3	3180.7	44.8	108.3	108.8	157.9
S_8	14402.3	3180.7	44.8	108.3	108.8	222.6

Table 5.13: case G4 orbital parameters

	Mean GDOP		Peak time %	
	MATLAB	STK	MATLAB	STK
Optimal solution	2.75	3.28	0.22 %	1.37 %

Table 5.14: case G4 GDOP values

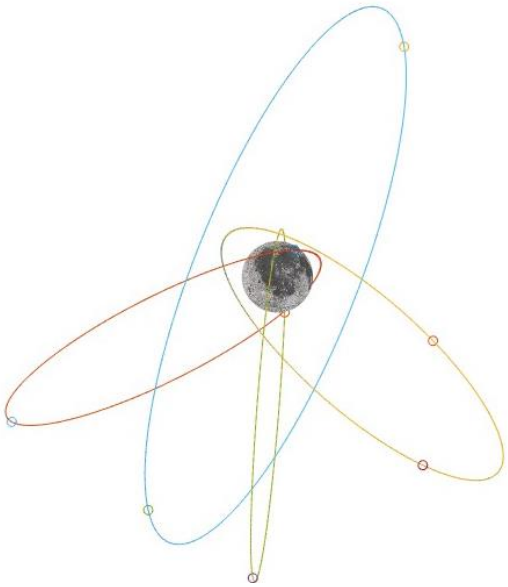

Figure 5.5: case G4 optimal solution

The solution obtained in case G4, as shown in Table 5.14, shows a more obvious difference between the Matlab and STK results, mainly due to the fact that the orbits are more modified under the dynamic perturbations. It could be useful to repeat the optimization with a perturbed dynamic mathematical model or to include different parameters in the optimization functions.

The following cases G5, G6 G7 represents a scenario with seven satellites. The total number of satellites is reduced in order to consider architectures with less complexity and a lower cost. Each satellite is defined by its six variables (42 total variables): apogee radius r_a, perigee radius r_p, inclination i, right ascension of the ascending node Ω, argument of perigee ω and the true anomaly ν. In each case are reported the variables defined for the optimization process while, if not specified, all the satellite variables are involved. If not specified, the mathematical model used for the optimization is represented by the two-body dynamics. The cases G6 and G7 report a limited number of orbital planes in order to reduce the complexity of the architectures, and to improve satellite operability.

5.2.5 Case G5

The case G5 presents a scenario with seven satellites and seven orbital planes. The mathematical model is described by the perturbed dynamics and the additional constraints on the final satellite perigee altitude (see expression 3.24) with $h_{pmin} = 100\ km$. The optimal results of case G5 are reported in Table 5.15, while in Table 5.16 are reported the orbital parameters of each satellite. In Figure 5.6 the optimal solution is represented.

	[km]	[km]	[deg]	[deg]	[deg]	[deg]
	r_a	r_p	i	Ω	ω	ν
S_1	12036.4	2477.8	42.8	259.0	92.9	269.7
S_2	14429.7	4765.7	87.38	38.9	88.8	144.3
S_3	14886.9	2329.1	40.88	163.8	88.1	23.1
S_4	12438.5	2086.9	141.08	172.5	84.4	199.3
S_5	10743.0	3693.7	142.08	254.4	90.3	79.1
S_6	14312.3	2672.3	96.78	290.6	78.6	221.4
S_7	14843.5	4584.8	85.9	356.9	102.5	73.4

Table 5.15: case G5 orbital parameters

	Mean GDOP		Peak time %	
	MATLAB	STK	MATLAB	STK
Optimal solution	4.70	4.70	5.1 %	5.1 %

Table 5.16: case G5 GDOP values

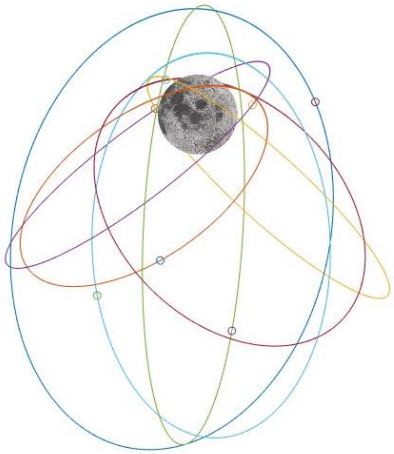

Figure 5.6: case G5 optimal solution

The solution obtained and reported in Table 5.16 solution satisfies the constraint on the final perigee altitude for each satellite but doesn't report good values of mean GDOP and mean peak time percentage values. The solution could be improved by increasing the computational effort. Although the solution is not the global optimum (see case G7 and case G15), it is still considered worthwhile thanks to the extensive use of all degrees of freedom.

5.2.6 Case G6

The case G6 presents a scenario with seven satellites and two orbital planes. The mathematical model is described by the perturbed dynamics and the additional constraints on the final satellite altitude (see expression 3.24). The optimal results of case G6 are reported in Table 5.19, while in Table 5.18 are reported the orbital parameters of each satellite. In Figure 5.7 the optimal solution is represented. The optimization variables selected are reported in Table 5.17.

S_1	S_2	S_3	S_4	S_5	S_6	S_7
r_{a1}				r_{a2}		
r_{p1}				r_{p2}		
i_1				i_2		
Ω_1				Ω_2		
ω_1				ω_2		
ν_1	ν_2	ν_3	ν_4	ν_5	ν_6	ν_7

Table 5.17: case G6 optimization variables

	[km]	[km]	[deg]	[deg]	[deg]	[deg]
	r_a	r_p	i	Ω	ω	ν
S_1	13185.4	5521.3	117.3	45.2	73.9	218.2
S_2	13185.4	5521.3	117.3	45.2	73.9	301.4
S_3	13185.4	5521.3	117.3	45.2	73.9	159.8
S_4	13185.4	5521.3	117.3	45.2	73.9	126.5
S_5	13368	3900.7	93.4	175.5	62.7	203.4
S_6	13368	3900.7	93.4	175.5	62.7	351.9

S_7	13368	3900.7	93.4	175.5	62.7	160.0

Table 5.18: case G6 orbital parameters

	Mean GDOP		Peak time %	
	MATLAB	STK	MATLAB	STK
Optimal solution	4.4	4.4	1.2 %	1.2 %

Table 5.19: case G6 GDOP values

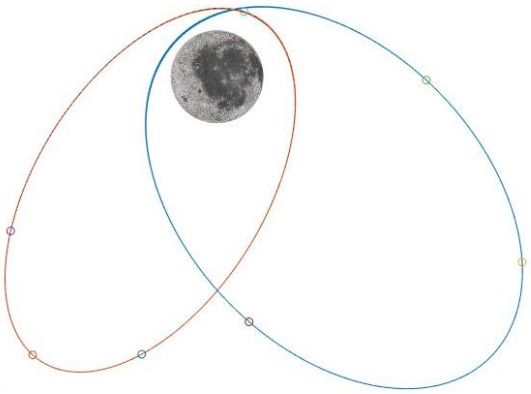

Figure 5.7: case G6 optimal solution

The solution obtained and reported in Table 5.19 satisfies the constraints on the final perigee altitude for each satellite and presents the mean GDOP value satisfying and the peak time percentage to be improved. The advantage is represented by the reduction of the orbital planes involved in the architecture.

5.2.7 Case G7

The optimal results of case G7 are reported in Table 5.22, while in Table 5.21 are reported the orbital parameters of each satellite. In Figure 5.8 the optimal solution is represented. The optimization variables selected are reported in Table 5.20: there are seven satellites and three orbital planes. The satellites S_1 and S_2 belong to the first plane so the variables are the plane orbital parameters (apogee radius r_{a1}, the perigee radius r_{p1}, the inclination i_1, the RAAN Ω_1 and the perigee argument ω_1) and the true anomaly of each satellite at $t = 0$. The satellites S_3 and S_4 belong to the second plane so the variables are the plane orbital parameters (r_{a2}, r_{p2}, i_2, Ω_2 and ω_2) and the true anomaly of each satellite at $t = 0$. The satellites S_5, S_6 and S_7 belong to the third plane so the variables are the plane orbital parameters (r_{a3}, r_{p3}, i_3, Ω_3 and ω_3) and the true anomaly of each satellite at $t = 0$.

S_1	S_2	S_3	S_4	S_5	S_6	S_7
r_{a1}		r_{a2}		r_{a3}		
r_{p1}		r_{p2}		r_{p3}		
i_1		i_2		i_3		
Ω_1		Ω_2		Ω_3		
ω_1		ω_2		ω_3		
ν_1	ν_2	ν_3	ν_4	ν_5	ν_6	ν_7

Table 5.20: case G7 optimization variables

	[km]	[km]	[deg]	[deg]	[deg]	[deg]
	r_a	r_p	i	Ω	ω	ν
S_1	14173.8	2585.7	37.5	335.4	69.4	187.3
S_2	14173.8	2585.7	37.5	335.4	69.4	358.7
S_3	11482.0	2101.7	144.6	316.9	93.0	237.5
S_4	11482.0	2101.7	144.6	316.9	93.0	171.4
S_5	11256.6	2461.2	97.7	305.9	95.8	135.4
S_6	11256.6	2461.2	97.7	305.9	95.8	173.7
S_7	11256.6	2461.2	97.7	305.9	95.8	213.7

Table 5.21: case G7 orbital parameters

	Mean GDOP		Peak time %	
	MATLAB	STK	MATLAB	STK
Optimal solution	2.27	2.80	0 %	0.16 %

Table 5.22: case G7 GDOP values

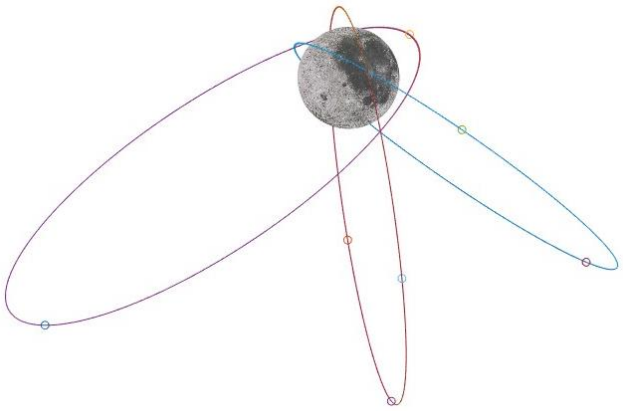

Figure 5.8: case G7 optimal solution

The solution obtained in case G7, as shown in Table 5.22, is a better solution with respect to cases G5 and G6, as can be seen from the mean GDOP and mean peak time percentage values. The architecture involves

three orbital planes. Recall that the algorithm adopted, been metaheuristic, cannot prove the optimality of the solution found.

5.2.8 Case G8

The optimal results of case G8 are reported in Table 5.25, while in Table 5.24 are reported the orbital parameters of each satellite. In Figure 5.9 the optimal solution is represented. The optimization variables selected are reported in Table 5.23: there are seven satellites and four orbital planes. The satellites S_1 and S_2 belong to the first plane so the variables are the plane orbital parameters (apogee radius r_{a1}, the perigee radius r_{p1}, the inclination i_1, the RAAN Ω_1 and the perigee argument ω_1) and the true anomaly of each satellite at $t = 0$. The satellites S_3 and S_4 belong to the second plane so the variables are the plane orbital parameters (r_{a2}, r_{p2}, i_2, Ω_2 and ω_2) and the true anomaly of each satellite at $t = 0$. The satellites S_5 and S_6 belong to the third plane so the variables are the plane orbital parameters (r_{a3}, r_{p3}, i_3, Ω_3 and ω_3) and the true anomaly of each satellite at $t = 0$. The satellites S_7 belongs to the fourth plane so the variables are the plane orbital parameters (r_{a4}, r_{p4}, i_4, Ω_4 and ω_4) and the true anomaly of each satellite at $t = 0$.

S_1	S_2	S_3	S_4	S_5	S_6	S_7
r_{a1}		r_{a2}		r_{a3}		r_{a4}
r_{p1}		r_{p2}		r_{p3}		r_{p4}
i_1		i_2		i_3		i_4
Ω_1		Ω_2		Ω_3		Ω_4
ω_1		ω_2		ω_3		ω_4
ν_1	ν_2	ν_3	ν_4	ν_5	ν_6	ν_7

Table 5.23: case G8 optimization variables

	[km]	[km]	[deg]	[deg]	[deg]	[deg]
	r_a	r_p	i	Ω	ω	ν
S_1	9909.1	2407.9	40.4	315.0	107.8	174.9
S_2	9909.1	2407.9	40.4	315.0	107.8	314.2
S_3	14600.0	2574.6	38.9	131.1	114.2	220.3
S_4	14600.0	2574.6	38.9	131.1	114.2	167.7
S_5	14878.9	2359.4	97.6	133.1	104.6	206.9
S_6	14878.9	2359.4	97.6	133.1	104.6	159.2
S_7	12415.8	2027.1	90.5	327.9	118.4	26.2

Table 5.24: case G8 orbital parameters

	Mean GDOP		Peak time %	
	MATLAB	STK	MATLAB	STK
Optimal solution	3.02	3.35	0.74 %	1.71 %

Table 5.25: case G8 GDOP values

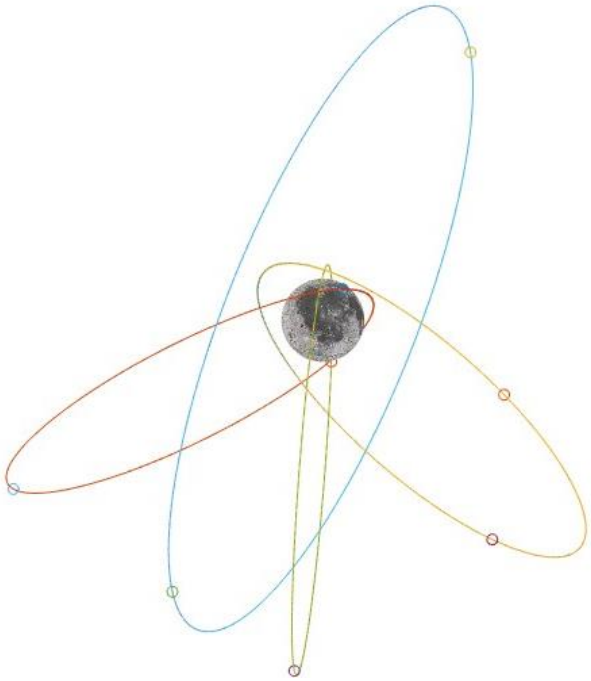

Figure 5.9: case G8 optimal solution

Case G8 represents a good solution with 4 orbital planes. The mean GDOP and peak time percentage could be improved by introducing, for example, the dynamic perturbations in the optimization mathematical model, or improving the genetic algorithm options.

The following case G9, G10 and G11 represents a scenario with six satellites. The total number of satellites is reduced in order to consider architectures with less complexity and a lower cost. Each satellite is defined by its six variables (36 total variables): apogee radius r_a, perigee radius r_p, inclination i, right ascension of the ascending node Ω, argument of perigee ω and the true anomaly ν. In each case are reported the variables defined for the optimization process while, if not specified, all the satellite variables are involved. If not specified, the mathematical model used for the optimization is represented by the two-body dynamics. The cases G10 and G11 report a limited number of orbital planes in order to reduce the complexity of the architectures, and to improve satellite operability.

5.2.9 Case G9

The optimal results of case G9 are reported in Table 5.27, while in Table 5.26 are reported the orbital parameters of each satellite. In Figure 5.10 the optimal solution is represented.

	[km]	[km]	[deg]	[deg]	[deg]	[deg]
	r_a	r_p	i	Ω	ω	ν
S_1	14311.2	2342.9	31.5	1.6	85.9	73.1
S_2	13106.8	2791.9	42.5	176.1	102.3	177.7
S_3	13846.0	2098.5	90.8	124.9	112.2	165.2
S_4	14772.8	2811.2	38.9	85.7	84.8	226.5
S_5	14264.1	2410.6	41.1	300.7	98.4	203.3
S_6	13310.1	2612.3	96.4	233.4	103.3	272.2

Table 5.26: case G9 orbital parameters

	Mean GDOP		Peak time %	
	MATLAB	STK	MATLAB	STK
Optimal solution	4.64	5.19	6.48 %	8.14 %

Table 5.27: case G9 GDOP values

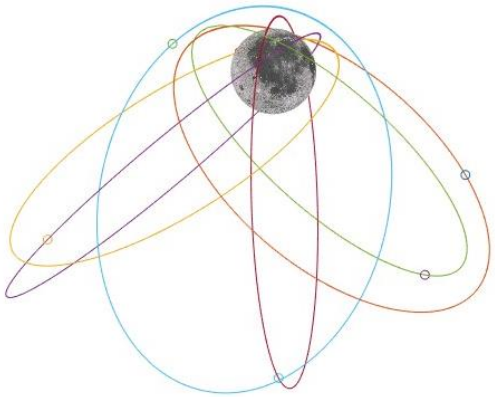

Figure 5.10: case G9 optimal solution

The solution obtained reports a high mean GDOP and mean peak time percentage. In order to improve the solution it is possible to repeat the optimization reducing the variables involved (reducing the number of orbital planes) or introducing the perturbations in the optimization mathematical model.

5.2.10 Case G10

The optimal results of case G10 are reported in Table 5.30, while in Table 5.29 are reported the orbital parameters of each satellite. In Figure 5.11 the optimal solution is represented. The optimization variables selected are reported in Table 5.28: there are six satellites and two orbital planes. The satellites S_1, S_2 and S_3 belong to the first plane so the variables are the plane orbital parameters (apogee radius r_{a1}, the perigee radius r_{p1}, the inclination i_1, the RAAN Ω_1 and the perigee argument ω_1) and the true anomaly of each satellite at $t = 0$. The satellites S_4, S_5 and S_6 belong to the second plane so the variables are the plane orbital parameters (r_{a2}, r_{p2}, i_2, Ω_2 and ω_2) and the true anomaly of each satellite at $t = 0$.

S_1	S_2	S_3	S_4	S_5	S_6
r_{a1}			r_{a2}		
r_{p1}			r_{p2}		
i_1			i_2		
Ω_1			Ω_2		
ω_1			ω_2		
ν_1	ν_2	ν_3	ν_4	ν_5	ν_6

Table 5.28: case G10 optimization variables

	[km]	[km]	[deg]	[deg]	[deg]	[deg]
	r_a	r_p	i	Ω	ω	ν
S_1	14654.3	2979.5	93.9	229.5	133.7	188.1
S_2	14654.3	2979.5	93.9	229.5	133.7	151.2
S_3	14654.3	2979.5	93.9	229.5	133.7	251.4
S_4	13733.1	3884.7	48.0	179.1	76.5	164.5
S_5	13733.1	3884.7	48.0	179.1	76.5	359.8
S_6	13733.1	3884.7	48.0	179.1	76.5	205.9

Table 5.29: case G10 orbital parameters

	Mean GDOP		Peak time %	
	MATLAB	STK	MATLAB	STK
Optimal solution	3.88	4.19	0.05 %	1.36 %

Table 5.30: case G10 GDOP values

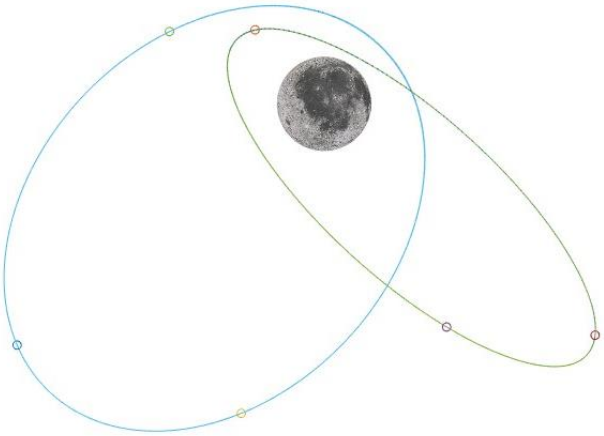

Figure 5.11: case G10 optimal solution

The solution obtained involves a reduced number of orbital planes and a better mean GDOP and peak time percentage compared to the previous solution G9.

5.2.11 Case G11

The optimal results of case G11 are reported in Table 5.33, while in Table 5.32 are reported the orbital parameters of each satellite. In Figure 5.12 the optimal solution is represented. The optimization variables selected are reported in Table 5.31: there are six satellites and three orbital planes. The satellites S_1 and S_2 belong to the first plane so the variables are the plane orbital parameters (apogee radius r_{a1}, the perigee radius r_{p1}, the inclination i_1, the RAAN Ω_1 and the perigee argument ω_1) and the true anomaly of each satellite at $t = 0$. The satellites S_3 and S_4 belong to the second plane so the variables are the plane orbital parameters (r_{a2}, r_{p2}, i_2, Ω_2 and ω_2) and the true anomaly of each satellite at $t = 0$. The satellites S_5 and S_6

belong to the third plane so the variables are the plane orbital parameters (r_{a3}, r_{p3}, i_3, Ω_3 and ω_3) and the true anomaly of each satellite at $t = 0$

S_1	S_2	S_3	S_4	S_5	S_6
r_{a1}		r_{a2}		r_{a3}	
r_{p1}		r_{p2}		r_{p3}	
i_1		i_2		i_3	
Ω_1		Ω_2		Ω_3	
ω_1		ω_2		ω_3	
ν_1	ν_2	ν_3	ν_4	ν_5	ν_6

Table 5.31: case G11 optimization variables

	[km]	[km]	[deg]	[deg]	[deg]	[deg]
	r_a	r_p	i	Ω	ω	ν
S_1	13311.8	2478.1	76.2	358.7	75.4	179.2
S_2	13311.8	2478.1	76.2	358.7	75.4	206.5
S_3	12747.9	3043.8	102.16	84.4	76.8	146.3
S_4	12747.9	3043.8	102.16	84.4	76.8	326.9
S_5	14633.8	2270.1	142.6	332.9	107.0	178.6
S_6	14633.8	2270.1	142.6	332.9	107.0	310.8

Table 5.32: case G11 orbital parameters

	Mean GDOP		Peak time %	
	MATLAB	STK	MATLAB	STK
Optimal solution	4.59	5.12	0.24 %	1.81 %

Table 5.33: case G11 GDOP values

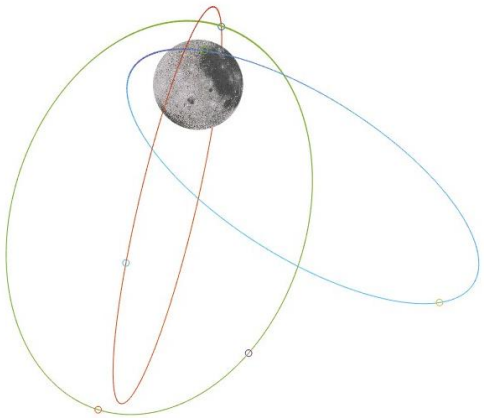

Figure 5.12: case G11 optimal solution

The solution obtained shows a higher mean GDOP and mean peak time percentage compared to the previous solution G10. In order to improve the solution, it is possible to repeat the optimization by introducing the perturbations in the optimization mathematical model.

5.2.12 Case G12

Case G12 is described by five satellites and five orbital planes. The optimization variables are orbital parameters of all the five orbital plans and the true anomalies of the five satellite at $t = 0$. The optimal results of case G12 are reported in Table 5.35, while in Table 5.34 are reported the orbital parameters of each satellite. In Figure 5.13 the optimal solution is represented.

	[km]	[km]	[deg]	[deg]	[deg]	[deg]
	r_a	r_p	i	Ω	ω	ν
S_1	14785.2	2069.9	140.9	3.6	91.9	331.8
S_2	14571.2	3841.9	90.9	94.9	93.5	156.8
S_3	14458.0	3958.9	90.7	89.4	93.1	229.9
S_4	14500.2	2347.2	142.3	222.4	96.1	327.1
S_5	14630.2	2216.2	139.8	115.2	86.0	311.9

Table 5.34: case G12 orbital parameters

	Mean GDOP		Peak time %	
	MATLAB	STK	MATLAB	STK
Optimal solution	6.98	7.35	21.34 %	22.9 %

Table 5.35: case G12 GDOP values

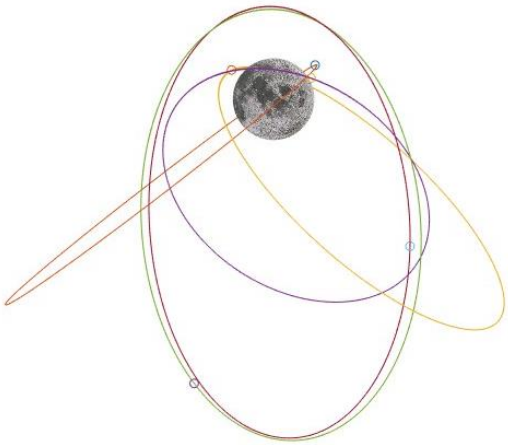

Figure 5.13: case G12 optimal solution

The solution obtained in case G12 have to be improved, since it doesn't report good performances. The case with five satellites represents an onerous scenario with respect to the one with eight satellites. In particular, the method could be improved by acting on different elements. The optimization could be improved with a mathematical model defined with the dynamic perturbations (to represent a more realistic scenario), or by modifying the genetic algorithm options, for example the total computation time.

5.2.13 Case G13

The optimal results of case G13 are reported in Table 5.38, while in Table 5.37 are reported the orbital parameters of each satellite. In Figure 5.14 the optimal solution is represented. The optimization variables selected are reported in Table 5.36: there are five satellites and two orbital planes. The satellites S_1, S_2 and S_3 belong to the first plane so the variables are the plane orbital parameters (apogee radius r_{a1}, the perigee radius r_{p1}, the inclination i_1, the RAAN Ω_1 and the perigee argument ω_1) and the true anomaly of each satellite at $t = 0$. The satellites S_4 and S_5 belong to the second plane so the variables are the plane orbital parameters (r_{a2}, r_{p2}, i_2, Ω_2 and ω_2) and the true anomaly of each satellite at $t = 0$.

S_1	S_2	S_3	S_4	S_5
r_{a1}			r_{a2}	
r_{p1}			r_{p2}	
i_1			i_2	
Ω_1			Ω_2	
ω_1			ω_2	
ν_1	ν_2	ν_3	ν_4	ν_5

Table 5.36: case G13 optimization variables

	[km]	[km]	[deg]	[deg]	[deg]	[deg]
	r_a	r_p	i	Ω	ω	ν
S_1	14372.5	2594.1	100.7	225.6	115.4	171.6
S_2	14372.5	2594.1	100.7	225.6	115.4	209.5
S_3	14372.5	2594.1	100.7	225.6	115.4	94.2
S_4	14946.3	2018.2	128.4	359.8	101.0	159.8
S_5	14946.3	2018.2	128.4	359.8	101.0	192.7

Table 5.37: case G13 orbital parameters

	Mean GDOP		Peak time %	
	MATLAB	STK	MATLAB	STK
Optimal solution	6.90	8.26	6.79 %	15.5 %

Table 5.38: case G13 GDOP values

Figure 5.14: case G13 optimal solution

As for case G12, the solution obtained from case G13 have to be improved, since doesn't represent acceptable performances. The same considerations are applied for the current solution.

5.2.14 Summary of global approach from scratch optimal solutions

Case	Total number of satellites	Total number of orbital planes	Mean GDOP	Peak time %
G1	8	8	2.65	0.38 %
G2	8	2	3.66	0.04 %
G3	8	3	2.50	0 %
G4	8	4	3.28	1.37 %
G5	7	7	4.7	5.1 %
G6	7	2	4.4	1.2 %
G7	7	3	2.80	0.16 %
G8	7	4	3.35	1.71 %
G9	6	6	5.19	8.14 %
G10	6	2	4.19	1.36 %
G11	6	3	5.12	1.81 %
G12	5	5	7.35	22.9 %
G13	5	2	8.26	15.5 %

Table 5.39: global approach optimal solutions:

The genetic algorithm efficiently finds satisfactory solutions without any initialization. To achieve more optimal solutions with higher degrees of freedom, new solutions are generated using a genetic algorithm in section 5.6. The algorithm starts with a population of individuals that includes the solutions obtained with the same number of satellites (see e.g., Table 5.39) and leave all the optimization variables unrestricted (one orbital plane for each satellite).

5.3 Local approach from guess solutions

In the following section the cases regarding the SQP algorithm, implemented in Matlab environment, are reported. The algorithm is typically seen as a global method, thanks to the use of the multi-start option available in Matlab. In this scenario the algorithm act as a local optimization, because the use of multi-start would request longer time calculation and no solutions improvements in short time computations. It is necessary to give in input a guess solution to be minimized. In the following cases the guess solution is the one with eight satellites presented in the article by Bhamidipati et al. (2023).

The following case S1, S2, S3, S4 represents a scenario with eight satellites. Each satellite is defined by its six variables (48 total variables): apogee radius r_a, perigee radius r_p, inclination i, right ascension of the ascending node Ω, argument of perigee ω and the true anomaly ν. In each case are reported the variables defined for the optimization process while, if not specified, all the satellite variables are involved. If not specified, the mathematical model used for the optimization is represented by the two-body dynamics.

5.3.1 Case S1

The optimal results of case S1 are reported in Table 5.41, while in Table 5.40 are reported the orbital parameters of each satellite. In Figure 5.16 the optimal solution is represented.

	[km]		[km]		[deg]		[deg]		[deg]		[deg]	
	r_a		r_p		i		Ω		ω		ν	
	Guess solution	Optimal solution	Guess solution	Optimal solution	Guess solution	Optimal solution	Guess solution	Optimal solution	Guess solution	Optimal solution	Guess solution	Optimal solution
S_1	9828.8	9828.7	2457.2	2461.4	51.7	51.78	0	0.002	90	90.0	0	0.0003
S_2	9828.8	9826.1	2457.2	2461.2	51.7	51.78	0	0.002	90	90.0	147.7	147.7
S_3	9828.8	9828.9	2457.2	2460.7	51.7	51.76	0	0.001	90	89.9	180	179.9
S_4	9828.8	9826.4	2457.2	2462.5	51.7	51.77	0	0.002	90	90.0	212.3	212.3
S_5	9828.8	9826.7	2457.2	2458.5	51.7	51.78	180	179.9	90	90.0	0	0.0015
S_6	9828.8	9825.5	2457.2	2458.9	51.7	51.78	180	180.0	90	89.9	147.7	147.7
S_7	9828.8	9825.6	2457.2	2458.6	51.7	51.79	180	180.0	90	89.9	180	180.0
S_8	9828.8	9826.1	2457.2	2457.8	51.7	51.77	180	179.9	90	90.0	212.3	212.3

Table 5.40: case S1 orbital parameters

	Mean GDOP	Peak time %
	MATLAB	MATLAB
Guess solution	4.3807	1.08 %
Optimal solution	4.3003	0.6 %

Table 5.41: case S1 GDOP values

From the optimal solution obtained, even if the objective function is minimized, the variables don't show effective variations and the difference between the guess solution orbital parameters are too small.

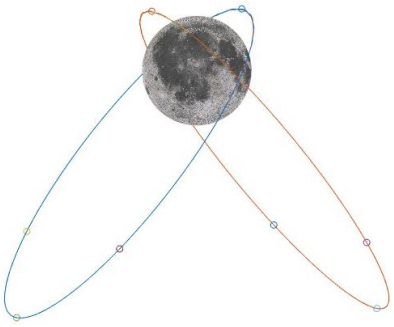

Figure 5.15: case S1 guess solution

Figure 5.16: case S1 optimal solution

5.3.2 Case S2

The optimal results of case S2 are reported in Table 5.44, while in Table 5.43 are reported the orbital parameters of each satellite. In Figure 5.18 the optimal solution is represented. The optimization variables selected are reported in Table 5.42: there are eight satellites and two orbital planes. The satellites S_1, S_2, S_3 and S_4 belong to the first plane so the variables are the plane orbital parameters (apogee radius r_{a1}, the perigee radius r_{p1}, the inclination i_1, the RAAN Ω_1 and the perigee argument ω_1) and the true anomaly of each satellite at $t = 0$. The satellites S_5, S_6, S_7 and S_8 belong to the second plane so the variables are the plane orbital parameters (r_{a2}, r_{p2}, i_2, Ω_2 and ω_2) and the true anomaly of each satellite at $t = 0$.

S_1	S_2	S_3	S_4	S_5	S_6	S_7	S_8
r_{a1}				r_{a2}			
r_{p1}				r_{p2}			
i_1				i_2			
Ω_1				Ω_2			
ω_1				ω_2			
ν_1	ν_2	ν_3	ν_4	ν_5	ν_6	ν_7	ν_8

Table 5.42: case S2 optimization variables

	[km]		[km]		[deg]		[deg]		[deg]		[deg]	
	r_a		r_p		i		Ω		ω		ν	
	Guess solution	Optimal solution	Guess solution	Optimal solution	Guess solution	Optimal solution	Guess solution	Optimal solution	Guess solution	Optimal solution	Guess solution	Optimal solution
S_1	9828.8	10469	2457.2	3820.9	51.7	49.8	0	37.2	90	124.4	0	17.3
S_2	9828.8	10469	2457.2	3820.9	51.7	49.8	0	37.2	90	124.4	147.7	137.8
S_3	9828.8	10469	2457.2	3820.9	51.7	49.8	0	37.2	90	124.4	180	183.0
S_4	9828.8	10469	2457.2	3820.9	51.7	49.8	0	37.2	90	124.4	212.3	222.8
S_5	9828.8	8785.7	2457.2	2246.3	51.7	81.2	180	152.2	90	135.5	0	24.08
S_6	9828.8	8785.7	2457.2	2246.3	51.7	81.2	180	152.2	90	135.5	147.7	156.9
S_7	9828.8	8785.7	2457.2	2246.3	51.7	81.2	180	152.2	90	135.5	180	186.2
S_8	9828.8	8785.7	2457.2	2246.3	51.7	81.2	180	152.2	90	135.5	212.3	225.6

Table 5.43: case S2 orbital parameters

	Mean GDOP		Peak time %	
	MATLAB	STK	MATLAB	STK
Guess solution	4.38	4.57	1.08 %	1.9%
Optimal solution	3.48	3.78	0.06 %	0.86 %

Table 5.44: case S2 GDOP values

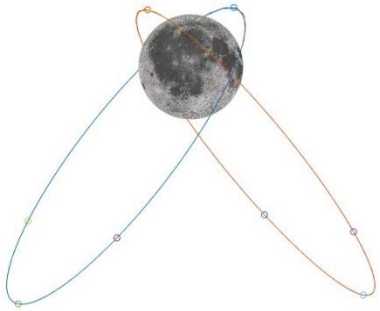

Figure 5.17: case S2 guess solution

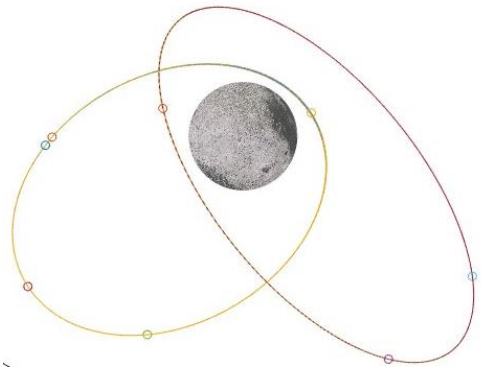

Figure 5.18: case S2 optimal solution

The solution S2 is improved with respect to the solution obtained in case S1. The mean GDOP and the peak time percentage are reduced and the orbital parameters are different. It can be seen that working with fewer variables with the SQP algorithm leads to a better solution and more visible changes in the architecture.

5.3.3 Case S3

The optimal results of case S3 are reported in Table 5.47, while in Table 5.46 are reported the orbital parameters of each satellite. In Figure 5.20 the optimal solution is represented. The optimization variables selected are reported in Table 5.45: there are eight satellites and two orbital planes. The satellites S_1, S_2, S_3 and S_4 belong to the first plane so the variables are the plane orbital parameters (apogee radius r_{a1}, the perigee radius r_{p1}, the inclination i_1 and the RAAN Ω_1) and the true anomaly of each satellite at $t = 0$. The satellites S_5, S_6, S_7 and S_8 belong to the second plane, which has the same apogee and perigee radius of the first plane, so the variables are the plane orbital parameters (r_{a1}, r_{p1}, i_2, and Ω_2) and the true anomaly of each satellite at $t = 0$. The perigee argument ω_1 and ω_2 of the two planes are equivalent to those of the guess solution ($\omega_1 = \omega_2 = 90$).

S_1	S_2	S_3	S_4	S_5	S_6	S_7	S_8
r_{a1}							
r_{p1}							
i_1				i_2			
Ω_1				Ω_2			
ν_1	ν_2	ν_3	ν_4	ν_5	ν_6	ν_7	ν_8

Table 5.45: case S3 optimization variables

	[km]		[km]		[deg]		[deg]		[deg]		[deg]	
	r_a		r_p		i		Ω		ω		ν	
	Guess solution	Optimal solution	Guess solution	Optimal solution	Guess solution	Optimal solution	Guess solution	Optimal solution	Guess solution	Optimal solution	Guess solution	Optimal solution
S_1	9828.8	9627.6	2457.2	2874.0	51.7	68.1	0	0	90	90	0	359.9
S_2	9828.8	9627.6	2457.2	2874.0	51.7	68.1	0	0	90	90	147.7	153.3
S_3	9828.8	9627.6	2457.2	2874.0	51.7	68.1	0	0	90	90	180	180.8
S_4	9828.8	9627.6	2457.2	2874.0	51.7	68.1	0	0	90	90	212.3	207.6
S_5	9828.8	9627.6	2457.2	2874.0	51.7	73.0	180	180.5	90	90	0	1.1
S_6	9828.8	9627.6	2457.2	2874.0	51.7	73.0	180	180.5	90	90	147.7	156.1
S_7	9828.8	9627.6	2457.2	2874.0	51.7	73.0	180	180.5	90	90	180	178.6
S_8	9828.8	9627.6	2457.2	2874.0	51.7	73.0	180	180.5	90	90	212.3	207.4

Table 5.46: case S3 orbital parameters

	Mean GDOP		Peak time %	
	MATLAB	STK	MATLAB	STK
Guess solution	4.38	4.57	1.08 %	1.9%
Optimal solution	4.24	4.18	0.44 %	0.81 %

Table 5.47: case S3 GDOP values

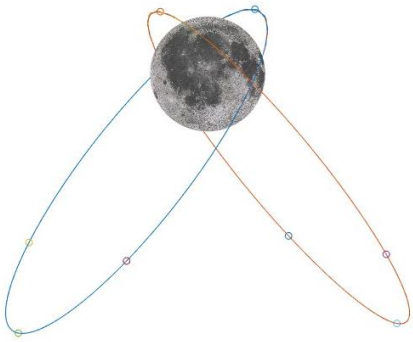

Figure 5.19: case S3 guess solution

Figure 5.20: case S3 optimal solution

The solution, with respect to case S3, improves the mean GDOP and peak time percentage values. As for case S2, using a reduced number of variables with the SQP algorithm, led to a better solution and more visible changes in the architecture and orbital parameters.

5.3.4 Case S4

The optimal results of case S4 are reported in Table 5.50, while in Table 5.49 are reported the orbital parameters of each satellite. In Figure 5.22 the optimal solution is represented. The optimization variables selected are reported in Table 5.48: there are eight satellites and eight orbital planes. Each satellite has the plane orbital parameters (apogee radius r_a, the perigee radius $r_p$and the inclination i) and the true anomaly of each satellite at $t = 0$. The perigee argument ω of each plane is equivalent to those of the guess solution ($\omega_1 = \omega_2 = \omega_3 = \omega_4 = \omega_5 = \omega_6 = \omega_7 = \omega_8 = 90°$). The RAAN Ω of each plane is equivalent to those of the guess solution ($\Omega_1 = \Omega_2 = \Omega_3 = \Omega_4 = 0°$, $\Omega_5 = \Omega_6 = \Omega_7 = \Omega_8 = 180°$).

S_1	S_2	S_3	S_4	S_5	S_6	S_7	S_8
r_{a1}	r_{a2}	r_{a3}	r_{a4}	r_{a5}	r_{a6}	r_{a7}	r_{a8}
r_{p1}	r_{p2}	r_{p3}	r_{p4}	r_{p5}	r_{p6}	r_{p7}	r_{p8}
i_1	i_2	i_3	i_4	i_5	i_6	i_7	i_8
ν_1	ν_2	ν_3	ν_4	ν_5	ν_6	ν_7	ν_8

Table 5.48: case S4 optimization variables

	[km]		[km]		[deg]		[deg]		[deg]		[deg]	
	r_a		r_p		i		Ω		ω		ν	
	Guess solution	Optimal solution	Guess solution	Optimal solution	Guess solution	Optimal solution	Guess solution	Optimal solution	Guess solution	Optimal solution	Guess solution	Optimal solution
S_1	9828.8	9828.8	2457.2	2457.2	51.7	67.3	0	1.4	90	90	0	0.4
S_2	9828.8	9828.8	2457.2	2457.2	51.7	82.9	0	4.7	90	90	147.7	147.7
S_3	9828.8	9828.8	2457.2	2457.2	51.7	71.6	0	0.0	90	90	180	173.4
S_4	9828.8	9828.8	2457.2	2457.2	51.7	60.6	0	0	90	90	212.3	210.7
S_5	9828.8	9828.8	2457.2	2457.2	51.7	77.4	180	178.7	90	90	0	1.1
S_6	9828.8	9828.8	2457.2	2457.2	51.7	60.1	180	180.4	90	90	147.7	153.7
S_7	9828.8	9828.8	2457.2	2457.2	51.7	75.9	180	184.2	90	90	180	185.8
S_8	9828.8	9828.8	2457.2	2457.2	51.7	82.9	180	176.9	90	90	212.3	221.4

Table 5.49: case S4 orbital parameters

	Mean GDOP		Peak time %	
	MATLAB	STK	MATLAB	STK
Guess solution	4.38	4.57	1.08 %	1.9%
Optimal solution	3.70	3.73	0.03 %	0.03 %

Table 5.50: case S4 GDOP values

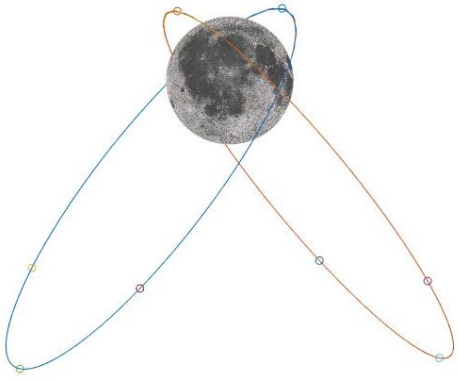

Figure 5.21: case S4 guess solution

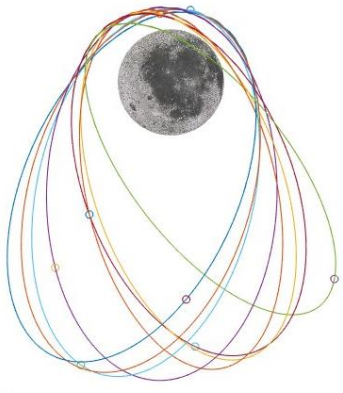

Figure 5.22: case S4 optimal solution

The obtained solution doesn't allow to reduce the complexity of the architecture. However, the algorithm can also be used with the inclusion of selected variables to reduce the model complexity and improve the objective function.

5.3.5 Case S5

The optimal results of case S5 are reported in Table 5.53, while in Table 5.52 are reported the orbital parameters of each satellite. In Figure 5.24 the optimal solution is represented. The optimization variables selected are reported in Table 5.51: there are 8 satellites and 8 orbital planes. Each satellite has the plane orbital parameters (inclination i) and the true anomaly of each satellite at $t = 0$. The perigee argument ω of each plane is equivalent to those of the guess solution ($\omega_1 = \omega_2 = \omega_3 = \omega_4 = \omega_5 = \omega_6 = \omega_7 = \omega_8 = 90°$). The RAAN Ω of each plane is equivalent to those of the guess solution ($\Omega_1 = \Omega_2 = \Omega_3 = \Omega_4 = 0°, \Omega_5 = \Omega_6 = \Omega_7 = \Omega_8 = 180°$). The perigee radius and apogee radius of each plane is equivalent to those of the guess solution ($r_a = 9828.8\ km, r_p = 2457.2\ km$).

S_1	S_2	S_3	S_4	S_5	S_6	S_7	S_8
r_{a1}	r_{a2}	r_{a3}	r_{a4}	r_{a5}	r_{a6}	r_{a7}	r_{a8}
r_{p1}	r_{p2}	r_{p3}	r_{p4}	r_{p5}	r_{p6}	r_{p7}	r_{p8}
i_1	i_2	i_3	i_4	i_5	i_6	i_7	i_8
ν_1	ν_2	ν_3	ν_4	ν_5	ν_6	ν_7	ν_8

Table 5.51: case S5 optimization variables

	[km]		[km]		[deg]		[deg]		[deg]		[deg]	
	r_a		r_p		i		Ω		ω		ν	
	Guess solution	Optimal solution	Guess solution	Optimal solution	Guess solution	Optimal solution	Guess solution	Optimal solution	Guess solution	Optimal solution	Guess solution	Optimal solution
S_1	9828.8	9830.9	2457.2	2461	51.7	51.75	0	0	90	90	0	0.000
S_2	9828.8	9829.5	2457.2	2459.7	51.7	51.76	0	0	90	90	147.7	147.68
S_3	9828.8	9829.7	2457.2	2459.8	51.7	51.75	0	0	90	90	180	179.98
S_4	9828.8	9831.2	2457.2	2461.4	51.7	51.76	0	0	90	90	212.3	212.3
S_5	9828.8	9826.9	2457.2	2456.7	51.7	51.76	180	180	90	90	0	0.001
S_6	9828.8	9825.4	2457.2	2455.4	51.7	51.76	180	180	90	90	147.7	147.7
S_7	9828.8	9825.5	2457.2	2455.5	51.7	51.77	180	180	90	90	180	180.0
S_8	9828.8	9826.8	2457.2	2456.8	51.7	51.75	180	180	90	90	212.3	212.3

Table 5.52: case S5 orbital parameters

	Mean GDOP	Peak time %
	MATLAB	MATLAB
Guess solution	4.3807	1.08 %
Optimal solution	4.3584	0.67 %

Table 5.53: case S5 GDOP values

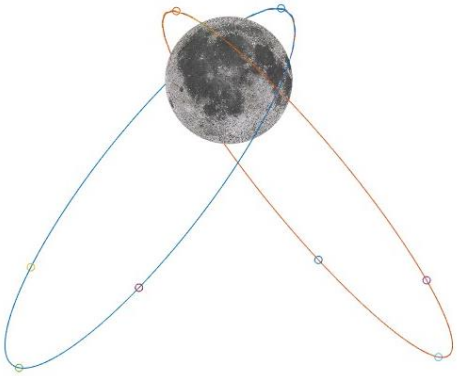

Figure 5.23: case S5 guess solution

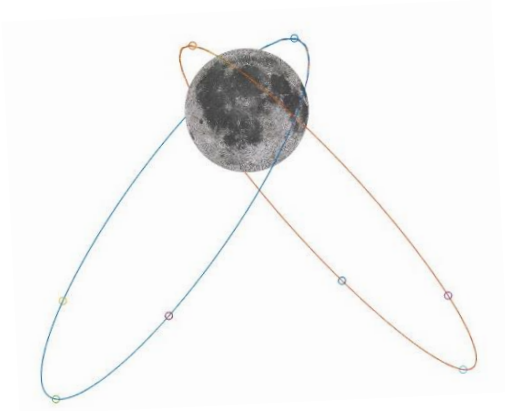

Figure 5.24: case S5 optimal solution

From the optimal solution obtained, even if the objective function is minimized, the variables don't show effective variations and the difference between the guess solution orbital parameters are not too small.

5.3.6 Summary of local approach optimal solution

Case	Total number of satellites	Total number of orbital planes	Mean GDOP	Peak time %
S2	8	2	3.79	0.86 %
S3	8	2	4.18	0.81 %
S4	8	8	3.74	0.03 %

Table 5.54: local approach optimal solutions

5.4 Orbit number reduction

The following section deals with the clustering method. The methodology proposed regards the K-means algorithm application, useful for solutions with independent satellite orbits, obtained from previous cases. Thanks to this approach it can be possible to reduce satellite variables into a defined number of clusters and to observe which satellite is assigned to each cluster. In general, the solutions obtained from the clustering are not good as the starting ones, so the choice was made to use the SQP algorithm to perform a local optimization from the new guess solutions obtained.

5.4.1 Case AK1: K-means clustering

The results of case AK1 are reported in Table 5.56. The guess solution from which starts the clustering is case G1. The clustering is made on orbital plane variables $r_a, r_p, i, \Omega, \omega$ with two clusters, in order to reduce the number of orbital planes from eight planes to two planes. The true anomaly of each satellite is defined externally in each plane. The Table 5.55 reports the orbital parameters of each satellite. In Figure 5.26 the clustering solution is represented.

	[km]		[km]		[deg]		[deg]		[deg]		[deg]	
	r_a		r_p		i		Ω		ω		ν	
	Guess solution	Optimal solution	Guess solution	Optimal solution	Guess solution	Optimal solution	Guess solution	Optimal solution	Guess solution	Optimal solution	Guess solution	Optimal solution
S_1	13348	13699	2943.2	2596.3	147.4	129.9	246.9	237.9	90.0	98.5	0	0
S_2	13585	13699	2594.0	2596.3	148.3	129.9	247.8	237.9	90.0	98.5	147.7	147.7
S_3	14996	13699	2525.6	2596.3	152.0	129.9	126.4	237.9	89.9	98.5	180	180
S_4	13289	13699	5177.1	2596.3	87.1	129.9	267.5	237.9	90.0	98.5	212.3	212.3
S_5	14827	14565	2797.5	3340.1	35.9	81.6	171.3	187.2	90.0	99.0	0	0
S_6	14827	14565	2738.6	3340.1	34.9	81.6	221.3	187.2	89.9	99.0	147.7	147.7
S_7	14166	14565	2248.9	3340.1	94.1	81.6	219.1	187.2	89.9	99.0	180	180
S_8	14919	14565	3554.9	3340.1	97.8	81.6	149.3	187.2	90.0	99.0	212.3	212.3

Table 5.55: case AK1 orbital parameters

	Mean GDOP		Peak time %	
	MATLAB	STK	MATLAB	STK
Guess solution	2.53	2.65	0.19 %	0.37 %
Optimal solution	4.27	4.48	0 %	0.02 %

Table 5.56: case AK1 GDOP values

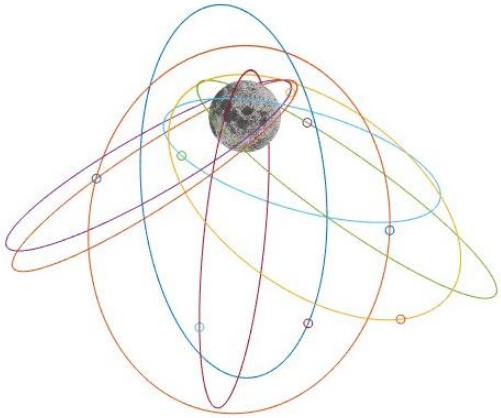

Figure 5.25: case AK1 guess solution

Figure 5.26: case AK1 clustering solution

In the following case, thanks to the use of the K-means algorithm, it is possible to reduce the number of orbital planes from eight (case G1) to two, without changing the total number of satellites involved in the architecture. Even if the mean peak time percentage is reduced, the mean GDOP value is higher. It is proposed a second local optimization (case BK1) starting from the clustering solution obtained with the present case AK1.

5.4.2 Case BK1: SQP optimization

The optimal results of case BK1 are reported in Table 5.59, while in Table 5.58 are reported the orbital parameters of each satellite. In Figure 5.28 the optimal solution is represented. The optimization variables selected are reported in Table 5.57: there are eight satellites and two orbital planes. The satellites S_1, S_2, S_3 and S_4 belong to the first plane so the variables are the plane orbital parameters (apogee radius r_{a1}, the perigee radius r_{p1}, the inclination i_1, the RAAN Ω_1 and the perigee argument ω_1) and the true anomaly of each satellite at $t = 0$. The satellites S_5, S_6, S_7 and S_8 belong to the second plane so the variables are the plane orbital parameters (r_{a2}, r_{p2}, i_2, Ω_2 and ω_2) and the true anomaly of each satellite at $t = 0$. The guess solution is the clustering solution of case AK1.

S_1	S_2	S_3	S_4	S_5	S_6	S_7	S_8
r_{a1}				r_{a2}			
r_{p1}				r_{p2}			
i_1				i_2			
Ω_1				Ω_2			
ω_1				ω_2			
ν_1	ν_2	ν_3	ν_4	ν_5	ν_6	ν_7	ν_8

Table 5.57: case BK1 optimization variables

	[km]		[km]		[deg]		[deg]		[deg]		[deg]	
	r_a		r_p		i		Ω		ω		ν	
	Guess solution	Optimal solution	Guess solution	Optimal solution	Guess solution	Optimal solution	Guess solution	Optimal solution	Guess solution	Optimal solution	Guess solution	Optimal solution
S_1	13699	14049	2596.3	5335.3	129.9	145.1	237.9	247.9	98.5	77.9	0	0
S_2	13699	14049	2596.3	5335.3	129.9	145.1	237.9	247.9	98.5	77.9	147.7	132.0
S_3	13699	14049	2596.3	5335.3	129.9	145.1	237.9	247.9	98.5	77.9	180	167.7
S_4	13699	14049	2596.3	5335.3	129.9	145.1	237.9	247.9	98.5	77.9	212.3	204.3
S_5	14565	12797	3340.1	3069.6	81.6	92.5	187.2	174.3	99.0	142.5	0	0.3
S_6	14565	12797	3340.1	3069.6	81.6	92.5	187.2	174.3	99.0	142.5	147.7	161.0
S_7	14565	12797	3340.1	3069.6	81.6	92.5	187.2	174.3	99.0	142.5	180	193.7
S_8	14565	12797	3340.1	3069.6	81.6	92.5	187.2	174.3	99.0	142.5	212.3	215.2

Table 5.58: case BK1 orbital parameters

	Mean GDOP		Peak time %	
	MATLAB	STK	MATLAB	STK
Guess solution	4.27	4.48	0 %	0.02 %
Optimal solution	3.64	3.96	2.01 %	3.10 %

Table 5.59: case BK1 GDOP values

Figure 5.27: case BK1 guess solution

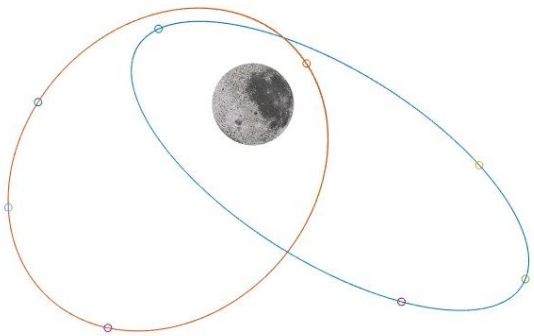

Figure 5.28: case BK1 optimal solution

In the present case, it can be seen that the SQP algorithm, in order to improve the solution, reduces the mean GDOP value by increasing the mean peak percentage value.

5.4.3 Case AK2: K-means clustering

The results of case AK2 are reported in Table 5.61. The guess solution from which starts the clustering is case G1. The clustering is made on orbital plane variables $r_a, r_p, i, \Omega, \omega$ with three clusters. The true anomaly of each satellite is defined externally in each plane. The Table 5.60 reports the orbital parameters of each satellite. In Figure 5.29 the clustering solution is represented.

	[km]		[km]		[deg]		[deg]		[deg]		[deg]	
	r_a		r_p		i		Ω		ω		ν	
	Guess solution	Optimal solution	Guess solution	Optimal solution	Guess solution	Optimal solution	Guess solution	Optimal solution	Guess solution	Optimal solution	Guess solution	Optimal solution
S_1	13348	13699	2943.2	2596.3	147.4	129.9	246.9	237.9	90.0	98.5	0	0
S_2	13585	13699	2594.0	2596.3	148.3	129.9	247.8	237.9	90.0	98.5	147.7	120
S_3	14996	13699	2525.6	2596.3	152.0	129.9	126.4	237.9	89.9	98.5	180	240
S_4	13289	14104	5177.1	4366.2	87.1	92.5	267.5	208.4	90.0	98.3	212.3	0
S_5	14827	14104	2797.5	4366.2	35.9	92.5	171.3	208.4	90.0	98.3	0	120
S_6	14827	14104	2738.6	4366.2	34.9	92.5	221.3	208.4	89.9	98.3	147.7	240
S_7	14166	14842	2248.9	2687.2	94.1	74.3	219.1	173.0	89.9	99.5	180	0
S_8	14919	14842	3554.9	2687.2	97.8	74.3	149.3	173.0	90.0	99.5	212.3	180

Table 5.60: case AK2 orbital parameters

	Mean GDOP		Peak time %	
	MATLAB	STK	MATLAB	STK
Guess solution	2.53	2.65	0.19 %	0.37 %
Cluster solution	4.96	5.43	2.15 %	3.31 %

Table 5.61: case AK2 GDOP values

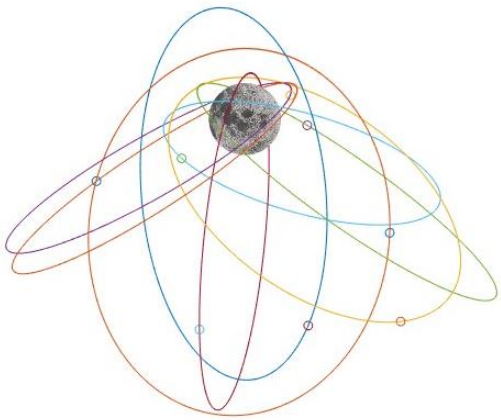

Figure 5.30: case AK2 guess solution

Figure 5.29: case AK2 clustering solution

By using the K-means algorithm, it is possible to reduce the number of orbital planes from eight (case G1) to three with the same total number of satellites in the architecture. The mean peak time percentage and the mean GDOP value are increased. A second local optimization (case BK2) is proposed starting from the clustering solution of case AK2.

5.4.4 Case BK2: SQP optimization

The optimal results of case BK2 are reported in Table 5.64, while in Table 5.63 are reported the orbital parameters of each satellite. In Figure 5.31 the optimal solution is represented. The optimization variables selected are reported in Table 5.62: there are eight satellites and three orbital planes. The satellites S_1, S_2 and S_3 belong to the first plane so the variables are the plane orbital parameters (apogee radius r_{a1}, the perigee radius r_{p1}, the inclination i_1, the RAAN Ω_1 and the perigee argument ω_1) and the true anomaly of each satellite at $t = 0$. The satellites S_4, S_5 and S_6 belong to the second plane so the variables are the plane orbital parameters (r_{a2}, r_{p2}, i_2, Ω_2 and ω_2) and the true anomaly of each satellite at $t = 0$. The satellites S_7 and S_8 belong to the second plane so the variables are the plane orbital parameters (r_{a3}, r_{p3}, i_3, Ω_3 and ω_3) and the true anomaly of each satellite at $t = 0$. The guess solution is the clustering solution of case AK2.

S_1	S_2	S_3	S_4	S_5	S_6	S_7	S_8
r_{a1}			r_{a2}			r_{a3}	
r_{p1}			r_{p2}			r_{p3}	
i_1			i_2			i_3	
Ω_1			Ω_2			Ω_3	
ω_1			ω_2			ω_3	
ν_1	ν_2	ν_3	ν_4	ν_5	ν_6	ν_7	ν_8

Table 5.62: case BK2 optimization variables

	[km]		[km]		[deg]		[deg]		[deg]		[deg]	
	r_a		r_p		i		Ω		ω		ν	
	Guess solution	Optimal solution	Guess solution	Optimal solution	Guess solution	Optimal solution	Guess solution	Optimal solution	Guess solution	Optimal solution	Guess solution	Optimal solution
S_1	13699	14165	2596.3	3560.8	129.9	149.5	237.9	252.9	98.5	113.8	0	0.2
S_2	13699	14165	2596.3	3560.8	129.9	149.5	237.9	252.9	98.5	113.8	120	161.3
S_3	13699	14165	2596.3	3560.8	129.9	149.5	237.9	252.9	98.5	113.8	240	197.5
S_4	14104	12461	4366.2	3509.3	92.5	107.2	208.4	188.1	98.3	136.9	0	5.3
S_5	14104	12461	4366.2	3509.3	92.5	107.2	208.4	188.1	98.3	136.9	120	166.7
S_6	14104	12461	4366.2	3509.3	92.5	107.2	208.4	188.1	98.3	136.9	240	208.2
S_7	14842	12484	2687.2	2417.7	74.3	43.2	173.0	172.5	99.5	165.8	0	1.2
S_8	14842	12484	2687.2	2417.7	74.3	43.2	173.0	172.5	99.5	165.8	180	205.2

Table 5.63: case BK2 orbital parameters

	Mean GDOP		Peak time %	
	MATLAB	STK	MATLAB	STK
Guess solution	4.96	5.43	0.19 %	3.31 %
Optimal solution	4.57	5.85	6.74 %	13.2 %

Table 5.64: case BK2 GDOP values

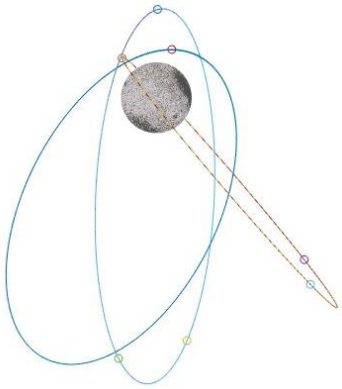

Figure 5.32: case BK2 guess solution

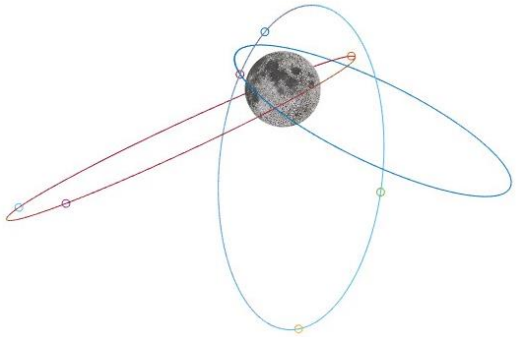

Figure 5.31: case BK2 optimal solution

From the results, it can be seen that SQP algorithm, in order to improve the solution, reduces the mean GDOP value by increasing the mean peak percentage value. The solution doesn't show good performance because the mean GDOP and peak time percentage values are too high.

5.4.5 Case AK3: K-means clustering

The results of case AK3 are reported in Table 5.66. The guess solution from which starts the clustering is case G5. The clustering is made on orbital plane variables $r_a, r_p, i, \Omega, \omega$ with two clusters. The true anomaly of each satellite is defined externally in each plane. The Table 5.65 reports the orbital parameters of each satellite. In Figure 5.34 the clustering solution is represented.

	[km]		[km]		[deg]		[deg]		[deg]		[deg]	
	r_a		r_p		i		Ω		ω		ν	
	Guess solution	Optimal solution	Guess solution	Optimal solution	Guess solution	Optimal solution	Guess solution	Optimal solution	Guess solution	Optimal solution	Guess solution	Optimal solution
S_1	14160	14553	2206.1	3595	79.5	94.8	237.1	209.1	97.0	93.1	359.7	0
S_2	14386	14261	5700.1	2141	120.4	57.8	254.9	233.5	90.3	97.3	35.2	0
S_3	14569	14261	3062.5	2141	148.7	57.8	170.1	233.5	90.4	97.3	254.2	150.3
S_4	14946	14553	2075.9	3595	36.1	94.8	230.0	209.1	97.6	93.1	132.6	180
S_5	12510	14261	2851.1	2141	82.7	57.8	301.9	233.5	105.3	97.3	329.2	171.8
S_6	14968	14261	4188.7	2141	84.5	57.8	187.6	233.5	98.9	97.3	268.9	188.1
S_7	14871	14261	2172.7	2141	38.1	57.8	131.4	233.5	80.6	97.3	285.8	209.6

Table 5.65: case AK3 orbital parameters

	Mean GDOP		Peak time %	
	MATLAB	STK	MATLAB	STK
Guess solution	4.70	4.70	5.1 %	5.1 %
Cluster solution	5.73	5.23	0 %	0.02 %

Table 5.66: case AK3 GDOP values

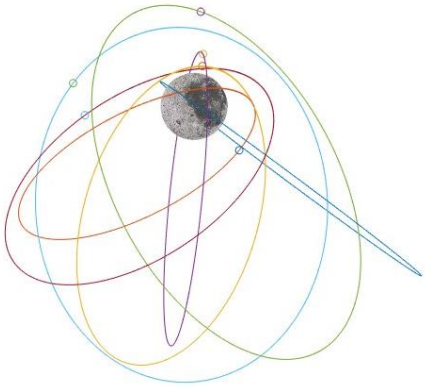

Figure 5.34: case AK3 guess solution

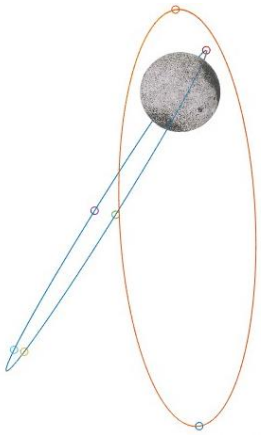

Figure 5.33: case AK3 clustering solution

By using the K-means algorithm, the number of orbital planes is reduced from seven (solution case G5) to two without changing the total number of satellites involved in the architecture. Although the mean peak time percentage is reduced, the mean GDOP value is increased. A second local optimization (case BK3) is proposed starting from the clustering solution of case AK3.

5.4.6 Case BK3: SQP optimization

The optimal results of case BK3 are reported in Table 5.69, while in Table 5.68 are reported the orbital parameters of each satellite. In Figure 5.36 the optimal solution is represented. The optimization variables selected are reported in Table 5.67: there are seven satellites and two orbital planes. The satellites S_1 and S_4 belong to the first plane so the variables are the plane orbital parameters (apogee radius r_{a1}, the perigee radius r_{p1}, the inclination i_1, the RAAN Ω_1 and the perigee argument ω_1) and the true anomaly of each satellite at $t = 0$. The satellites S_2, S_3, S_5, S_6 and S_7 belong to the second plane so the variables are the plane orbital parameters ($r_{a2}, r_{p2}, i_2, \Omega_2$ and ω_2) and the true anomaly of each satellite at $t = 0$. The guess solution is the clustering solution of case AK3.

S_1	S_4	S_2	S_3	S_5	S_6	S_7
r_{a1}		r_{a2}				
r_{p1}		r_{p2}				
i_1		i_2				
Ω_1		Ω_2				
ω_1		ω_2				
ν_1	ν_2	ν_3	ν_4	ν_5	ν_6	ν_7

Table 5.67: case BK3 optimization variables

	[km]		[km]		[deg]		[deg]		[deg]		[deg]	
	r_a		r_p		i		Ω		ω		ν	
	Guess solution	Optimal solution	Guess solution	Optimal solution	Guess solution	Optimal solution	Guess solution	Optimal solution	Guess solution	Optimal solution	Guess solution	Optimal solution
S_1	14553	14628	3595	4185.5	94.8	104.5	209.1	211.5	93.1	79.9	0	0
S_2	14261	14294	2141	2927.7	57.8	49.7	233.5	231.6	97.3	105.1	0	0
S_3	14261	14294	2141	2927.7	57.8	49.7	233.5	231.6	97.3	105.1	150.3	147.0
S_4	14553	14628	3595	4185.5	94.8	104.5	209.1	211.5	93.1	79.9	180	172.6
S_5	14261	14294	2141	2927.7	57.8	49.7	233.5	231.6	97.3	105.1	171.8	171.8
S_6	14261	14294	2141	2927.7	57.8	49.7	233.5	231.6	97.3	105.1	188.1	188.6
S_7	14261	14294	2141	2927.7	57.8	49.7	233.5	231.6	97.3	105.1	209.6	212.2

Table 5.68: case BK3 orbital parameters

	Mean GDOP		Peak time %	
	MATLAB	STK	MATLAB	STK
Guess solution	5.73	5.23	0 %	0.02 %
Optimal solution	5.43	5.45	0.63 %	1.33 %

Table 5.69: case BK3 GDOP values

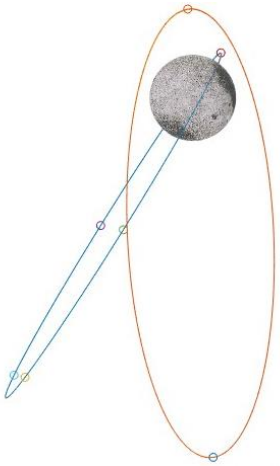

Figure 5.35: case BK3 guess solution

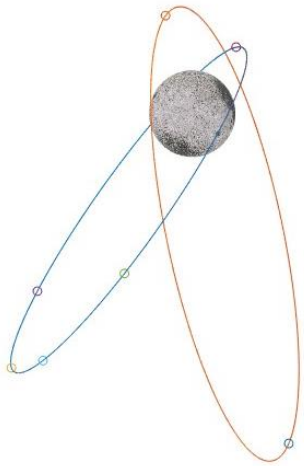

Figure 5.36: case BK3 optimal solution

In this case, to improve the solution, SQP algorithm reduces the
mean GDOP value by increasing the mean peak percentage value. The solution could be improved by defining a perturbed dynamic model or by adding different parameters to be optimized.

5.4.7 Case AK4: K-means clustering

The results of case AK4 are reported in Table 5.71. The guess solution from which starts the clustering is case G5. The clustering is made on orbital plane variables $r_a, r_p, i, \Omega, \omega$ with three clusters. The true anomaly of each satellite is defined externally in each plane. The Table 5.70 reports the orbital parameters of each satellite. In Figure 5.38 the clustering solution is represented.

	[km]		[km]		[deg]		[deg]		[deg]		[deg]	
	r_a		r_p		i		Ω		ω		ν	
	Guess solution	Optimal solution	Guess solution	Optimal solution	Guess solution	Optimal solution	Guess solution	Optimal solution	Guess solution	Optimal solution	Guess solution	Optimal solution
S_1	14553	14229	3595	3068.7	94.8	88.5	209.1	197.7	93.1	93.7	0	0
S_2	14261	14553	2141	2141.0	57.8	57.8	233.5	233.5	97.3	97.3	0	0
S_3	14261	14386	2141	5700.1	57.8	120.4	233.5	254.9	97.3	90.3	150.3	0
S_4	14553	14229	3595	3068.7	94.8	88.5	209.1	197.7	93.1	93.7	180	180
S_5	14261	14386	2141	5700.1	57.8	120.4	233.5	254.9	97.3	90.3	171.8	134.6
S_6	14261	14386	2141	5700.1	57.8	120.4	233.5	254.9	97.3	90.3	188.1	180
S_7	14261	14386	2141	5700.1	57.8	120.4	233.5	254.9	97.3	90.3	209.6	225.4

Table 5.70: case AK4 orbital parameters

	Mean GDOP		Peak time %	
	MATLAB	STK	MATLAB	STK
Guess solution	4.70	4.70	5.1 %	5.1 %
Cluster solution	5.03	5.43	2.95 %	4.54 %

Table 5.71: case AK4 GDOP values

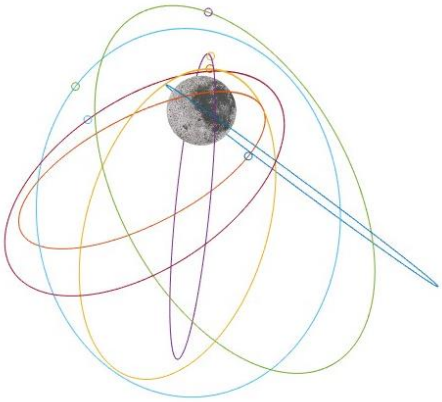

Figure 5.37: case AK4 clustering solution

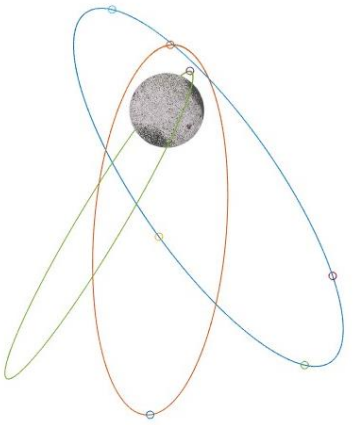

Figure 5.38: case AK4 guess solution

As reported in the previous cases, the number of orbital planes is reduced from seven (case G5) to three with the same total number of satellites. Although the mean peak time percentage is reduced, the mean GDOP value is increased. A second local optimization (case BK4) is proposed starting from the clustering solution of case AK4.

5.4.8 Case BK4: SQP optimization

The optimal results of case BK4 are reported in Table 5.74, while in Table 5.73 are reported the orbital parameters of each satellite. In Figure 5.40 the optimal solution is represented. The optimization variables selected are reported in Table 5.72: there are seven satellites and three orbital planes. The satellites S_1 and S_4 belong to the first plane so the variables are the plane orbital parameters (apogee radius r_{a1}, the perigee radius r_{p1}, the inclination i_1, the RAAN Ω_1 and the perigee argument ω_1) and the true anomaly of each satellite at $t = 0$. The satellites S_2 belongs to the second plane so the variables are the plane orbital parameters (r_{a2}, r_{p2}, i_2, Ω_2 and ω_2) and the true anomaly of each satellite at $t = 0$. The satellites S_3, S_5, S_6 and S_7 belong to the second plane so the variables are the plane orbital parameters (r_{a3}, r_{p3}, i_3, Ω_3 and ω_3) and the true anomaly of each satellite at $t = 0$ The guess solution is the clustering solution of case AK4.

S_1	S_4	S_2	S_3	S_5	S_6	S_7
r_{a1}		r_{a2}	r_{a3}			
r_{p1}		r_{p2}	r_{p3}			
i_1		i_2	i_3			
Ω_1		Ω_2	Ω_3			
ω_1		ω_2	ω_3			
ν_1	ν_2	ν_3	ν_4	ν_5	ν_6	ν_7

Table 5.72: case BK4 optimization variables

	[km]		[km]		[deg]		[deg]		[deg]		[deg]	
	r_a		r_p		i		Ω		ω		ν	
	Guess solution	Optimal solution	Guess solution	Optimal solution	Guess solution	Optimal solution	Guess solution	Optimal solution	Guess solution	Optimal solution	Guess solution	Optimal solution
S_1	14229	14177	3068.7	2945.2	88.5	101.9	197.7	196.2	93.7	100.4	0	0
S_2	14553	14350	2141.0	2092.6	57.8	37.9	233.5	235.5	97.3	106.8	0	0.1
S_3	14386	14007	5700.1	5615.5	120.4	140.8	254.9	254.3	90.3	92.2	0	0
S_4	14229	14177	3068.7	2945.2	88.5	101.9	197.7	196.2	93.7	100.4	180	180.6
S_5	14386	14007	5700.1	5615.5	120.4	140.8	254.9	254.3	90.3	92.2	134.6	141.6
S_6	14386	14007	5700.1	5615.5	120.4	140.8	254.9	254.3	90.3	92.2	180	188.3
S_7	14386	14007	5700.1	5615.5	120.4	140.8	254.9	254.3	90.3	92.2	225.4	222.0

Table 5.73: case BK4 orbital parameters

	Mean GDOP		Peak time %	
	MATLAB	STK	MATLAB	STK
Guess solution	5.03	5.43	2.95 %	4.54 %
Optimal solution	4.21	4.83	4.22 %	6.2 %

Table 5.74: case BK4 GDOP values

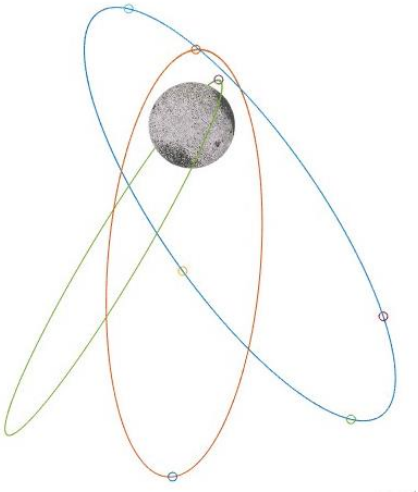

Figure 5.40: case BK4 guess solution

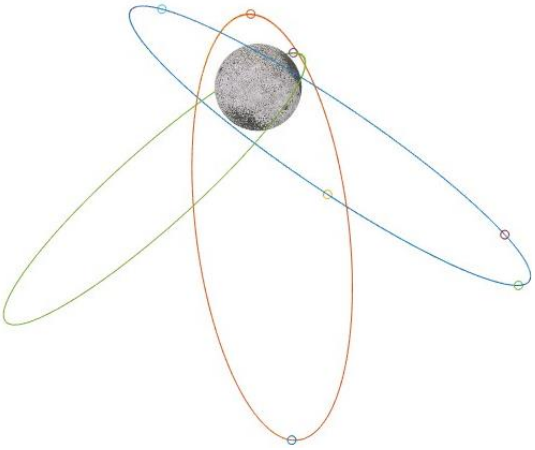

Figure 5.39: case BK4 optimal solution

As reported for case BK3, to improve the solution, the SQP algorithm reduces the mean GDOP value by increasing the mean peak percentage value. The solution can be improved by defining a perturbed dynamic model or by adding different parameters to be optimized.

5.5 Path-relinking solutions

The following section reports the solutions obtained through the application of the Path-relinking technique. The relevant solutions obtained through the application of the method are reported below. The aim of this section is to propose a different methodology to obtain new solutions starting from others previously known. The initial solutions are cases G1 (see e.g. Fig 5.41) and G2 (see e.g. Fig 5.42) obtained from the genetic algorithm.

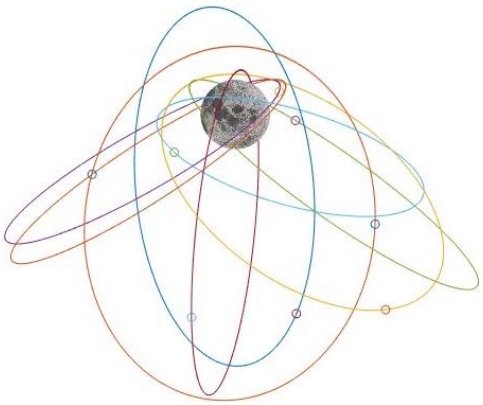

Figure 5.41: case G1 genetic algorithm

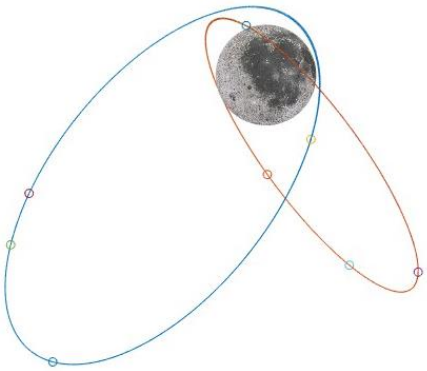

Figure 5.42: case G2 genetic algorithm

Starting from the orbital parameters of each satellite respectively (satellite S_1 of case G1 and of case G2, satellite S_2 of case G1 and of case G2, …), are obtained ten evenly spaced subintervals. The following table describe the concept:

r_{aG1}	r_{ai}	r_{aG2}
r_{pG1}	r_{ai}	r_{pG2}
i_{G1}	i_i	i_{G2}
Ω_{G1}	Ω_i	Ω_{G2}
ω_{G1}	ω_i	ω_{G2}
ν_{G1}	ν_i	ν_{G2}

Table 5.75: orbital parameters subdivision

Where $i = 1, 2, \dots, 8$.
The intermediate solutions represent the new guess solutions from which start the optimization. The genetic algorithm is implemented for the process, defining new upper and lower bounds around the new guess solution:

	[km]	[km]	[deg]	[deg]	[deg]	[deg]
	r_a	r_p	i	Ω	ω	ν
Lower bound	$r_{aG} + 200$	$r_{pG} + 200$	$i_G + 10°$	$\Omega_G + 10°$	$\omega_G + 10°$	$\nu_G + 30°$
Upper bound	$r_{aG} - 200$	$r_{pG} - 200$	$i_G - 10°$	$\Omega_G - 10°$	$\omega_G - 10°$	$\nu_G - 30°$

Table 5.76: upper and lower bounds

Where:

- r_{aG} is the orbit apogee radius of the guess solution;
- r_{pG} is the orbit perigee radius of the guess solution;
- i_G is the orbit inclination of the guess solution;
- Ω_G is the orbit RAAN of the guess solution;
- ω_G is the perigee argument of the guess solution;
- ν_G is the satellite true anomaly at $t = 0$ of the guess solution;

The following case P1, P2 and P3 represents a scenario with eight satellites. Each satellite is defined by its six variables (48 total variables): apogee radius r_a, perigee radius r_p, inclination i, right ascension of the ascending node Ω, argument of perigee ω and the true anomaly ν. All the satellite variables are involved in the optimization process. The basic assumptions described in Section 5.1 are considered. The mathematical model used for the optimization is represented by the perturbed dynamic.

5.5.1 Case P1

The optimal results of case P1 are reported in Table 5.78, while in Table 5.77 are reported the orbital parameters of each satellite. In Figure 5.43 the optimal solution is represented.

	[km]	[km]	[deg]	[deg]	[deg]	[deg]
	r_a	r_p	i	Ω	ω	ν
S_1	12171.3	4032.6	137.9	248.2	89.6	199.8
S_2	12405.4	3774.6	143.2	243.2	110.1	316.1
S_3	13418.9	3523.4	140.4	150.5	96.4	134.3
S_4	12045.8	5897.9	77.8	267.3	102.9	137.2
S_5	14152.4	2733.4	41.4	192.3	106.3	159.5
S_6	14210.9	2817.9	46.5	236.3	98.4	236.0
S_7	13480.5	2356.2	93.6	231.3	92.6	163.4
S_8	14499.1	3475.0	97.3	171.5	79.5	222.0

Table 5.77: case P1 orbital parameters

	Mean GDOP		Peak time %	
	MATLAB	STK	MATLAB	STK
Optimal solution	3.68	3.68	1.4 %	1.45 %

Table 5.78: case P1 GDOP values

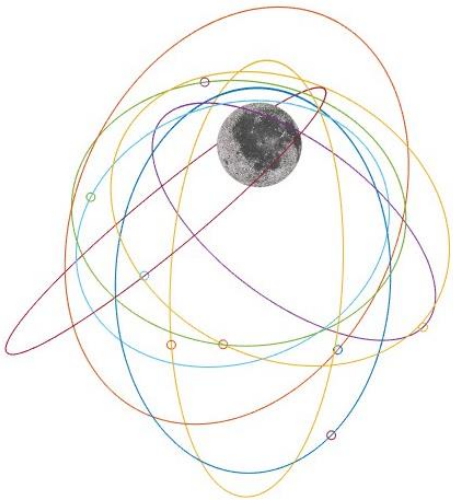

Figure 5.43: case P1 optimal solution

The new solution obtained reports an architecture of eight satellites and eight orbital planes. The complexity can be reduced by applying the clustering method, as explained in Section 5.4, to reduce the total number of orbital planes. The mean GDOP and mean peak percentage values shown in Table 5.78 are satisfactory.

5.5.2 Case P2

The optimal results of case P2 are reported in Table 5.80, while in Table 5.79 are reported the orbital parameters of each satellite. In Figure 5.44 the optimal solution is represented.

	[km]	[km]	[deg]	[deg]	[deg]	[deg]
	r_a	r_p	i	Ω	ω	ν
S_1	10796.6	5240.2	141.8	252.3	98.0	198.1
S_2	11209.2	4720.5	139.8	241.2	111.9	306.3
S_3	12013.4	4732.4	142.7	149.9	105.0	141.3
S_4	10948.4	7013.7	79.2	257.8	107.2	134.7
S_5	13488.1	2710.6	46.0	211.0	90.1	155.1
S_6	13656.3	2643.9	55.5	240.1	99.9	212.7
S_7	13206.0	2302.4	96.5	247.4	92.4	148.1
S_8	13606.0	3185.5	99.7	198.1	93.2	234.0

Table 5.79: case P2 orbital parameters

	Mean GDOP		Peak time %	
	MATLAB	STK	MATLAB	STK
Optimal solution	4.30	4.30	2.75 %	2.76 %

Table 5.80: case P2 GDOP values

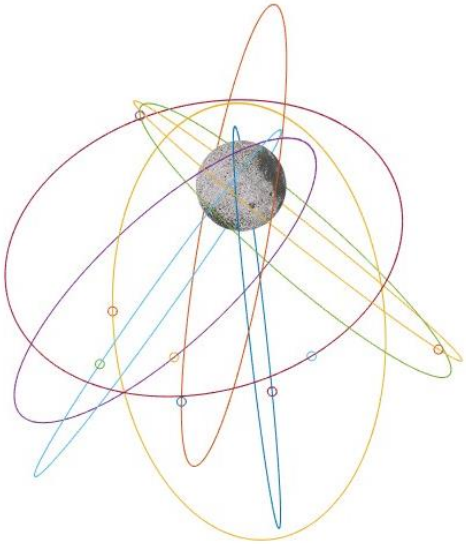

Figure 5.44: case P2 optimal solution

As explained for case P2, the new solution obtained reports an architecture of eight satellites and eight orbital planes. The complexity can be reduced by applying the clustering method, as explained in Section 0, in order to reduce the total number of orbital planes. The mean GDOP and mean peak percentage values reported in Table 5.80 are higher with respect to case P1 and could be improved, for example by applying the SQP algorithm.

5.5.3 Case P3

The optimal results of case P3 are reported in Table 5.82, while in Table 5.81 are reported the orbital parameters of each satellite. In Figure 5.45 the optimal solution is represented.

	[km]	[km]	[deg]	[deg]	[deg]	[deg]
	r_a	r_p	i	Ω	ω	ν
S_1	11785.2	3262.7	93.8	248.4	134.4	163.3
S_2	11770.4	3261.3	88.3	249.7	129.6	98.7
S_3	11550.6	3455.1	86.1	252.6	125.9	189.4
S_4	11772.8	3252.8	76.3	263.9	130.8	223.5
S_5	10176.5	2441.5	122.4	330.9	83.3	164.1
S_6	10031.3	2627.0	103.7	328.0	96.2	203.7
S_7	10104.3	2481.4	128.7	336.8	95.2	186.4
S_8	10054.5	2571.7	129.7	324.8	88.9	359.9

Table 5.81: case P3 orbital parameters

	Mean GDOP		Peak time %	
	MATLAB	STK	MATLAB	STK
Optimal solution	3.43	3.45	0.11 %	0.11 %

Table 5.82: case P3 GDOP values

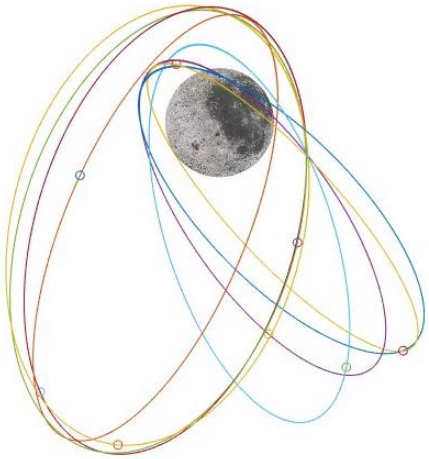

Figure 5.45: case P3 optimal solution

The new solution obtained report an architecture of eight satellites and eight orbital planes. As for the previous cases of this section, the complexity can be reduced. The mean GDOP and mean peak percentage values reported in Table 5.82 are represent good performances with respect to cases P1 and P2.

5.6 Global approach from guess solutions

The solutions obtained through the use of the genetic algorithm are reported in this section. To begin the optimization process, a population of individuals, including the optimal solutions obtained in the previous sections, is initialized. The optimization analysis is performed in the Matlab environment, while the results are verified in the System Tool kit (STK) environment. The mathematical model used for the optimization is based on the assumptions reported in section 5.1. Two cases are presented, one involving eight satellites (case G14) and the other involving seven satellites (case G15).

5.6.1 Case G14

The case reports 8 satellites and 8 orbital planes (48 total variables). The optimal results of case G14 are reported in Table 5.83, while in Table 5.84 are reported the orbital parameters of each satellite. In Figure 5.46 the optimal solution is represented. The initial population of individuals include the solutions with eight satellites obtained in the previous sections.

	[km]	[km]	[deg]	[deg]	[deg]	[deg]
	r_a	r_p	i	Ω	ω	ν
S_1	14893.8	2634.6	93.3	156.6	95.5	137.3
S_2	14893.8	2634.6	91.6	170.9	93.7	184.6
S_3	14893.8	2689.3	93.8	156.6	93.7	258.9
S_4	13158.5	3798.6	45.6	163.7	99.6	197.0
S_5	13158.5	3798.6	42.0	163.7	99.6	147.7
S_6	13158.5	3798.6	31.3	163.7	99.6	344.6
S_7	14429.7	2548.6	150.1	152.1	70.3	177.2
S_8	14429.7	2548.6	150.1	146.7	70.3	253.2

Table 5.83: case G14 orbital parameters

	Mean GDOP		Peak time %	
	MATLAB	STK	MATLAB	STK
Optimal solution	2.39	2.41	0%	0 %

Table 5.84: case G14 GDOP values

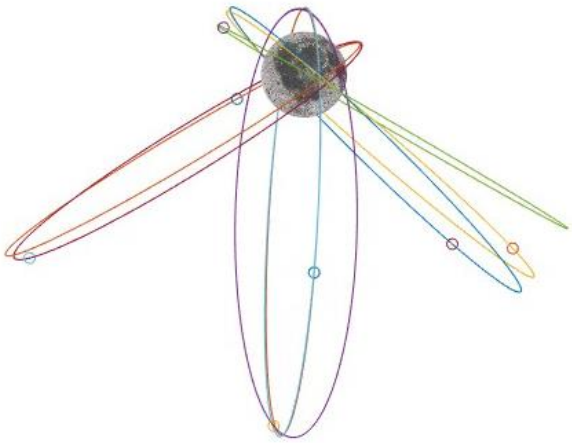

Figure 5.46: case G14 optimal solution

Case G14 presents a solution with eight satellites and eight orbital planes. The mean GDOP and mean peak time percentage values are satisfactory. The solution demonstrates that increasing the degrees of freedom leads to an improved solution.

5.6.2 Case G15

The case reports 7 satellites and 7 orbital planes (42 total variables). The optimal results of case G15 are reported in Table 5.86, while in Table 5.85 are reported the orbital parameters of each satellite. In Figure 5.44 5.47 the optimal solution is represented. The initial population of individuals include the solutions with seven satellites obtained in the previous sections.

	[km]	[km]	[deg]	[deg]	[deg]	[deg]
	r_a	r_p	i	Ω	ω	ν
S_1	14173.8	2620.9	30.3	335.4	69.4	187.3
S_2	14173.8	2585.7	37.5	335.4	69.4	358.7
S_3	11482	2101.7	144.6	316.9	93.0	237.5
S_4	11482	2101.7	144.6	316.9	93.0	171.4
S_5	11256.6	2461.2	97.7	305.9	92.6	128.2
S_6	11256.6	2461.2	97.7	313.1	95.8	173.7
S_7	11256.6	2461.2	90.5	312.2	95.8	213.7

Table 5.85: case G15 orbital parameters

	Mean GDOP		Peak time %	
	MATLAB	STK	MATLAB	STK
Optimal solution	2.62	2.69	0 %	0.11 %

Table 5.86: case G15 GDOP values

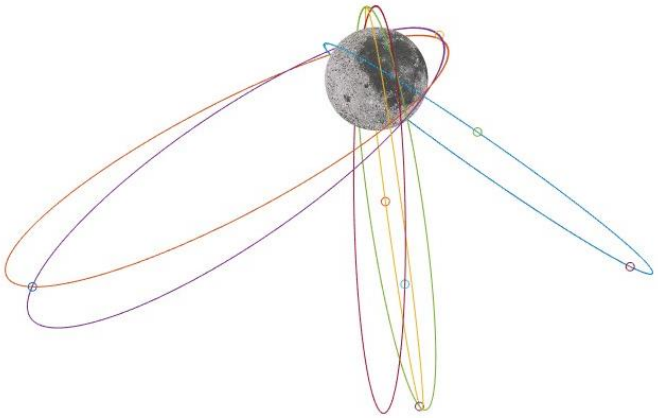

Figure 5.47: case G15 optimal solution

Case G15 presents a solution with seven satellites and seven orbital planes. The mean GDOP and mean peak time percentage values are satisfactory. The solution demonstrates that increasing the degrees of freedom leads to an improved solution.

A summary of all the optimal solutions obtained from the experimental analysis is presented in Section 5.8.

5.7 Solution analysis

This section presents a perturbation analysis conducted on two significant solutions. Specifically, STK was used to perform a high-fidelity propagation of satellite orbits, taking into account the following perturbations:

- Moon gravity field,
- Earth gravity field,
- Sun gravity field,
- Earth zonal harmonics (up to J_7),
- Moon zonal harmonics (up to J_{50}).

Here, the notation J_n represents the degree order considered in the gravity harmonics formulation. The propagation is defined (see Section 5.1) for a total time of 28 days. The comparison is made between the solution obtained in case G1 with the genetic algorithm and the guess solution of case S1, as reported in the work by Bhamidipati et al. (2023). The aim of this analysis is to present the different percentages of variations for the satellite orbital parameters. Case G1 represents a scenario with generic high elliptical orbits, while case S1 reports two frozen orbits. Case G1, as reported in the Chapter 5, Figures out a lower mean GDOP and mean peak time percentage values. On the other hand, the frozen orbits represent a class of Table orbits around the Moon. These orbits are elliptical, with their line of apsides librating in the polar region and exhibiting a lifetime of ten years.
The solutions of cases G1 and S1 are reported in figures Figure 5.48, Figure 5.49, Figure 5.50, Figure 5.51, Figure 5.52 respectively, where the percentage variations, relative to the orbital parameters of each satellite (S_1, S_2, …, S_8), are represented.

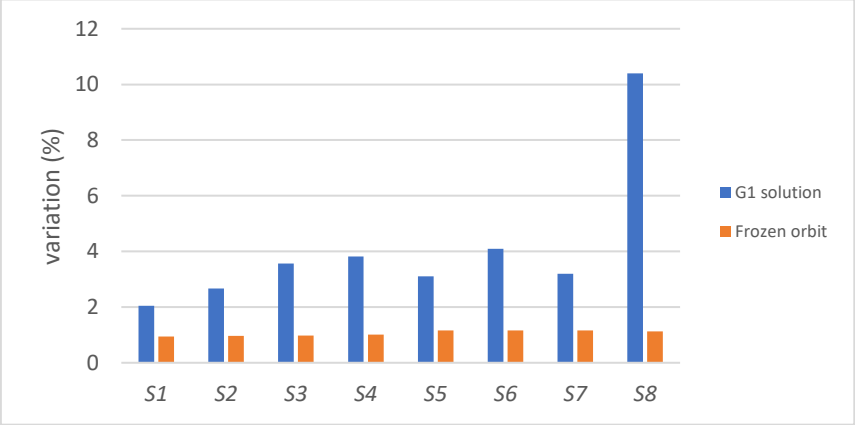

Figure 5.48: apogee radius variation (%)

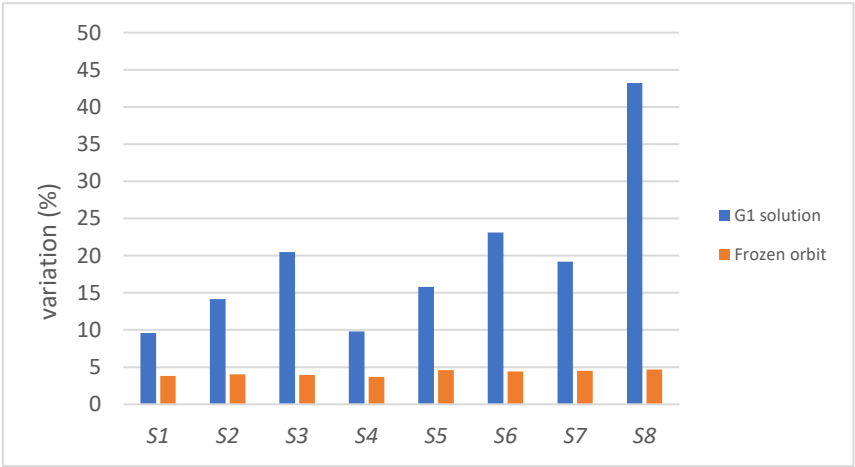

Figure 5.49: perigee radius variation (%)

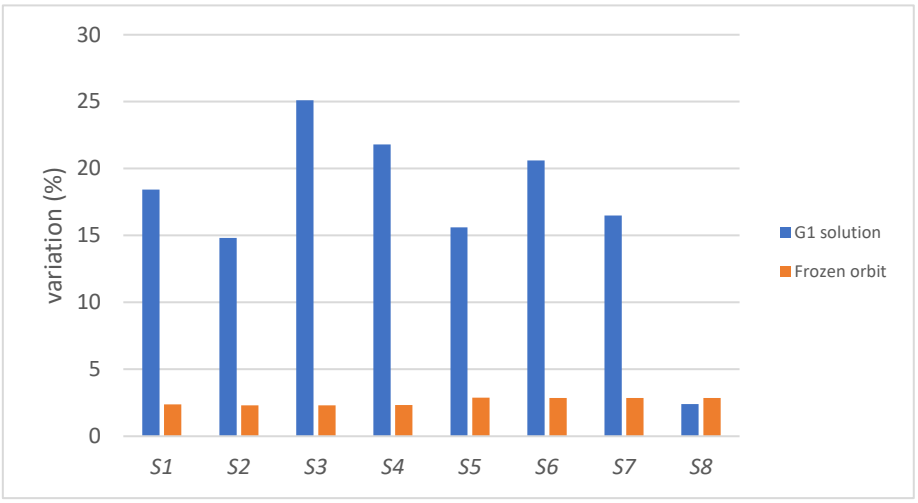

Figure 5.50: perigee argument variation (%)

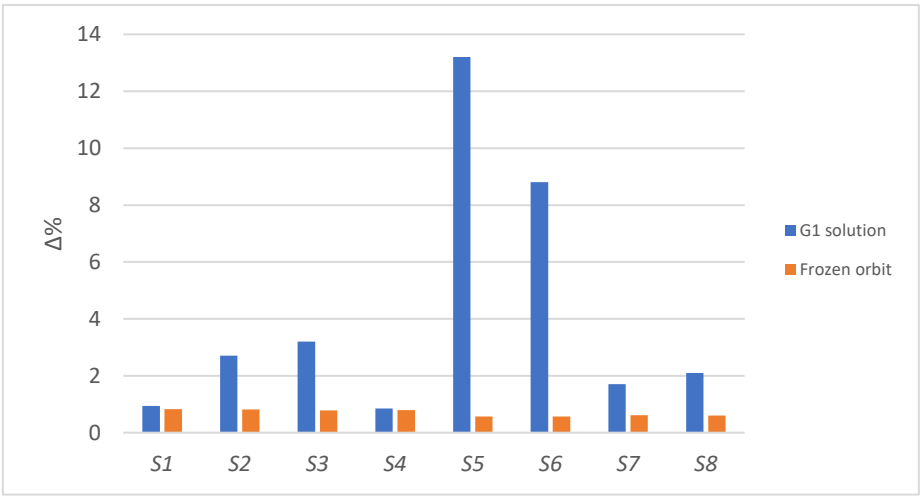

Figure 5.51: inclination variation (%)

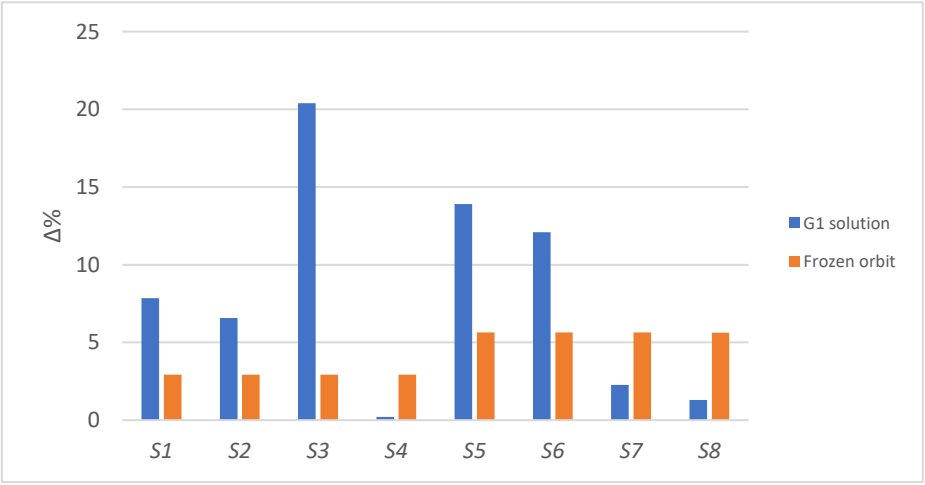

Figure 5.52: RAAN variation (%)

From the results shown, it can be observed that non-frozen orbits manifest a greater variation in orbital parameters over the time. The value of variation strongly depends on the orbit considered and the effect of relevant perturbations.

5.8 Analysis summary

In this section a summary of all the optimal solutions obtained are reported in Table 5.87, with a discussion about the related results.

Case	Total number of satellites	Total number of orbital planes	Mean GDOP	Peak time %
G1	8	8	2.65	0.38 %
G14	8	8	2.41	0 %
S4	8	8	3.74	0.03 %
P1	8	8	3.68	1.45 %
P2	8	8	4.30	2.73 %
P3	8	8	3.43	0.11 %
G2	8	2	3.66	0.04 %
S2	8	2	3.79	0.86 %
S3	8	2	4.18	0.81 %
AK1	8	2	4.48	0.02 %
BK1	8	2	3.96	3.10 %
G3	8	3	2.50	0.01 %
AK2	8	3	5.43	3.31 %
BK2	8	3	5.85	13,2 %
G4	8	4	3.28	1.37 %
G5	7	7	4.7	5.1 %
G15	7	7	2.69	0.11 %
G6	7	2	4.4	1.2 %
AK3	7	2	5.23	0.02 %
BK3	7	2	5.45	1.33 %
G7	7	3	2.80	0.16 %
AK4	7	3	5.43	4.54 %
BK4	7	3	4.83	6.2 %
G8	7	4	3.35	1.71 %
G9	6	6	5.19	8.14 %
G10	6	2	4.19	1.36 %
G11	6	3	5.12	1.81 %
G12	5	5	7.35	22.98 %
G13	5	2	8.26	15.52 %

Table 5.87: summary of the optimal solutions obtained

Scenarios with higher degrees of freedom, where each satellite has its own orbital plane, could lead to better solutions in terms of mean GDOP values and mean peak time percentage. This way each satellite can select its position using Keplerian orbital parameters within assigned bounds. On the other side, they require more computational effort. The genetic algorithm led to the solutions G14 and G15 with the lowest mean values of GDOP and peak time percentage. The SQP algorithm can hardly improve the solution when about forty variables or more are involved (see case S1 and S5). Using the SQP algorithm with fewer free variables (as reported in cases S2, S3 and S4) is more advantageous, resulting in improved results and different constellation architectures. The path-relinking method can be used to obtain new solution architectures. The genetic algorithm is then applied to optimize the new solutions by restricting variable bounds and using six variables for each satellite (as represented by cases P1, P2, and P3 with eight satellites). By means of the genetic algorithm, the solutions could be improved increasing the computational time. In order to reduce the constellation complexity and improve the satellite operability, the number of orbital planes can be defined externally, by defining each satellite to a plane. Cases G2, G3, G4, S2, S3, AK1, BK1, AK2 and BK2 report good solutions with eight satellites and limited number of orbital planes. The advantage of reducing the number of orbital planes involved is shown in the clustering cases AK1, AK2, AK3 and AK4. On the other side, subsequent optimization by means of the SQP algorithm can reduce the mean GDOP value as the expense of an increment of mean peak time percentage value. In general, not all the solutions resulted in being acceptable because featuring high mean GDOP value and/or a significant number of peak percentages over time. By using a perturbed-dynamics model and appropriate additional constraints (e.g., on the perigee altitude) the optimization leads to improved solutions (see case G5 and G6). The best solution obtained with seven satellites is represented by case G15, while, for the scenario with six satellites, the best one is represented by case G10. The scenarios with five satellites (G12 and G13) are less efficient, in fact the GDOP is reduced with a higher number of satellites involved. In the whole analysis performed here, the genetic algorithm proved to be effective. The SQP method is a local approach for improving a known solution. It is strongly dependent on the trend of the objective function and the provided guess solution. By applying the K-means algorithm, the clustering approach is an effective method for reducing the number of orbital planes involved.

Finally, a Pareto-front approach is adopted to select the solutions obtained: non-dominated solutions are considered equivalent. The cases considered concern different numbers of orbital planes but the same numbers of satellites. Two objective functions are considered, i.e., mean GDOP value and mean peak time percentage, both to be minimized. Figure 5.53 shows that in scenarios with eight satellites, there is one dominant solution (G14) followed closely by G3. Neglecting G3 and G14 the G1, P3, G2, S4, and AK1 are mutually non-dominated solutions (the one that are still good from an engineering point of view are mutually non dominated and can be considered as equivalent). The remaining solutions in the top right-hand side are dominated by the previous.

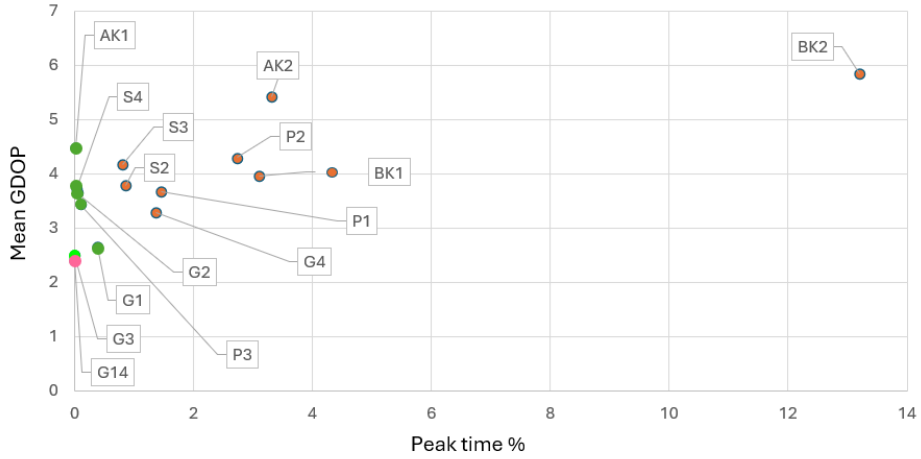

Figure 5.53: non-dominated solution selection for eight satellite scenarios

The same selection approach has been followed concerning the scenarios involving seven satellites. Figure 5.54 shows that there is one dominant solution (G15) followed closely by G7. AK3 and G7 are mutually non-dominated. The remaining solutions in the top right-hand side are dominated by the previous.

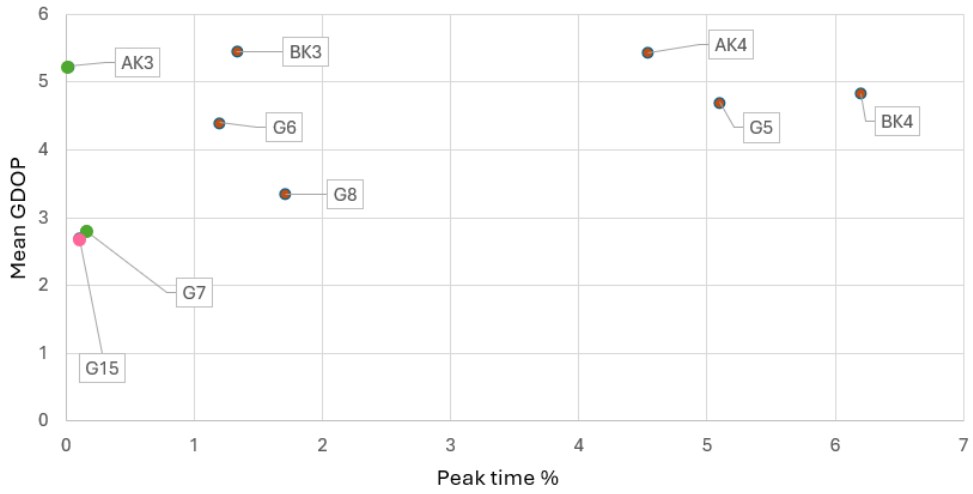

Figure 5.54: non-dominated solution selection for seven satellite scenarios

6 Extensions and future improvements

In relation to the experimental analysis proposed in Chapter 5, the following discussion concern possible future developments to improve the methodologies and the optimization approach adopted. In this section a different area of interest is considered. A test case regarding the arrangement of 16 satellites, covering the Moon equatorial area, is reported. The geographical coordinates of the grid points considered are reported below:

Minimum latitude	-10°
Maximum latitude	-10°
Minimum longitude	0°
Maximum longitude	360°
Number of points	36

Table 6.1: equatorial target area coordinates

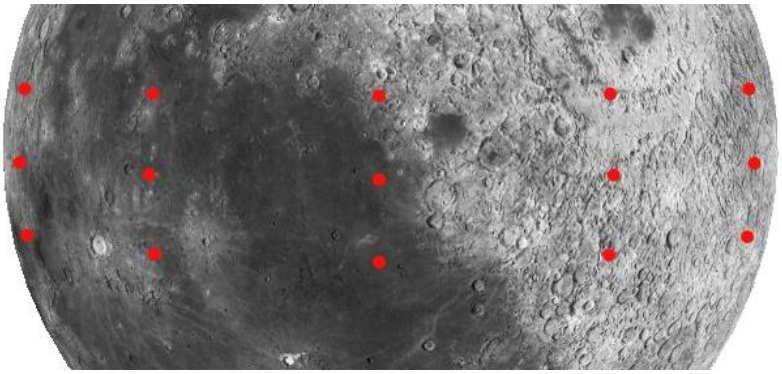

Figure 6.1: representation of the equatorial target area (STK)

The orbit propagation considers the perturbation effects due to the Earth gravity and the Sun gravity. The satellites and positions of the target points are calculated for a total time of $28\,days$. This total time is partitioned in subintervals of 10 minutes each, to calculate satellite / target point locations and the relevant GDOP values. The visibility constraint is defined by a minimum elevation angle between the surface point and the satellite position (see 3.13):

$$\gamma = 5°.$$

The variables bounds are defined as follows:

	[km]	[km]	[deg]	[deg]	[deg]	[deg]
	r_a	r_p	i	Ω	ω	ν
Lower bound	2000	2000	0	0	0	0
Upper bound	15000	15000	180	360	360	360

Table 6.2: variable upper and lower bounds

The mean GDOP value and the mean peak time percentage is minimized. Each satellite is defined by its six variables: apogee radius r_a, perigee radius r_p, inclination i, right ascension of the ascending node Ω, argument

of perigee ω and the true anomaly ν. The optimal results are reported in Table 6.4, while in Table 6.3 the orbital parameters of each satellite are reported. In Figure 6.2 the optimal solution is represented. The optimization involves sixteen satellites and two orbital planes. Satellites S_1, S_2, S_3, S_4, S_5, S_6, S_7 and S_8 belong to the first plane, therefore the variables involved are the plane orbital parameters, in addition to the true anomaly of each satellite, at $t = 0$. Satellites S_9, S_{10}, S_{11}, S_{12}, S_{13}, S_{14}, S_{15} and S_{16} belong to the first plane, therefore the variables involved are the plane orbital parameters, in addition to the true anomaly of each satellite, at $t = 0$. The test case-reported in Figure 6.2 represents an example of the possible applicability of the algorithm to different areas to be observed.

	[km]	[km]	[deg]	[deg]	[deg]	[deg]
	r_a	r_p	i	Ω	ω	ν
S_1	12805.3	10832.7	148.4	254.8	19.5	263.8
S_2	12805.3	10832.7	148.4	254.8	19.5	68.8
S_3	12805.3	10832.7	148.4	254.8	19.5	234.8
S_4	12805.3	10832.7	148.4	254.8	19.5	155.9
S_5	12805.3	10832.7	148.4	254.8	19.5	318.5
S_6	12805.3	10832.7	148.4	254.8	19.5	205.3
S_7	12805.3	10832.7	148.4	254.8	19.5	28.8
S_8	12805.3	10832.7	148.4	254.8	19.5	103.4
S_9	12543.7	11704.9	44.7	207.1	142.8	324.7
S_{10}	12543.7	11704.9	44.7	207.1	142.8	210.6
S_{11}	12543.7	11704.9	44.7	207.1	142.8	79.8
S_{12}	12543.7	11704.9	44.7	207.1	142.8	258.9
S_{13}	12543.7	11704.9	44.7	207.1	142.8	27.1
S_{14}	12543.7	11704.9	44.7	207.1	142.8	159.1
S_{15}	12543.7	11704.9	44.7	207.1	142.8	124.0
S_{16}	12543.7	11704.9	44.7	207.1	142.8	290.6

Table 6.3: equatorial area orbital parameters

	Mean GDOP		Peak time %	
	MATLAB	STK	MATLAB	STK
Optimal solution	2.59	2.59	0 %	0 %

Table 6.4: equatorial area GDOP values

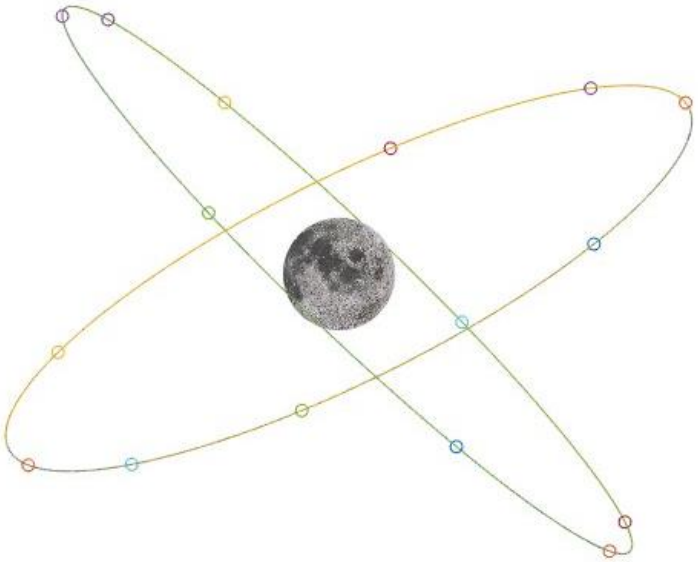

Figure 6.2: equatorial optimal solution

The study of the orbital station keeping issue is discussed hereinafter. The station-keeping is defined by the maneuvers required to maintain a spacecraft at a fixed distance from another spacecraft or planet/celestial body. It is performed through a series of orbital maneuvers made by the satellite thrusters to keep the spacecraft in the designed path. The perturbations present in the outer space are the major causes of the deviations from the theoretical trajectory. For example, the Earth's oblateness, the gravitational forces from other celestial bodies, solar radiation pressure or atmospheric drag are typical perturbations. Station keeping is strictly correlated with the satellite constellation considered. The maintaining cost of the satellites in their nominal position is the fundamental scope of the station keeping. This cost is expressed in terms of number of maneuvers required and consequently the propellant mass consumed. In Figure 6.3, the maximum percentage variations of the orbital parameters are reported. The case studies considered compare a stabilized lunar satellite orbit with an unstable one. Station keeping could help improving maneuvers with low fuel consumption. In this case an optimization strategy can be adopted by acting on the constellation variables.

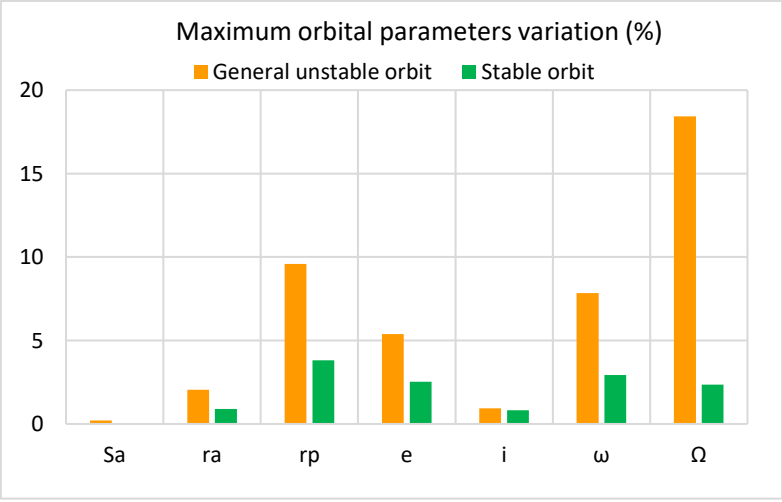

Figure 6.3: stable and unstable orbits comparison

With respect to the satellite trajectory, the GDOP function is closely related to the instantaneous satellite position in 3D space, and the number of satellites involved in the positioning. Generally, the function exhibits a highly irregular trend over time, often varying by many orders of magnitude within a short period (see e.g., Fig. 6.4). Major aspects concerning each optimal solution consists in the mean GDOP value and the mean peak percentage over time. It is expected that more or less stable solutions can occur. Specifically, if small variations in the parameters that characterize the optimal solution result in large variations in the GDOP value, the solution is considered unstable and vice versa. A sensitivity analysis could therefore be carried out to investigate the stability of the GDOP function (w.r.t. the control variables values found).

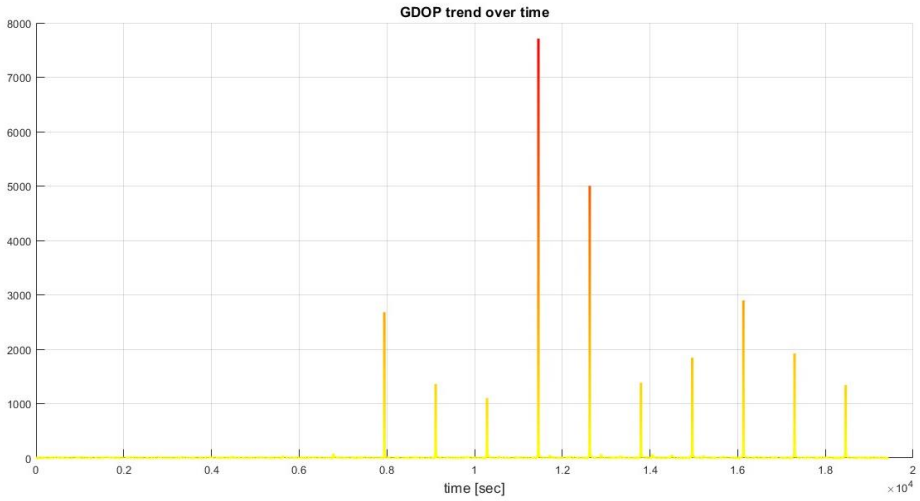

Figure 6.4: GDOP trend over time

Finally, a relevant aspect in the development of a constellation architecture, is the relative communication between satellites (see e.g., Fig 6.5). It is important to understand which spacecraft can communicate with each other and with those connected to Earth. This ensures communication between the satellite constellation and surface points of the observed area, even when they are hidden on the dark side of the Moon. The inclusion of communication aspects between satellites in the mathematical model allows for more realistic solutions. In fact, the need for constant communication from the ground with the relevant points on the surface observed by the constellation would be fully covered.

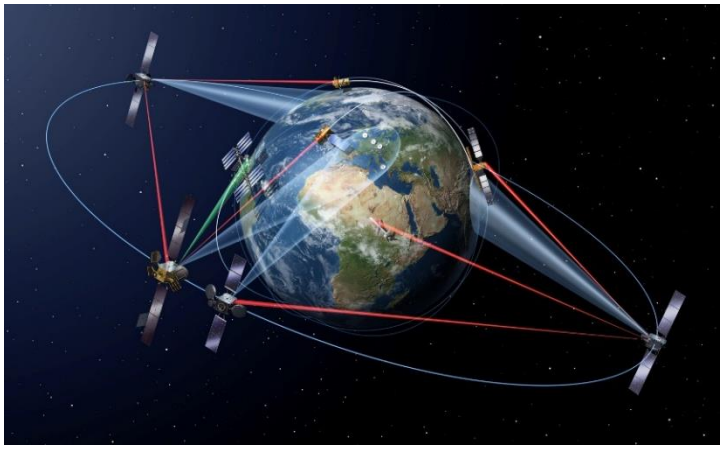

Figure 6.5: satellite inter-link communication

7 Conclusions

In the upcoming years, the exploration of the Moon will be a primary focus of global space initiatives. Satellite constellations orbiting the Moon will play a central role in these endeavors by providing essential navigation, communication, and data relay services. These architectures will enable precise positioning for lunar landers and rovers, facilitate real-time communication with Earth-based mission control, and support the establishment of sustainable lunar habitats. The South Pole region of the Moon is of particular interest due to its water ice deposits, ample sunlight for generating solar power, and significant scientific potential. Lunar exploration presents valuable opportunities to develop and refine capabilities essential for more ambitious ventures, such as crewed missions to Mars.

The objective of this thesis is to propose methodologies and algorithms for obtaining optimized architectures of lunar satellites visible from the lunar South Pole area, while minimizing the global dilution of precision (GDOP). The solutions obtained ensure that at least one satellite is always visible from Earth and at least four satellites are visible from every point in the lunar South Pole area. The basics of GPS positioning systems and the relevant triangulation concept are considered in depth. The dilution of precision and its relative factors, including the GDOP, determine the precision of the positioning system and represents the main objective of the constellation.

In this work, the mean GDOP is minimized, in addition to the mean percentage of times the GDOP exceeds a given acceptability limit. A novel overall approach is put forward, combining various methods and techniques. In this perspective, ad-hoc algorithms have been developed using several mathematical concepts. A genetic algorithm is used to arrange the satellite positions, following a global optimization point of view. Additionally, a different approach utilizes the sequential quadratic programming algorithm to locally optimize architectures known a priori. Another method aims to decrease the constellation complexity and improve satellite operability by reducing the number of orbital planes in the constellations. This is achieved through a specific clustering technique based on the K-means algorithm.

The experimental analysis carried out is aimed at obtaining a number of satisfactory solutions applicable to different operational scenarios, rather than a single result, albeit globally optimal. The proposed methods are applied to various cases involving different optimization variables, total number of satellites, and orbital planes. For example, constellations with eight satellites are investigated, distributed on eight or less orbital planes (e.g., two orbits). The results obtained from different cases confirm the efficiency of the overall methodology proposed. The optimization process can be applied flexibly to scenarios with different areas of observation and on other celestial bodies like Earth or Mars. A constellation architecture is additionally considered to cover the equatorial region of the Moon, using two orbital planes and sixteen satellites.

Future improvements will focus on major aspects, such as orbital station keeping and satellite inter-link communication. These enhancements will address the challenges posed by perturbations in outer space, leading to specific optimization strategies to minimize the costs associated with satellite positioning, such as the propellant required for station keeping maneuvers.

8 Bibliography

Arthur, D. and Vassilvitskii, S. (2007). K-Means++: The Advantages of Careful Seeding. Society for Industrial and Applied Mathematics, USA.

Alarie, S., Audet C., Gheribi, A.E., Kokkolaras, M., and Le Digabel, S. (2021). «Two decades of blackbox optimization applications». EURO Journal on Comuputational Optimization, 9.

Bhamidipati, S., Mina, T., Sanchez, A., and Gao, G. (2023). Satellite constellation design for a lunar navigation and communication system. NAVIGATION, 70 (4).

Ben-Israel, A. and Greville, T. (2003). Generalized inverses: Theory and applications. Springer, New York.

Bryson, A. and Ho, Y. (1969). Applied optimal control, Blaisdell, New York.

ESA (2020). Types of orbits. https://www.esa.int/Enabling_Support/Space_Transportation/Types_of_orbits Accessed on April 1,.2024.

ESA (2024a). About satellite navigation. https://www.esa.int/Applications/Navigation/About_satellite_navigation . Accessed on April 1, 2024.

ESA (2024b). Lunar satellites. https://www.esa.int/Applications/Connectivity_and_Secure_Communications/Lunar_satellites . Accessed on April 1, 2024.

Fletcher R. (2010). The Sequential Quadratic Programming Method, Springer, Berlin Heidelberg.

Langley, R. B. (1999a). Dilution of Precision. GPS World, Vol. 10 (5), 52-59.

Langley, R. B. (1999b). The Mathematics of GPS. GPS World, Vol. 10 (5), 52-59.

GISgeography (2024). How GPS Receivers Work – Trilateration vs Triangulation. https://gisgeography.com/trilateration-triangulation-gps/.

Minoux, M. and Vaida, S. (1986). Mathematical programming: theory and algorithms. John Wiley & Sons, London.

The MathWorks Inc. (2022). MATLAB version: 9.13.0 (R2022b), Natick, Massachusetts: The MathWorks Inc. https://www.mathworks.com.

Systems Tool Kit (STK). https://www.agi.com/products/stk.

Tsui, J. B. (2000). Fundamentals of Global Positioning System Receivers: A Software Approach, John Wiley & Sons.

Walker, J. (1984). Satellite constellations. Journal of the British Interplanetary Society, 37, 559-571.

Vallado, D. A. (2013). Fundamental of Astrodynamics and Applications, 4.

9 Acknowledgements

Vorrei dedicare il presente lavoro a tutte le persone che mi hanno accompagnata e supportata durante l'intero percorso universitario e, in particolar modo, in questi mesi conclusivi in Thales Alenia Space a Torino.
In particolare, vorrei ringraziare il mio relatore, il Prof. Lorenzo Casalino, che mi ha seguita durante l'intero sviluppo della tesi, fornendomi preziosi consigli e senza i quali non avrei raggiunto i risultati ottenuti. Ringrazio in particolare il Dott. Giorgio Fasano che mi ha aiutata in questi mesi, introducendomi nel vasto mondo dell'ottimizzazione, e rappresentando per me un punto di riferimento importante nei momenti di difficoltà. Grazie alla sua passione e disponibilità ho potuto apprendere concetti e sperimentare argomenti che non avevo mai affrontato nel mio percorso, arricchendomi e migliorando le mie capacità.
Ringrazio l'Ing. Marco Berga e tutto l'ufficio di Mission Analysis and Operations di Thales Alenia Space a Torino, per avermi accolto in questi mesi e avermi permesso lo svolgimento di un'esperienza stimolante e arricchente. Il loro costante supporto ed i loro consigli sono stati un prezioso aiuto non solo per gli aspetti tecnici della tesi e le relative difficoltà della materia, ma mi hanno permesso anche di osservare da vicino le varie fasi operative aziendali.
Infine, dedico questo lavoro alle persone a me più care. La mia famiglia (mio papà Paolo, mia mamma Gabriella e mia sorella Greta), che in questi anni non mi hanno mai fatto mancare nulla, al contrario mi hanno sempre dato la motivazione giusta, insegnandomi a non farmi scoraggiare dalle difficoltà ma a dare sempre il massimo dell'impegno. In particolare, mio papà, che mi ha trasmesso la sua passione fin da bambina, facendomi sentire sempre all'altezza di ogni situazione. Ringrazio il mio fidanzato Federico, che in questi anni mi ha sempre dimostrato il suo sostegno, assecondando le mie necessità e insegnandomi a guardare "un gradino alla volta" al posto dell'intera scala. Il raggiungimento di questo traguardo è grazie a voi e ai vostri costanti sacrifici.
In ultimo dedico un ringraziamento a tutti i miei amici, a quelli che ci sono da sempre, fin dall'asilo, e a quelli nuovi conosciuti in questi anni. Con loro ho condiviso tutte le mie esperienze più belle e grazie ai momenti passati insieme il percorso è stato meno faticoso.
A tutti voi, grazie.